https://doi.org/10.35662/unine-thesis-2954

PhD Thesis

Thin-disk lasers and their applications for nonlinear frequency conversion toward THz and XUV

Presented by

Jakub Drs

A dissertation submitted to:

University of Neuchâtel
Faculty of science

PhD jury:

Prof. Thomas Südmeyer	Director
Dr. Valentin Wittwer	Examiner
Prof. Clara Saraceno	Examiner
PD Dr. Christian Kränkel	Examiner

Neuchâtel, 2022

UNIVERSITÉ DE NEUCHÂTEL

Faculté des Sciences
Secrétariat-décanat de Faculté
Rue Emile-Argand 11
2000 Neuchâtel – Suisse
Tél : + 41 (0)32 718 21 00
E-mail : secretariat.sciences@unine.ch

IMPRIMATUR POUR THESE DE DOCTORAT

La Faculté des sciences de l'Université de Neuchâtel autorise l'impression de la présente thèse soutenue par

Monsieur Jakub DRS

Titre:

"Thin-disk lasers and their applications for nonlinear frequency conversion toward THz and XUV"

sur le rapport des membres du jury composé comme suit:

- Prof. Thomas Südmeyer, directeur de thèse, Université de Neuchâtel, Suisse
- Dr Valentin Wittwer, Université de Neuchâtel, Suisse
- Prof. Clara Saraceno, Ruhr-Universität Bochum, Allemagne
- Dr Christian Kränkel, Leibniz-Institut für Kristallzüchtung, Berlin, Allemagne

Neuchâtel, le 5 mai 2022

Le Doyen, Prof. A. Bangerter

Abstract

This thesis is devoted to the development of ultrafast thin-disk lasers (TDL) oscillators and their use for intra-oscillator high-harmonic generation (HHG). The main motivation was to develop a simple and compact source of coherent extreme ultraviolet (XUV) light. Conventionally, coherent XUV radiation can be found in large scale synchrotron or free-electron laser facilities. Laser driven HHG systems have long strived to become a lab-scale alternative to these sources. The major challenge has been the low conversion efficiency of the HHG process and the high demands on the driving laser. With the advancing laser technology, this situation is rapidly improving and several state-of-the-art HHG systems can nowadays reach an XUV flux which is in certain aspects comparable to synchrotrons.

The intra-laser-oscillator HHG approach is inspired by femtosecond enhancement cavities. Driving HHG inside an enhancement cavity allows for recycling the unconverted pulse energy, while increasing the available power by the cavity enhancement factor. An enhancement cavity, however, requires coherent coupling of the femtosecond pulses into the cavity which is a demanding task. The intra-oscillator HHG approach offers a simplified concept using directly the cavity of the laser instead of an external enhancement cavity.

To achieve sufficiently high driving power for efficient intra-oscillator HHG, the existing TDL technology had to be significantly improved and optimized for intracavity performance. Within the scope of this thesis, a strong focus was placed on the development of the driving laser and significant progress has been achieved. To this purpose, we investigated and demonstrated Kerr lens mode-locked TDL oscillators based on the gain material Yb:YAG, which achieved several records in terms of their output performance. Using our system we have demonstrated the shortest pulse duration of any TDL oscillator of 27 fs, as well as the highest average power in the sub-100-fs regime of 100 W and the highest peak power of 100 MW.

The corresponding increase of intracavity performance of our laser allowed us to significantly improve the HHG operation in terms of the generated XUV flux and photon energies. Starting from 0.5 nW generated at 13 eV demonstrated five years ago, we have improved the XUV flux to 10 µW at 30 eV at the current state. Although this is not yet the highest performance among other HHG systems, the flux value is becoming competitive to the results of enhancement cavities operating at similar photon energy.

The improved output performance of the demonstrated TDLs is also highly attractive for nonlinear conversion toward longer wavelengths of the electromagnetic spectrum. A part of this thesis is, thus, dedicated to terahertz genera-

tion. We have demonstrated the first TDL driven terahertz generation in 2018, through optical rectification in GaP. Later, we used the tunability and the high average power of our self-built TDL oscillator to experimentally investigate in detail the properties of optical rectification in GaP driven by 1-µm high-power Yb-based lasers. Finally, having the experience from intra-oscillator HHG, we have shown that the high-power driving laser can be replaced by driving the THz generation directly inside the cavity of a small KLM bulk laser oscillator.

Résumé

Cette thèse est consacrée au développement d'oscillateurs lasers ultrarapides à disques minces (TDL pour « thin-disk-laser » en anglais) et à leur utilisation pour la génération d'harmoniques d'ordres élevés (HHG pour « high-harmonic-generation » en anglais) à l'intérieur de l'oscillateur laser. La motivation principale était de développer une source simple et compacte de lumière cohérente XUV (pour « extreme ultraviolet » en anglais). Traditionnellement, une radiation cohérente de XUV peut être trouvé dans les installations à grande échelle comme les synchrotrons ou les lasers à électrons libres. Les systèmes HHG entrainés par laser ont longtemps cherché à devenir une alternative à échelle de laboratoire à ces sources. Le défi majeur était la faible efficacité de conversion du HHG et les exigences élevées du system de laser. Avec le progrès de la technologie laser, la situation s'améliore rapidement et plusieurs systèmes HHG peuvent aujourd'hui atteindre un flux XUV qui est, à certains égards, comparable à celui des synchrotrons.

L'approche HHG à l'intérieur de l'oscillateur laser est inspirée des cavités d'amélioration femtosecondes. L'entrainement de HHG à l'intérieur d'une cavité d'amélioration permet de recycler l'énergie non converties, tout en augmentant la puissance disponible par le facteur d'amélioration de la cavité. Cependant, une cavité d'amélioration nécessite un couplage cohérent des impulsions femtosecondes dans la cavité, ce qui est une tâche exigeante. L'approche HHG intra-oscillateur offre un concept simplifié utilisant directement la cavité du laser au lieu d'une cavité d'amélioration externe.

Pour atteindre une puissance d'entrainement suffisamment élevée pour un HHG intra-oscillateur efficace, la technologie TDL existante a dû être améliorée de manière significative et être optimisée pour les performances intra-cavité. Dans le cadre de cette thèse, l'accent a été mis sur le développement du laser d'entrainement et des progrès significatifs ont été réalisés. Dans ce but, nous avons étudié et démontré des oscillateurs TDL à mode verrouillé par lentille de Kerr basés sur le matériau de gain Yb :YAG, qui ont atteint plusieurs records en termes de performance de sortie. Notre système fournit la durée d'impulsion la plus courte de tous les oscillateurs TDL, soit 27 fs, ainsi que la puissance moyenne la plus élevée dans le régime sub-100-fs, soit 100 W, et la puissance de crête la plus élevée, soit 100 MW.

L'augmentation correspondante des performances intra-cavité de notre laser nous a permis d'améliorer considérablement le fonctionnement du HHG en termes de flux de XUV et d'énergie des photons générés. Partant du 0,5 nW généré à 13 eV démontré il y a cinq ans, nous avons amélioré le flux XUV à 10 µW à 30 eV à l'état actuel. Bien que ce ne soit pas encore la meilleure perfor-

mance parmi d'autres systèmes HHG, la valeur du flux est en train de devenir compétitive par rapport aux résultats des cavités d'amélioration fonctionnant à une énergie de photon similaire.

Les performances de sortie améliorées des TDLs démontrées sont également très intéressantes pour la conversion non linéaire vers des longueurs d'onde plus longues du spectre électromagnétique. Une partie de cette thèse est donc consacrée à la génération térahertz. Nous avons démontré la première génération térahertz entrainé par TDL en 2018, par rectification optique dans GaP. Par la suite, nous avons utilisé l'accordabilité et la puissance moyenne élevée de notre oscillateur TDL auto-construit pour étudier expérimentalement en détail les propriétés de la rectification optique dans GaP entrainé par des lasers à base d'Yb de haute puissance à 1 µm. Enfin, forts de l'expérience de la HHG intra-oscillateur, nous avons montré que le laser haute puissance d'entrainement peut être remplacé en entrainant le THz directement à l'intérieur de la cavité d'un petit oscillateur en volume à mode verrouillé par lentille de Kerr.

Contents

List of acronyms

AOM	Acousto-optic modulator
CPA	Chirped pulse amplifier
CW	Continuous-wave
DFG	Difference frequency generation
DPSSL	Diode-pumped solid-state laser
EOS	Electro-optic Sampling
FWHM	Full width at half maximum
GDD	Group delay dispersion
GaP	Gallium phosphide
HA	Hard aperture
HC-PCF	Hollow-core photonic crystal fibers
HHG	High harmonic generation
HR	Highly-reflective
IR	Infrared
KLM	Kerr lens mode-locking
KM	Kerr medium
NLM	Nonlinear mirror mode-locking
NPR	Nonlinear polarization rotation mode-locking
RoC	Radius of curvature
SESAM	Semiconductor saturable absorber mirror
SFG	Sum-frequency generation
SHG	Second-harmonic generation
SPM	Self-phase modulation
TDL	Thin-disk laser
TEM	Transverse electromagnetic modes
THz-TDS	Terahertz time-domain spectroscopy
TPF	Thin-film polarizer
XUV	Extreme ultraviolet
YAG	Yttrium aluminium garnet

Publication list

Articles in peer-reviewed journals:

1. Paradis, C., Drs, J., Modsching, N., Razskazovskaya, O., Meyer, F., Kränkel, C., Saraceno, C. J., Wittwer, V. J. & Südmeyer, T. Broadband terahertz pulse generation driven by an ultrafast thin-disk laser oscillator. *Optics Express* **26**, 26377 (2018).
2. Modsching, N., Drs, J., Fischer, J., Paradis, C., Labaye, F., Gaponenko, M., Kränkel, C., Wittwer, V. J. & Südmeyer, T. Sub-100-fs Kerr lens mode-locked Yb:Lu_2O_3 thin-disk laser oscillator operating at 21 W average power. *Optics Express* **27**, 16111 (2019).
3. Drs, J., Modsching, N., Paradis, C., Kränkel, C., Wittwer, V. J., Razskazovskaya, O. & Südmeyer, T. Optical rectification of ultrafast Yb lasers: pushing power and bandwidth of terahertz generation in GaP. *JOSA B* **36**, 3039 (2019).
4. Fischer, J., Drs, J., Labaye, F., Modsching, N., Wittwer, V. & Südmeyer, T. Intra-oscillator high harmonic generation in a thin-disk laser operating in the 100-fs regime. *Optics Express* **29**, 5833 (2021).
5. Modsching, N., Drs, J., Brochard, P., Fischer, J., Schilt, S., Wittwer, V. J. & Südmeyer, T. High-power dual-comb thin-disk laser oscillator for fast high-resolution spectroscopy. *Optics Express* **29**, 15104 (2021).
6. Hamrouni, M., Drs, J., Modsching, N., Wittwer, V. J., Labaye, F. & Südmeyer, T. Intra-oscillator broadband THz generation in a compact ultrafast diode-pumped solid-state laser. *Optics Express* **29**. Publisher: Optical Society of America, 23729 (2021).
7. Drs, J., Fischer, J., Modsching, N., Labaye, F., Wittwer, V. J. & Südmeyer, T. Sub-30-fs Yb:YAG thin-disk laser oscillator operating in the strongly self-phase modulation broadened regime. *Optics Express* **29**. Publisher: Optical Society of America, 35929 (2021).
8. Fischer, J., Drs, J., Modsching, N., Labaye, F., Wittwer, V. J. & Südmeyer, T. Efficient 100-MW, 100-W, 50-fs-class Yb:YAG thin-disk laser oscillator. *Optics Express* **29**. Publisher: Optical Society of America, 42075 (2021).
9. Drs, J., Fischer, J., Modsching, N., Labaye, F., Müller, M., Wittwer, V. J. & Südmeyer, T. A decade of sub-100-fs thin-disk laser oscillators. Submitted to: Laser & Photonics Reviews (2022).

Conference contributions (first or presenting author):

10. Drs, J., Fischer, J., Modsching, N., Labaye, F., Wittwer, V. J. & Südmeyer, T. *69-W Sub-100-fs Yb: YAG Thin-Disk Laser Oscillator* in *2021 Conference on Lasers and Electro-Optics Europe and European Quantum Electronics Conference (2021)* (Optical Society of America, 2021), ca_7_1.

11. Drs, J., Fischer, J., Labaye, F., Modsching, N., Wittwer, V. J. & Südmeyer, T. *10-μW, 30-eV High Harmonic Generation inside an Yb:YAG Thin-Disk Laser Oscillator* in *Advanced Solid State Lasers (2021)* (Optical Society of America, 2021), ATh3A.2.

12. Drs, J., Modsching, N., Paradis, C., Kränkel, C., Wittwer, V. J., Razskazovskaya, O. & Südmeyer, T. *High-Power 0.33 mW Broadband THz Source Driven by an Ultrafast Yb-based Thin-Disk Laser Oscillator* in *2019 Conference on Lasers and Electro-Optics Europe and European Quantum Electronics Conference (2019)* (Optical Society of America, 2019), cc_6_6.

13. Drs, J., Modsching, N., Paradis, C., Kränkel, C., Wittwer, V. J., Razskazovskaya, O. & Südmeyer, T. *New horizons for high power broadband THz sources driven by ultrafast Yb-based thin-disk laser oscillators* in *Conference on Lasers and Electro-Optics (2019)* (Optical Society of America, 2019), STh3F.5.

14. Drs, J., Fischer, J., Labaye, F., Modsching, N., Wittwer, V. J. & Südmeyer, T. *Recent Progress and Perspectives of High-Harmonic Generation Inside Thin-Disk Laser Oscillators* in *Conference on Lasers and Electro-Optics (2021)* (Optical Society of America, 2021), SW3Q.7.

15. Drs, J., Fischer, J., Labaye, F., Modsching, N., Kränkel, C., Wittwer, V. J. & Südmeyer, T. *High Harmonic Generation Inside an Ultrafast Kerr-Lens Mode-Locked Thin-Disk Laser Oscillator* in *OSA High-brightness Sources and Light-driven Interactions Congress 2020 (EUVXRAY, HILAS, MICS) (2020)* (Optical Society of America, 2020), EM2A.4.

16. Drs, J., Fischer, J., Modsching, N., Labaye, F., Wittwer, V. J. & Südmeyer, T. *100-W, 100-MW, 50-fs thin-disk laser oscillator based on Yb:YAG* in *EOSAM conference* (European Optical Society, Rom, Italy, 2021), TOM13 S07:1.

17. Paradis, C., Modsching, N., Razskazovskaya, O., Drs, J., Wittwer, V. J., Sudmeyer, T., Meyer, F. & Saraceno, C. J. *Thin-Disk Laser Oscillator Driving THz Generation Up To 6 THz* in *2018 43rd International Conference on Infrared, Millimeter, and Terahertz Waves (IRMMW-THz)* (IEEE, Nagoya, 2018), Tu–P1–1c.

18. Drs, J., Fischer, J., Labaye, F., Modsching, N., Wittwer, V. J. & Südmeyer, T. *High-harmonic generation inside a 100-fs Yb:YAG Kerr-lens mode-locked thin-disk laser oscillator* in *9th EPS-QEOD Europhoton* (2020), Tu_M1.3.

1 Introduction

Being it four years since the beginning of my PhD, it is now time to stop, turn around, and reflect on the gained experience. Physics is an interesting domain. Since the times of Einstein, Bohr, Heisenberg, Schrödinger, Dirac, Pauli, Fermi, Higgs, Born, and Feynman the number of big ground-breaking discoveries has been slowly decreasing. The major physical theories such as general relativity, quantum mechanics and the standard model of the particle physics have long remained unchanged, while the physics literature has been exponentially growing together with the number of physicists [1]. The difficult and fundamental questions such as the possibility of unifying all these theories have been already pondered by generations of genius scientists. The probability of an important discovery without a significant technological advantage compared to previous generations is nowadays very low. The recent progress in physics has been, thus, mostly enabled by the slow ongoing progress of the technology. The ever growing energy of particle colliders has finally led to the detection of long predicted Higgs Boson, the increasing sensitivity of laser interferometers has allowed measurements of gravitational waves foreseen already by Einstein, the improving resolution of optical and radio telescopes has allowed for observation of an increasing number of cosmic objects, the growing capacity of super-computers permits to simulate properties of molecular structures as complex as proteins and the stronger energy confinement inside tokamaks might one day allow for positive net energy obtained from nuclear fusion after decades of development. It has been, thus, clearly the technological progress which has been pushing the frontiers of physics and this thesis is no exception to this trend. The main motivation of this work was driving high harmonic generation (HHG) directly inside the cavity of a mode-locked thin-disk laser (TDL) oscillator. Although this approach is relatively new, first demonstrated only one year before the beginning of my thesis, mode-locked TDL oscillators have been around since more than two decades, while HHG has been known since the 1960s. The key challenge was improving the performance of these lasers in order to efficiently drive the peak-power-hungry HHG.

Improving the laser performance has been, however, the main goal in the TDL oscillator domain since the last 20 years. Assuming an average duration of a PhD thesis to be 4 years, I would call myself a fifth generation PhD student

working on this topic. Given the number of PhD theses written on the subject, I don't find necessary to repeat the well-established theory, which can be found in many articles and thesis introductions. Instead, I will compose this thesis in a cumulative format based on the published peer-reviewed journal articles. The main introduction and overview of the current state-of-the-art will be provided by a recently submitted review article entitled "A decade of sub-100-fs thin-disk laser oscillators".

References

1. Sinatra, R., Deville, P., Szell, M., Wang, D. & Barabási, A.-L. A century of physics. *Nature Phys* **11**, 791 (2015).

A decade of sub-100-fs thin-disk laser oscillators

Jakub Drs, Julian Fischer, Norbert Modsching, François Labaye, Michael Müller, Valentin J. Wittwer, Thomas Südmeyer*

Laboratoire Temps-Fréquence (LTF), Institut de Physique, Université de Neuchâtel, Avenue de Bellevaux 51, 2000 Neuchâtel, Switzerland
E-mail: jakub.drs@unine.ch

Keywords: thin-disk laser, Kerr-lens mode-locking, SESAM mode-locking, high harmonic generation

Abstract

Thin-disk lasers (TDL) are best known for their high-power continuous-wave industrial applications. Nonetheless, the thin-disk geometry is also highly attractive for ultrafast laser oscillators. The short propagation distance and large beam diameter inside the gain crystal allows for very low induced nonlinearity, low dispersion, and extreme peak powers inside the laser cavity. The path toward TDL oscillators directly delivering high average power at ultrafast pulse duration required for many scientific applications has, however, been tangled and is still ongoing. A decade ago, the first sub-100-fs laser oscillator was demonstrated, initiating the pursuit of even shorter pulses. Since then, many gain materials have been investigated in the thin-disk geometry as well as various mode-locking mechanisms for their suitability for efficient short-pulse operation. In this review, we will discuss the fast-evolving development trends of TDL oscillators, as well as their scientific applications, and prospects.

1. Introduction

The thin-disk laser (TDL) concept, first demonstrated in 1993 [1], has been designed and optimized for most efficient cooling of the laser gain material while maximizing the beam size inside the gain crystal. This endowed the TDL technology with a unique suitability for high-power applications. A single thin-disk gain crystal with a ~100-µm thickness can provide several kilowatts of average power [2] and withstand many gigawatts of peak power [3]. The small thickness of the disk directly contacted onto a very good heat sink, nowadays diamond in most systems, results in a very uniform single-dimensional heat flow inside the disk, minimizing the induced thermal lens [1]. In addition, the very short interaction length in the crystal keeps the dispersive and nonlinear response of the gain medium at a very low level, benefitting ultrafast operation.

The most common use of TDLs are high-power continuous-wave (CW) industrial lasers. Here, the thin-disk geometry allows to efficiently convert the high average power of low-brightness laser diodes into a high-brightness laser beam suitable for remote welding and cutting applications [4–6]. The vast use in industrial applications have led to the development of highly efficient multi-pass pumping solutions. Pumping TDL heads with up to 72-passes through the disk are nowadays commercially available, allowing for nearly 100% absorption of the pump power inside the gain crystal. Similarly, the production of high-quality industrial-grade Yb:YAG disks has been optimized to near perfection.

These developments later also benefitted pulsed operation of TDLs. Most notably, multi-pass and regenerative amplifiers have reached tremendous success, both industrially and scientifically. Up to 1.9 kW of average power in 1.3-ps pulses have been demonstrated from a multi-pass TDL amplifier [3] as well as 200 mJ in 1-ps pulses and 1 kW of average power out of a regenerative amplifier [7].

However, due to the narrow gain bandwidth of Yb:YAG disks, the pulse duration of these amplifier systems is typically limited to ~200 fs. Shorter pulses can be achieved by operating TDLs as high-power mode-locked laser oscillators. Thanks to the soliton mode-locking, TDL oscillators can reach significantly shorter pulse durations than Yb-based laser amplifier systems. In addition, ultrafast TDL oscillators typically emit nearly transform-limited soliton pulses with clean sech^2 spectrum in an excellent transverse-mode TEM_{00} Gaussian beam.

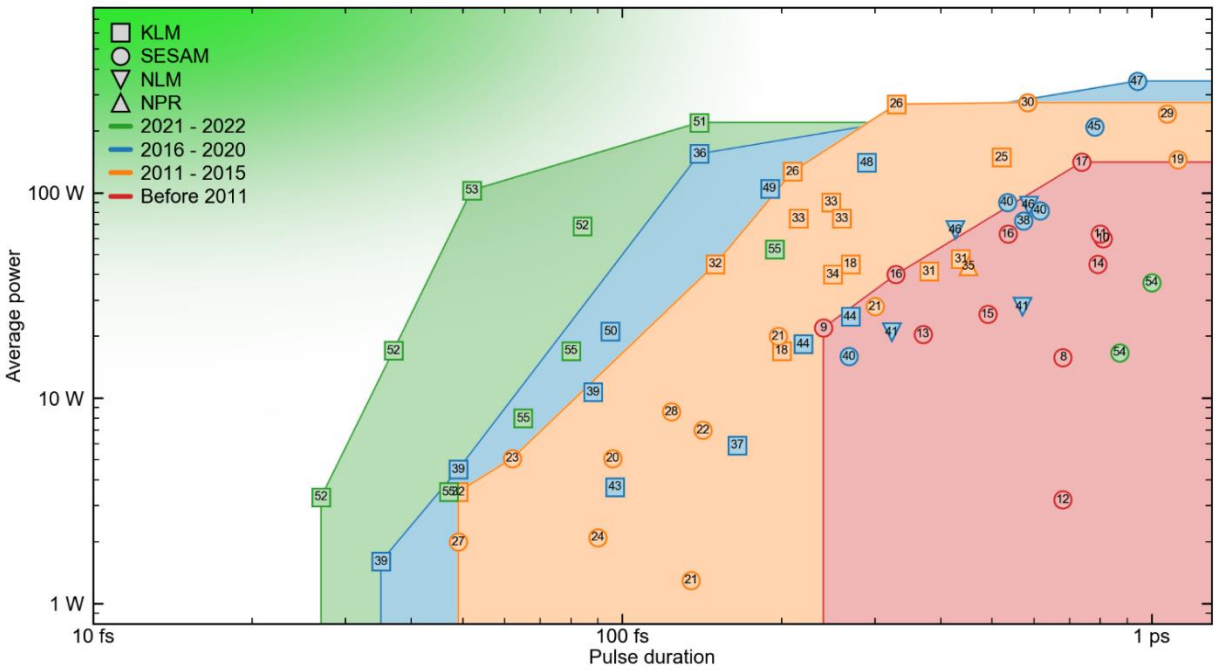

Figure 1. Overview of state-of-the-art TDL oscillators operating with > 1 W of average power and sub-picosecond pulse duration. The markers depict the mode-locking scheme: KLM – Kerr-lens mode-locking, SESAM – semiconductor saturable absorber mirror mode-locking, NLM – nonlinear mirror mode-locking, NPR – nonlinear polarization rotation mode-locking. The color scheme shows the historical evolution of the technology, categorizing the individual results into several time frames. A trade-off between average power and pulse duration can be observed within each time frame, which is moving over time toward the green-shaded corner indicating the desired parameter range. The numbers in the markers correspond to references [8–55].

Development of mode-locked TDL oscillators, thus, became an important research direction aiming for obtaining ultrafast pulses from Yb-doped gain materials at tens to hundreds of watts of average power and megahertz repetition rates. In Fig. 1, we show a historical overview of state-of-the-art TDL oscillators in terms of pulse duration and average output power. The color scheme together with the colored polygons categorize the results into several time frames revealing a trade-off between achievable pulse duration and average power within each time frame. During the first decade of development indicated in red, TDL oscillators strongly increased their average power starting from initial 16 W [8] up to 141 W [17] and reached pulse durations as short as 240 fs [9]. In 2012, the first sub-100-fs TDL oscillator was demonstrated [20] triggering the pursuit of even shorter pulses. Within the following decade the frontier of achievable performance shown by the colored polygons has been pushed strongly into the sub-100-fs domain. This transition was allowed by using broadband Yb-doped gain materials as well as by the transition from semiconductor saturable absorber mirror (SESAM) mode-locking to Kerr-lens mode-locking (KLM). Interestingly, a very large step in this direction has been made only since 2021 as could be seen from the green markers. The strive towards short pulse duration at high-power levels is still a highly active research direction and will most likely enable many research and industrial

breakthroughs. In this paper, we will discuss in detail this progress into the sub-100-fs domain and identify the current trends and prospects of the technology.

We will start with a discussion on the gain materials for ultrafast TDLs in section 2. Initially, it appeared mandatory to switch to more broadband gain materials than Yb:YAG in order to progress into the sub-100-fs regime [56]. Numerous materials were evaluated and optimized in the thin-disk geometry, which will be discussed. Over time it turned out that in high-power ultrafast TDLs the mode-locking method is more important than initially considered, which will be discussed in section 3. Surprisingly, it has been shown that efficient ultrafast operation can be also achieved with Yb:YAG in KLM TDL oscillators. In section 4, we will focus on nonlinear pulse compression, where the clean sech^2 optical spectrum and beam quality of TDL oscillators provides an ideal starting point for reaching few-cycle pulses. In section 5, we will review the methods of carrier-envelope-offset stabilization of these lasers, which is a necessary ingredient for frequency comb and attosecond science applications. Finally, these lasers have been successfully used for further nonlinear conversion toward longer wavelengths for field-resolved mid-infrared (MIR) [57] and terahertz [58–62] spectroscopy applications or toward shorter wavelengths through high harmonic generation (HHG) [63]. The high average power from the laser oscillator has been also harnessed by single-cavity dual-comb systems [64,65]. Another very important potential of TDL oscillators is driving nonlinear processes at extremely high intensities directly inside the laser cavity such as intra-oscillator HHG [66–68]. In section 6 we provide a quick overview on those application areas for sub-100-fs TDLs.

2. Gain materials

After the first demonstration of a mode-locked TDL oscillator in 2000 based on Yb:YAG and SESAM mode-locking [8], one development direction soon oriented toward shorter pulses. The evolution of the shortest achieved pulse duration with respect to mode-locking scheme and gain materials is depicted in Fig. 2. During the first decade of development, mode-locked TDL oscillators have been enabled by SESAM technology. The initial studies showed that decreasing the pulse duration of SESAM mode-locked Yb:YAG TDL oscillators is very difficult due to the narrow gain bandwidth of Yb:YAG. This can be also seen in the Fig. 2 from the green circle markers, which show that the pulse duration of these lasers has decreased only marginally since the first demonstration. The focus was therefore put on mode-locking studies using more broadband Yb-doped gain materials. Already in 2002, the pulse duration dropped from the initial 730 fs [8] down to 240 fs using an Yb:KYW disk [9].

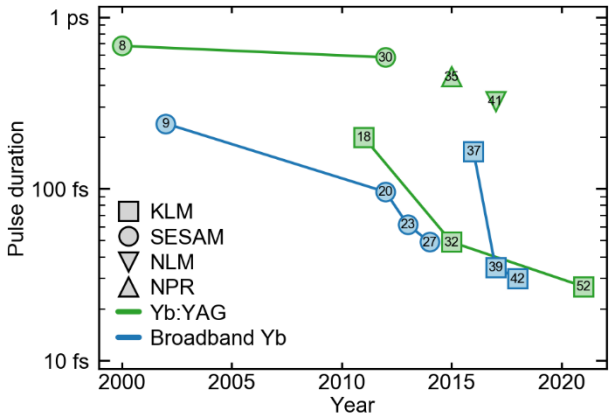

Figure 2. Historical evolution of the shortest pulse duration achieved by TDL oscillators. The markers depict the mode-locking scheme, while the color code differentiates between Yb:YAG and other more broadband Yb-doped host materials. SESAM mode-locked lasers have achieved short-pulse operation only with broadband gain materials, whereas KLM laser can reach the short pulses also with Yb:YAG.

The direction toward even shorter pulses was outlined in 2009 in a detailed review article highlighting the challenges and necessary steps for TDL oscillators operating in the sub-100-fs regime [56]. The first TDL oscillator which reached the 100-fs milestone was demonstrated three years later in 2012 using Yb:LuScO as gain medium and an optimized fast-recovery-time SESAM [20]. Many other gain materials have been utilized in the thin-disk geometry in order to allow for efficient short-pulse operation including Yb:KLuW [15], Yb:CALGO [21,23,24,27,42], Yb:LuO [13,16,17,22,39,40,50], Yb:ScO [28], and Yb:LuScO [20], as shown in Fig. 3. Another development direction of TDL oscillators leads toward operation at longer wavelength of 2 µm based on Ho:YAG [44,54]. The 2-µm TDLs have been recently reviewed in detail in [69] and will not be discussed further in the context of this review.

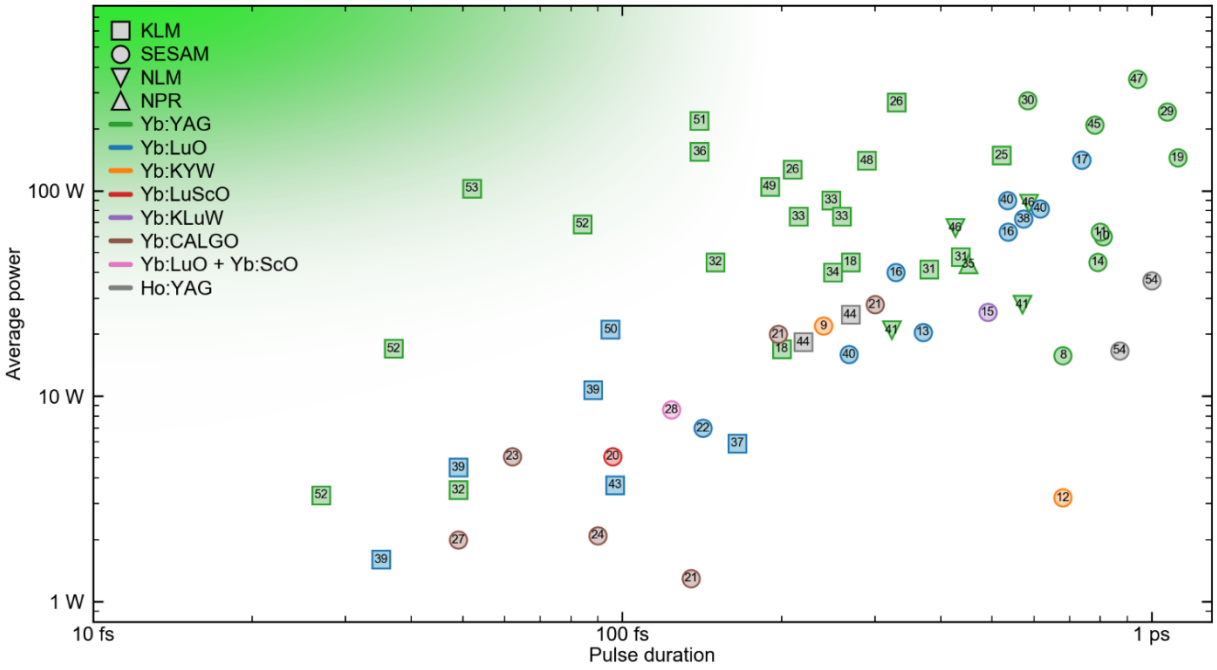

Figure 3. Overview of average power and pulse duration of TDL oscillators with respect to the gain materials used, depicted by the color scheme. The green-shaded corner shows the desired parameter range.

A great challenge for gain materials in the thin-disk geometry is not only the gain bandwidth but equally important the thermal properties, achievable doping concentration, and homogeneity. A high thermal conductivity is required for efficient heat removal and reduced thermal lensing. A high homogeneity in terms of thermo-mechanical and optical properties over the disk is a necessary ingredient for efficient operation in TEM_{00} mode.

Among all tested gain materials shown in Fig. 3, we will focus on the most abundant ones of Yb:YAG, Yb:LuO, and Yb:CALGO, which also form a good representative sample of the Yb-doped family in terms of performance trade-offs and technical challenges. The first and also by far the most used material in the thin-disk geometry has been Yb:YAG. It was selected as an industrial standard for high-power CW applications and optimized to a great degree for the thin-disk geometry in terms of crystal growth quality, doping concentration, thermal properties, and bonding procedure. It features a relatively narrow gain bandwidth of 8-nm full-width at half maximum (FWHM), shown in Fig. 4. The thermal conductivity amounts to 11 W m^{-1} K^{-1}, which however drops for high doping concentrations down to 7 W m^{-1} K^{-1} [70]. The crystal can be optically pumped at wavelengths around 940 nm or 969 nm.

Yb:LuO was introduced to the TDL family in 2001 as the most promising representative of Yb-doped sesquioxides and a potential successor of Yb:YAG for shorter pulse durations [71]. It features a broader gain bandwidth of ~13 nm (Fig. 4.) and slightly higher thermal conductivity of 12.8 W m^{-1} K^{-1} compared to Yb:YAG. Thanks to the very close weight ratio between lutetium and ytterbium, Yb:LuO allows for higher doping concentrations than Yb:YAG without compromising the thermal conductivity

of the gain crystal [70]. Initial studies characterizing Yb:LuO disks also showed unprecedented multimode slope efficiencies, exceeding 80% with > 70% of optical-to-optical efficiency in CW operation [70,72]. In mode-locked operation, also very promising initial results were demonstrated, reaching 141 W of average power in 738 fs pulses and 40% optical-to-optical efficiency [17].

These first results and the remarkable properties of Yb:LuO have motivated many further mode-locking studies with this material [13,16,17,22,39,40,50], as shown in Fig. 3. However, despite the theoretical advantage of Yb:LuO, up to nowadays, these lasers have not yet managed to outperform the ones based on Yb:YAG, as can be clearly seen in Fig. 3. This rather surprising outcome can be mostly attributed to the great difficulty of growing Yb:LuO crystals connected to its high melting point of ~2500°C [73]. This temperature exceeds the capabilities of the commonly used iridium crucibles. Rhenium is the only suitable material sustaining such temperatures and allowing for the use of the Czochralski growth method. Unfortunately, the production of rhenium crucibles is very costly and time consuming, since it involves galvanic deposition of the material. This technical difficulty has resulted in only few growth attempts of Yb:LuO crystals for thin disk laser applications, which have not yet allowed to reach a comparable level of optimization as for Yb:YAG.

A promising approach towards further development in this direction is based on compositions of Lu_2O_3 with other sesquioxides such as Sc_2O_3 and Y_2O_3, which have significantly lower melting temperatures. Recently, the first high-quality mixed sesquioxides crystal has been grown by conventional Czochralski method using an iridium crucible [74]. This approach might allow for a new generation of Yb-doped sesquioxide crystals with suitable properties for the thin-disk geometry in the near future [75].

Yb:CALGO is another notable gain material for TDLs. It offers a very broad gain bandwidth with > 60 nm FWHM (Fig. 4). In principle, such bandwidth should support ~20 fs pulse durations without requiring any further nonlinear spectral broadening effects. Its thermal conductivity of 6.3 W m^{-1} K^{-1} is lower than for Yb:YAG, but still sufficiently high for the use in TDLs. The first CW Yb:CALGO TDL oscillator was demonstrated in 2011 and showed a 40% slope efficiency with 32% optical-to-optical efficiency [76]. A SESAM mode-locked version followed already in 2012 [21]. The laser was operated in three configurations, delivering 28 W with 300 fs pulses, 20 W with 200 fs, and 1.3 W with 135 fs, respectively. Later studies showed even shorter pulse durations of 62 fs and 49 fs using SESAM mode-locking [23,27] and 30 fs using a KLM TDL oscillator [42]. All these short-pulse lasers, however, operated at rather low average powers for TDLs of < 6 W.

In contrast to the TDL results, Yb:CALGO lasers have proven to be very successful in the bulk geometry, where they even outperform their thin-disk counterparts. In CW operation, slope efficiencies of 73% with optical-to-optical efficiencies up to 65% have been demonstrated [77]. In mode-locked operation, up to 12.5 W has been obtained from a 94-fs laser oscillator with 20% optical-to-optical efficiency [78]. Shorter pulse durations of 22 and 31 fs at average powers of 0.7 W and 1.6 W have been shown using another Yb:CALGO bulk oscillator [79]. The bottleneck hindering the efficient operation of Yb:CALGO lasers in the thin-disk geometry seems to be again connected

to the crystal growth quality. So far, the distorted crystalline structure of Yb:CALGO has not provided sufficiently homogeneous gain over the disk surface [23,27,42], which prevents efficient operation in the fundamental TEM_{00} mode and limits the performance in mode-locked operation.

Up to nowadays, the production of high-quality thin disks comes at a great effort and has been difficult to achieve outside of an industrial environment. It can be also noticed, that several research groups have been recently returning back to Yb:YAG [47,49,53]. The commercial availability and the suitability for high average powers seem to outweigh the narrower gain bandwidth. Moreover, with the recent progress of Kerr-lens mode-locked TDL oscillators, it has been shown that the narrow gain bandwidth can be compensated by the self-phase modulation (SPM) inside the laser [32,39,52], as will be discussed in the next section. Recently, the shortest pulse durations achieved with Yb:LuO and Yb:CALGO TDL oscillators have been even surpassed by an Yb:YAG laser [52]. We, thus, expect that Yb:YAG will continue to dominate the realm of 1-µm TDL oscillators also in the next years.

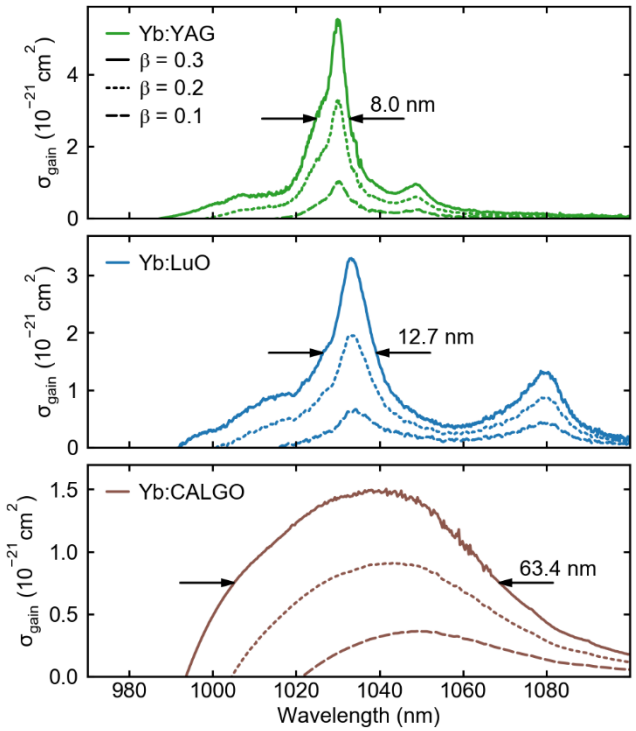

Figure 4. Gain cross-section of Yb:YAG, Yb:LuO and Yb:CALGO which are the three most commonly used gain materials in thin-disk lasers. The gain cross sections, σ_{gain}, are calculated from the emission and absorption cross sections as $\sigma_{gain} = \beta \cdot \sigma_{emission} - (1 - \beta) \cdot \sigma_{absorption}$, for the inversion levels of $\beta = 0.1$, 0.2, and 0.3. The underlying data was obtained from [56,77].

3. Mode-locking mechanisms

Nearly every ultrafast TDL oscillator operates in the soliton mode-locked regime yielding high-contrast soliton pulses without pre- or post-temporal features, typically at very good transverse beam quality with M^2 values < 1.1. TDLs are known to be power-scalable, meaning that the average power can be scaled by increasing the pumped surface of the disk and adapting the cavity to adjust the laser mode. This power-scaling principle is easily applicable in CW operation of these lasers, where the average power has been pushed toward the 10-kW levels. In mode-locked operation, the bottleneck is often the mode-locking mechanism itself, which needs to withstand the high peak and average powers, while providing sufficient self-amplitude modulation for soliton mode-locking. Various trade-offs are typically involved in the design of these lasers including the selection of the mode-locking mechanism in order to meet the desired parameters. The historical evolution of the highest average power with respect to pulse duration is shown in Fig. 5. It can be clearly identified that the technology has been constantly evolving and that both SESAM and KLM lasers have their important role in this evolution.

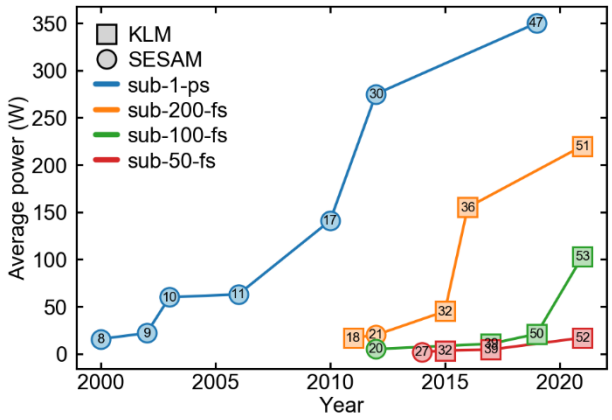

Figure 5. Historical evolution of the highest average power achieved by mode-locked TDL oscillators. SESAM mode-locked lasers depicted by circles dominate the long pulse duration category, whereas KLM lasers depicted by squares excel in shorter pulse durations.

3.1. SESAM mode-locking

SESAM mode-locked TDLs have opened up the possibility of obtaining tens to hundreds of watts directly from a laser oscillator, while also offering the favorable self-starting operation. Initial designs of SESAMs were originally inspired by saturable absorbers used for all-optical switches based on InGaAs/GaAs quantum wells grown on AlAs/GaAs dielectric Bragg reflector mirror [80,81]. But since the first demonstration, the technology has been constantly evolving and experiencing strong improvements [40,82–85].

There are various requirements for SESAMs operating inside high-power TDL oscillators. They need to provide sufficient modulation depth, typically around 1%, for stable mode-locking, while featuring fast recovery time for short-pulse operation. For reaching high average power and high pulse energies inside the oscillator, low non-saturable losses and high damage threshold as well as a reflectivity rollover shifted

towards highest fluences are essential. Since some residual losses always occur in the SESAM, efficient heat removal is also of high importance to prevent thermal lensing.

As these parameters have been improving, SESAM mode-locked TDLs have been continuously pushing the frontier of high-power laser oscillators, as can be seen in Fig. 5. The hundred-watt-level was reached in 2010 using Yb:LuO gain material [17]. In 2012, this level has been pushed to 275 W [30] and in 2019, 350 W was demonstrated using Yb:YAG [47].

On the other hand, decreasing the pulse duration of SESAM mode-locked TDLs has been much more challenging. Due to the moderate modulation depth of only few percent, SESAM mode-locked TDLs require broadband gain materials to reach short pulse durations. Further, the requirement of a short recovery time typically comes at a trade-off with other SESAM parameters required for high-power operation, such as damage threshold or rollover fluence [40,84]. Thus, in shorter pulse durations below 200 fs, SESAM mode-locked TDLs have not allowed for high average power, so far. Nevertheless, at lower powers below 10 W, shorter pulse duration has been achieved. For instance the first sub-100-fs TDL oscillator was based on SESAM mode-locking [20], and a pulse duration as short as 49 fs has been demonstrated using Yb:CALGO [27].

3.2. Nonlinear polarization rotation mode-locking

The concept of nonlinear polarization rotation (NPR), commonly utilized in fiber-based laser oscillators, has been demonstrated inside a TDL oscillator in 2015 [35].
Here, the nonlinear polarization rotation was induced by a phase-mismatched second harmonic generation in an LBO nonlinear crystal. The study used two nonlinear crystals at orthogonal orientation with 20-mm and 19-mm lengths, where the effective propagation length corresponds to the difference between both crystals. This allowed for a long interaction length inside the crystal for strong polarization rotation while maintaining broadband properties. The mode-locked laser emitted 44 W of average power with ~500 fs pulse duration. Although this more exotic mode-locking mechanism offers some theoretical advantages compared to the SESAM mode-locking, such as no absorptive losses and instantaneous response of the second order nonlinear process, the required propagation trough centimeter-long nonlinear crystals would likely prevent significant power-scaling or decrease of pulse duration.

3.3. Nonlinear mirror mode-locking

Another mode-locking scheme aiming to reduce the pulse duration of TDL oscillators is frequency-doubling nonlinear mirror mode-locking (NLM). In this scheme, the saturable losses are formed by an intracavity second harmonic nonlinear crystal followed by a spectrally tailored output coupler, having partial reflection for the fundamental wavelength but full reflection at the second harmonic wavelength. This way, the low intensity light passes through the nonlinear crystal without significant second harmonic conversion and experiences a partial transmission on the output coupler. In contrast, the high intensity light is partially transferred to the second harmonic which experiences complete reflection on the output coupler. On the way back through the nonlinear crystal, the second harmonic light is back-converted to the fundamental wavelength through optical parametric amplification.

The NLM concept has been first applied to a TDL oscillator in 2017 [41]. Compared to the bulk oscillators operating with NLM, the TDL oscillators are much more promising candidates for this technique. Thanks to the high peak intensities inside TDL cavities, it is possible to use much shorter nonlinear crystals and thus increase the mode-locking bandwidth and reach shorter pulse durations. The first NLM mode-locked TDL oscillator has reached 323 fs pulse duration at 21 W of average power using a 0.5-mm long BBO crystal. In a later study, the authors combined the NLM with SESAM mode-locking, reaching more than three times higher average power of 66 W with 426 fs pulses in a self-starting laser operation [46].

3.4. Kerr-lens mode-locking

The most commonly used approach for reaching shortest pulses is Kerr-lens mode-locking (KLM). Accidently discovered in 1990 [86] together with the novel Ti:sapphire gain material [87], KLM has revolutionized the ultrafast world. Conventionally, KLM lasers utilize the naturally occurring self-focusing inside the gain crystal, which leads to better pump overlap for high intensity light, so called soft-aperture mode-locking. The same effect can be used in combination with a physical hard aperture inside the laser, so called hard-aperture mode-locking. Here, the self-focused high-intensity light passes better through the aperture and experiences lower losses. The instantaneous effect of the Kerr lens together with high reachable modulation losses allow for the shortest pulse generation of all mode-locking mechanisms [88].

In TDLs, the large beam size inside the gain material usually does not provide sufficient self-focusing for KLM. For this purpose, an additional Kerr medium is placed close to an intra-cavity focus and a hard aperture is used for KLM. An often-emphasized drawback of KLM lasers is the coupling between the self-amplitude modulation required for the mode-locking and the cavity dynamics, leading toward changing beam size between CW and mode-locked operation. This also makes it difficult to quantitatively characterize the modulation losses inside the laser. The KLM mechanism cannot be easily taken out of the cavity and independently characterized as it is in the case for the SESAM, thus hindering theoretical studies. Another difficulty originates from the requirement of a laser perturbation to initiate the mode-locked operation, since KLM lasers are typically not self-starting. Typically, this is achieved via shaking or moving a cavity mirror. Nevertheless, the short achievable pulse duration and the simple implementation makes this approach very popular.

The first KLM TDL was demonstrated in 2011 [18] and reached a pulse duration of 200 fs at 17 W of average power using Yb:YAG gain material. This was by far the shortest pulse duration achieved by any Yb:YAG TDL oscillator, way below the 680 fs of SESAM mode-locked TDLs [8]. The next demonstration in 2016 has manifested the potential even clearer, showing a 155-W Yb:YAG TDL oscillator delivering 140-fs pulses [36]. The bandwidth of the demonstrated pulses has fully covered the available gain bandwidth of Yb:YAG, suggesting that the optimal operation point in terms of pulse duration for Yb:YAG has been reached.

Several attempts have been made to reach even shorter pulse durations using more broadband gain materials such as Yb:LuO or Yb:CALGO in the KLM TDL

configuration. These lasers have reached very short pulse durations of 35 fs [39], or 30 fs [42], however, at relatively low average powers of 1.5 W and 150 mW, respectively. KLM TDLs typically operate at higher cavity losses compared to SESAM mode-locked ones. This requires sufficient roundtrip gain to cover these losses while maintaining comparably high output coupling rate in order to operate efficiently. Unfortunately, the more broadband gain materials typically provide lower gain compared to Yb:YAG. The roundtrip cavity gain can be increased by implementing several bounces over the disk in order to allow for higher output coupling rates and reach more efficient operation. This has been shown by several studies [26,44,48,50]. However, implementing several passes over the disk also increases the sensitivity of the laser cavity to the thermal lens induced by the disk. So far, the highest power of broadband Yb-doped gain material TDLs in the sub-200-fs category has been limited to ~20 W, utilizing a double pass over an Yb:LuO disk [50].

The so far limited performance of the broadband gain material disks and the narrow gain bandwidth of Yb:YAG hindered power scaling in the sub-100-fs regime for a long time. In 2015, it was shown that by placing several additional Brewster plates inside the cavity, the pulse duration of a KLM Yb:YAG TDL oscillator can be significantly decreased down to 49 fs [32]. The corresponding 23-nm FWHM optical bandwidth by far exceeded the 8 nm gain bandwidth of Yb:YAG. A similar result was shown in 2017, reaching 35-fs pulses using an Yb:LuO disk, exceeding the gain bandwidth by a similar factor [39]. This operation beyond gain bandwidth was allowed by strong SPM inside the laser cavity, which generated the additional frequencies not covered by the gain material. Nevertheless, both these results showed only several watts of average power at a few percent optical-to-optical efficiency. Up to very recently, it was not believed that efficient operation is feasible with the pulse spectral bandwidth exceeding the gain bandwidth.

In spite of these assumptions, two recent studies have shown that the narrow gain bandwidth of Yb:YAG is not as a strongly limiting factor for reaching short pulse durations as originally expected. The first study investigated the limits of decreasing the pulse duration of a KLM Yb:YAG TDL oscillator operating in a strongly SPM-broadened regime [52]. It showed an overall better performance of Yb:YAG in the sub-100-fs regime compared to the more broadband Yb-doped hosts. The higher gain cross-section of Yb:YAG combined with the SPM-broadened regime has outperformed the broadband gain materials both in terms of average power, demonstrating 69 W at 84 fs, as well as in pulse duration, reaching the shortest pulses of any TDL oscillator with a duration of 27 fs at 3.3 W of average power. The second study utilizing the same laser system has pushed the frontier in the sub-100-fs regime even further by demonstrating 100 W of average power at 52 fs pulse duration [53]. Importantly, the latter result was achieved at an optical-to-optical efficiency of 26% which is comparable to the TDL oscillators operating within their gain bandwidth.

These experimental results seem to be enabled by using broadband dispersive mirrors and by operation at high intracavity peak power in the gigawatt range allowed by a vacuum environment. Both these technologies have been, however, long available in the domain and to fully explain this sudden gain in performance, a quantitative simulation will be needed. Nevertheless, these results suggest that further power scaling in the sub-100-fs regime is well within reach, even without development of any new

technology. For instance, a 220-W, 140-fs TDL oscillator operating at 24% efficiency has been recently demonstrated [51] and it seems reasonable to assume that the pulse duration of this laser could be also significantly reduced without compromising the efficiency.

3.5. Comparison of mode-locking schemes

Each of the individually discussed mode-locking schemes has its favored parameter range and different operating conditions. The SESAM mode-locked lasers have been pushing the highest achievable average powers, whereas KLM shines at short pulse durations. For the NPR and NLM, at the current state of development, the performance cannot yet compete with the well-established KLM and SESAM mode-locked TDLs.

One of the crucial parameters for TDL oscillators, as a high-power laser technology, is the optical-to-optical efficiency. Operation at high efficiency is crucial for decreasing the demand on high-power pump diodes while limiting the excessive parasitic heat, which typically causes further problems such as thermal lensing or misalignment. An overview of the achieved optical-to-optical efficiency with respect to pulse duration and average power is shown in Fig. 6. It can be seen that the highest efficiency of up to 40% [17] as well as highest average power has been achieved using SESAM mode-locked TDLs. This is due to the very low non-saturable losses in the range of a few per mil for SESAMs which allows for efficiencies close to the CW operation. The high efficiency together with the high average power of SESAM mode-locked lasers have allowed for significant pulse energies. Up to 80 µJ has been demonstrated at 3 MHz repetition rate and 1-ps pulse duration [29]. However, the long pulse duration puts SESAM mode-locked TDLs in competition with Yb-based laser amplifier systems, which easily outperform them both in terms of average power and pulse energy. Although much shorter pulses have been achieved using SESAM mode-locked TDLs, extending far into the sub-100-fs domain, we assume that several of these lasers could have been SESAM-assisted soft-aperture KLM due to the presence of a Brewster plate for polarization selection and additional SPM, similarly as implemented in [18].

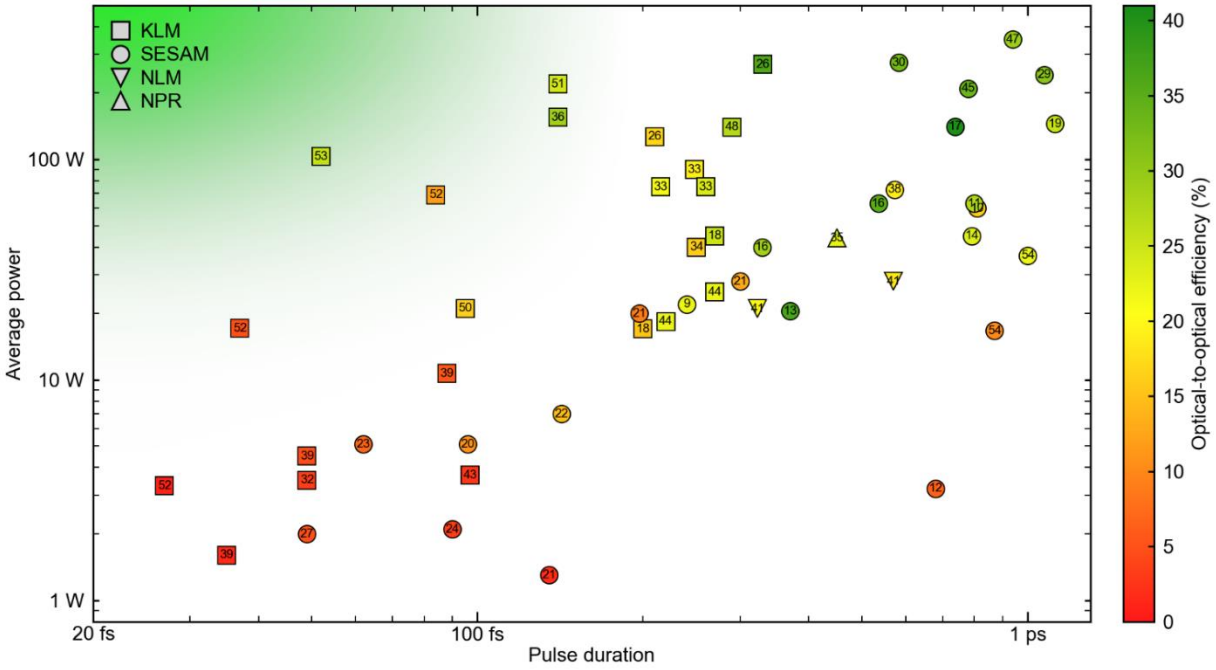

Figure 6. Overview of the optical-to-optical efficiency depicted by color with respect to average power and pulse duration. The highest optical-to-optical efficiencies of ~40% have been typically achieved by SESAM mode-locked lasers at > 500 fs pulse durations. At shorter pulse durations KLM lasers typically offer higher efficiencies than SESAM mode-locked lasers.

In contrast, KLM TDLs typically operate at lower optical-to-optical efficiencies but much shorter pulse durations, which distinguishes them from amplifier systems. As can be seen in Fig. 5, KLM TDLs have completely taken over the sub-100-fs domain since the last decade. The optical-to-optical efficiency of these lasers have been typically ranging between 10% to 30% at > 100 fs pulse durations but dropped significantly in the sub-100-fs domain as shown in Fig. 6. Recently, this limitation has been overcome by the demonstration of a SPM-broadened KLM TDL oscillator delivering 52-fs pulse duration with 26% optical-to-optical efficiency [53]. Thus, it is likely that more efficient TDL oscillators will soon operate in the sub-50-fs domain, which will also allow to increase their average power in this regime.

4. Peak power scaling and pulse compression

One of the most important parameters for many applications is the peak power of the driving laser, which rules the efficiency of many nonlinear processes. TDL oscillators are very interesting for scaling the peak power since the thin-disk gain medium does not pose a strong limitation in this sense. Several studies have investigated scaling of this parameter in TDL oscillators. In SESAM mode-locked lasers, the peak power is mainly determined by the design of the SESAM, mostly through the reflectivity rollover induced by two-photon absorption and by the gain bandwidth of the gain crystal [40]. In KLM TDL oscillators, the intra-cavity peak power has been shown to scale with the beam size inside the Kerr medium [26].

Toward high intra-cavity peak powers, a further challenge arises from the nonlinear response of the air inside the cavity. Several approaches have been proposed to mitigate this issue. The laser can be operated in a low-nonlinearity atmosphere such as helium [11] or the SPM can be canceled using a phase-mismatched second-harmonic crystal [45]. The most frequently employed method is, however, based on operating the laser in a vacuum environment [29–31,36,40,47,52], which also prevents the gas thermal lens induced by the multi-pass pumping scheme [89].

Figure 7 depicts the historical evolution of the highest peak power reached by TDL oscillators. Whereas SESAM mode-locked lasers had been continuously increasing their peak power up to 66 MW demonstrated in 2014 [29], KLM lasers have very rapidly surpassed this value in 2013 [25], three years after their first demonstration, and nowadays reach values of 100 MW [51,53]. It can be also noticed that most of the recent high-peak-power systems are operated in vacuum as indicated by the bell jar symbol around the markers, shown in Fig. 7.

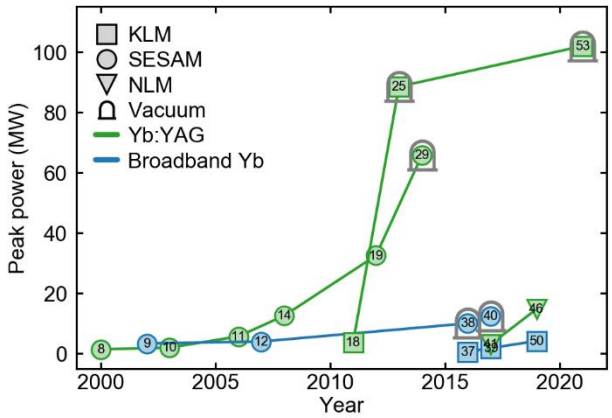

Figure 7. Historical evolution of the highest peak power achieved by TDL oscillators based on different mode-locking mechanisms. The bell jar symbol indicates systems operated in vacuum.

Further increase of the peak power can be achieved by nonlinear pulse compression that relies on SPM to induce spectral broadening. Driving this process in an anomaly dispersive medium can lead to self-compression of the pulse, whereas subsequent chirp removal is required for compression in normal-dispersive media. Both approaches have been pursued in numerous studies that are summarized in Fig. 8. The first compression experiments were based on micro-structured large-mode-area fibers [90,91] and reached ~30 fs pulse duration and 10-MW-level peak power. These were followed by very-large-mode-area rod-type gain fibers [92] generating 50-MW-level peak power and then by gas-filled hollow-core photonic crystal fibers [63,93] surpassing 100 MW peak power levering the scalability of the compression schemes. All experiments showed that the nearly transform-limited soliton pulses and the excellent beam quality of the TDL oscillators allow for high-quality pulse compression. Unfortunately, the average power generally remains limited to several tens of Watts for practical application due to the damage vulnerability of the fiber tips.
More recently, multi-pass cells were employed for nonlinear compression, both in the normal [94] and the net-anomalous dispersive regime [95]. Their high overall

transmission and their robustness against beam pointing instabilities allows for reliable operation at average powers well above the 100 W. The highest demonstrated peak power is close to 170 MW [96] in approximately 30 fs pulses. Compression into the few-cycle regime (≤10 fs at 1 µm) has been demonstrated as well using single- or multi-plate compressors to avoid the need for broadband, dispersion-engineered multi-pass cell mirrors [34,97].

Overall, nonlinearly compressed TDL oscillators generate peak power on the 100 MW-level, which already suffices for many nonlinear applications. Only for the efficient generation of high harmonics the peak power is still about an order of magnitude too low. In the future, this can change with the availability of oscillators directly emitting 100 MW peak power [51,53] combined with nonlinear compression in gas-based multi-pass cells, which support both few-cycle pulses and high average power [98,99].This allows envisioning GW-class sources suitable for high-harmonic generation in near future.

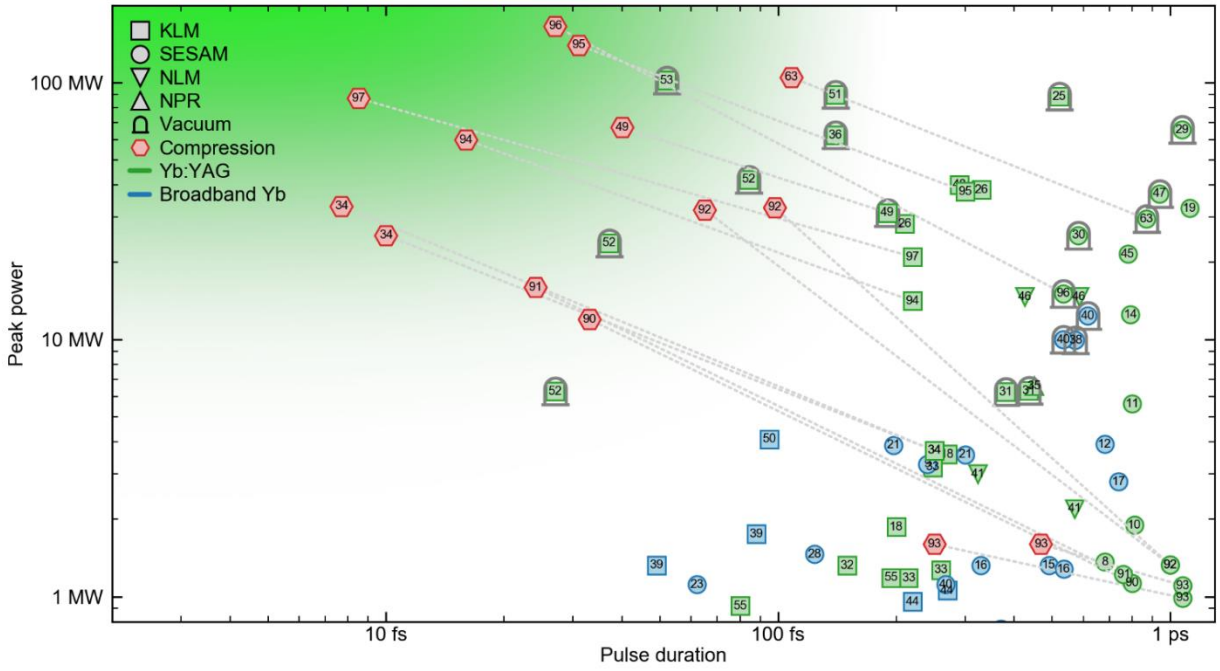

Figure 8. Overview of peak power and pulse duration of state-of-the-art TDL oscillators operating at sub-picosecond pulse duration. The red hexagon markers depict the parameters after nonlinear pulse compression [34,49,63,90–97]. The bell jar symbols indicate systems operated in vacuum. For references [34,97], the peak power was calculated based on the compression ratio, power efficiency and compression efficiency stated in the manuscripts, which is likely an overoptimistic estimate.

5. CEO frequency stabilization

An attractive application field of ultrafast oscillators is precision spectroscopy based on optical frequency combs. Here, the high average power and short pulse duration of TDL oscillators are especially attractive for efficient nonlinear conversion toward mid-infrared or extreme-ultraviolet frequencies, where directly emitting laser sources are not readily available. The key requirement for optical frequency-comb applications is the carrier-envelope offset frequency (f_{CEO}) stability of the source.

The most common way to access the f_{CEO} is using *f*-to-2*f* interferometry after coherent super-continuum generation [100]. Here, the low-frequency part of an octave-spanning optical spectrum is frequency doubled and interfered with the high-frequency part of the fundamental spectrum. The resulting optical beat note provides access to measuring the f_{CEO}. The f_{CEO} is affected by many parameters of the laser such as nonlinearity and dispersion providing wide range of options for an active stabilization. The most common method is modulation of the pump current. However, this method has a limitation for Yb-based lasers given by the long upper-state lifetime of the Yb-ion in the millisecond range. Correspondingly, the response of the f_{CEO} to a pump current modulation is limited to a few kilohertz range in bandwidth. An additional challenge of TDL oscillators compared to bulk lasers is the high amount of acoustical noise introduced by turbulent water cooling of the thin disk [34,65]. The high noise level increases the demand on the bandwidth of the control loop in order to cancel the noise. Many different modulation schemes have been investigated in order to stabilize the f_{CEO} of TDL oscillators which will be discussed in more detail in the following.

5.1. Pump current modulation

Regardless of the bandwidth limitation of the pump current modulation in Yb-based lasers, several studies have utilized this technique for f_{CEO} stabilization in TDL oscillators. The first f_{CEO}-stable TDL oscillator was demonstrated in 2013 [24]. The laser was a SESAM mode-locked Yb:CALGO TDL delivering 2 W of average power in 90-fs pulses. The octave-spanning supercontinuum spectrum was obtained by optical broadening in a highly nonlinear photonic-crystal fiber and the f_{CEO} was detected using a conventional *f*-to-2*f* interferometer. The f_{CEO} lock was implemented using the pump current modulation and resulted in a residual in-loop integrated phase noise of 120 mrad (1 Hz – 1 MHz).

Another challenge for the f_{CEO} stabilization over the pump current is the difficulty to modulate a high-power pump diode which generally involves custom-made electronics. An approach circumventing this issue was demonstrated in 2016, introducing dual wavelength pumping of a KLM Yb:YAG TDL [101]. This concept uses a high-power 940-nm pump diode for pumping the laser combined with a low-power 969-nm diode for fast f_{CEO} modulation. The difference in wavelength allows for applying a simple dichroic mirror to combine both pump beams. The octave-spanning supercontinuum spectrum was obtained by first compressing the 250-fs pulses down to 20-25 fs pulses in a large mode area fiber followed by multiple bounces on chirped mirrors and then further optical broadening in an all-normal-dispersion fiber and the f_{CEO} was detected using a conventional *f*-to-2*f* interferometer. The achieved residual in-loop integrated phase noise amounted to 390 mrad (1 Hz – 500 kHz) at 250 fs pulse duration and 45 W of average power.

A third demonstration of f_{CEO} stabilization modulating the pump current has been demonstrated for a KLM Yb:LuO TDL oscillator operating in a strongly SPM-broadened regime [102]. The laser generated 50-fs pulses at 4.4 W of average power and the f_{CEO} current-based lock resulted in a residual in-loop integrated phase noise of 197 mrad (1 Hz – 1 MHz). Also, in this result, the short pulse duration allowed to directly generate the coherent octave-spanning supercontinuum spectrum in a highly

nonlinear photonic-crystal fiber to detect the f_{CEO} using a conventional f-to-2f interferometer.

5.2. Intracavity AOM

A different approach to act on the f_{CEO} is based on modulating the intracavity losses. This can be achieved by placing an acousto-optic modulator (AOM) directly inside the cavity of the laser, as first demonstrated in 2015 [34]. This remarkable study utilized a nonlinearly compressed KLM TDL oscillator reaching a pulse duration of 7.7 fs at 6 W of average power. The AOM inside the cavity was capable of inducing up to 2% of losses, withstanding the average intracavity power of 280 W. The resulting residual in-loop integrated phase noise amounted to 180 mrad (1 Hz – 1 MHz). The out-of-loop measurement was also implemented in this work, revealing a value of 270 mrad, showing the importance of the out-of-loop measurement. The concept has been further scaled toward 100-W level in 2019, demonstrating 40-fs nonlinearly-compressed pulses at 105 W of average power and residual in-loop integrated phase noise of 90 mrad [49].

5.3. Depletion control

The most recently published method of f_{CEO} stabilization of a TDL oscillator is based on controlling the depletion of the gain through bouncing part of the laser output beam back over the disk [103]. The fraction of the laser output was controlled by an AOM and bounced 4 times over the disk depleting part of the available gain for the laser. This method is similar in its principle to pump current modulation and a similar control bandwidth can be expected. In this first study, the high free-running noise of the laser oscillator only allowed for a comparably poor stabilization with a residual integrated phase noise amounting to 1.5 rad (100 Hz to 500 kHz).

6. Applications

Over the last decade TDL oscillators have not only gained significant performance, but also reached sufficiently mature state of development to become driving sources for further experiments and applications.

6.1. High harmonic generation

One of the first applications of TDL oscillators clearly manifesting the importance of high repetition rate and short pulse duration was nonlinear conversion toward extreme ultraviolet (XUV) through high harmonic generation (HHG) in a noble gas target. Many applications such as photoelectron spectroscopy or XUV diffractive imaging have been relying on coherent XUV radiation delivered by large scale synchrotron facilities. HHG in a noble gas target is a lab-scale alternative which is constantly growing in popularity and finding more and more applications [104]. Historically, the biggest challenge of HHG systems has been the low conversion efficiency from the driving laser to the XUV light. The efficiency strongly increases with the peak power of the driving laser, while also benefiting from short pulse durations. Thus, HHG systems have been often driven by kilohertz-repetition-rate Ti:sapphire laser amplifiers. Unfortunately, some experiments such as photoelectron spectroscopy suffer from space-charge effects, meaning that when multiple photoelectrons are ejected by an XUV pulse from the sample, their trajectories are affected by their mutual coulomb interaction which limits the measurement resolution. In this case, lower-energy pulses emitting only a few

electrons at higher repetition rates are favored in order to maximize the resolution while allowing for short acquisition times. Regardless of space charge effects, the higher repetition rate is often useful for increasing the photon flux of these systems, benefiting most of the XUV applications. Compared to systems based on Ti:sapphire, Yb-based lasers are able to reach considerably higher average powers due to their lower quantum defect and well-developed high-power pump diodes. Hence, Yb-based lasers are much better suited for reaching the HHG required pulse energies at high repetition rates, enabling the transition from kilohertz- to megahertz-repetition rate HHG systems.

The first TDL driven HHG source was presented in 2015, based on a 70-W, 780-fs SESAM mode-locked oscillator operating at 2.4 MHz [63]. The laser output was nonlinearly compressed in a krypton filled HC-PCF fiber to 105 fs at 105 MW of peak power. HHG was obtained from a xenon gas target and reached photon energies up to 30 eV with an extracted XUV flux in a single harmonic of 0.18 nW. These were, however, rather modest values which have been surpassed by orders of magnitude by high-power Yb-based laser amplifier systems [105].

In the recent years, a new avenue for TDL oscillators has been opening up in the XUV realm. With the increasing capabilities of nonlinear pulse compression combined with the decreasing pulse duration of high average power KLM oscillators, there is a potential that these sources will reach single-cycle pulse duration in the near future. This would allow for generation of isolated attosecond pulses at megahertz repetition rates. Such a megahertz-rate isolated attosecond pulse source would highly benefit many applications in the attosecond domain, in particular attosecond streaking experiments [106]. Recently several major steps have been made in this direction. The demonstration of CEO stabilization of a 100-W class TDL oscillator [49] followed by another 100-MW class oscillator directly emitting 50-fs pulses [53] is highly promising. Especially, in combination with the advances in multi-pass cell bulk compression schemes, which have been routinely reaching sub-30-fs pulses at these power levels [94,96] and most recently even 8.5 fs [97]. Combining these recent results will likely provide a CEO-stable single-cycle 100-W-class laser source capable of generating isolated attosecond pulses at megahertz repetition rates.

6.2. Intra-oscillator high harmonic generation

A high potential of TDL oscillators is driving extreme nonlinear processes such as HHG directly inside the laser cavity since this enables the utilization of the very high intra-cavity peak powers. This concept is similar in its principle to femtosecond enhancement cavities [104,107]. In both concepts, the unconverted energy of the driving laser pulse is recycled inside the cavity, while increasing the available peak power by the enhancement factor of the cavity. In comparison to femtosecond enhancement cavities, the laser oscillator is a free-running system which does not require active phase lock and coherent coupling of fs-pulses into the enhancement cavity, thus, further simplifying the concept.

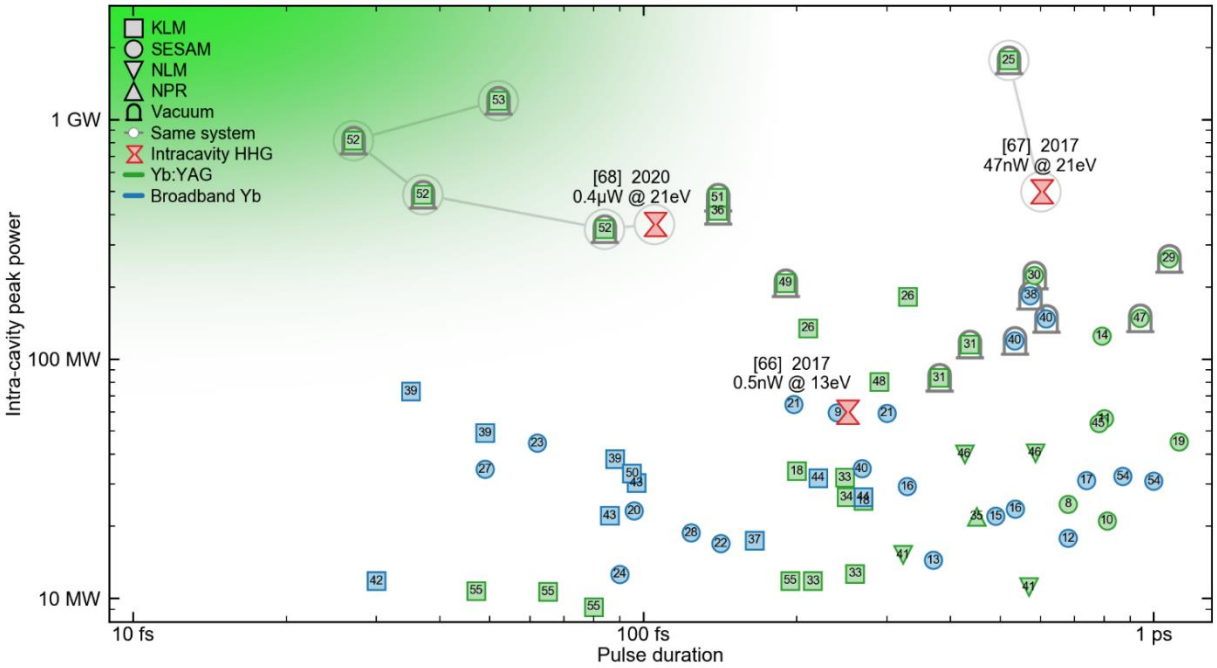

Figure 9. Overview of intracavity peak power with respect to pulse duration of state-of-the-art TDL oscillators operating at sub-picosecond pulse duration. The red hourglass symbols depict intra-oscillator HHG systems [66–68], labeled with the year and the generated XUV flux within the highest harmonic and its photon energy. The bell jar symbols indicate systems operated in vacuum. The gray connecting line indicates laser results, which were obtained with the systems developed for driving intra-oscillator HHG, showing that development of these systems has been also driving the progress in the TDL oscillator technology.

The high peak power and short pulse duration required for efficient HHG [108] makes TDL oscillators ideal candidates for this task. An overview of the intra-cavity peak power with respect to the pulse duration of TDL oscillators including intra-oscillator HHG systems (red hourglass markers) is shown in Fig. 9. The first HHG inside a TDL oscillator was demonstrated in 2017 [66]. The SESAM mode-locked Yb:LuO TDL operated at 320 W of average intra-cavity power, 255 fs pulse duration, and 17.4 MHz repetition rate, corresponding to 64 MW of intra-cavity peak power. The XUV average power generated in xenon was very modest in this first demonstration and amounted to only 0.5 nW in a single harmonic at 13 eV. This first demonstration was closely followed in the same year by a different system based on a KLM Yb:YAG TDL oscillator operating at 500 MW of intra-cavity peak power and 600 fs pulse duration at 3 MHz repetition rate [67]. The intra-oscillator HHG yielded an XUV flux of 47 nW at 21 eV generated in argon. The next intra-oscillator HHG system was published in 2021 [68]. The KLM TDL used Yb:YAG gain material and operated at 365 MW with 105 fs pulse duration at 11 MHz. HHG was driven in argon and the generated XUV photon flux at 30 eV amounted to 0.4 µW. This value has been recently increased to 10 µW by further optimization of the laser system [109].

The connecting line in Fig. 9 indicates the results obtained with the same laser systems developed for intra-oscillator HHG. It can be noticed that even much higher performance has been achieved by these lasers when not driving HHG. This can be attributed to the plasma effects inside the HHG gas target which typically limit the laser performance [68]. Without HHG, intra-cavity peak powers as high as 1.7 GW at 600 fs pulse duration [25] as well as 1.2 GW at 52 fs [53] have been shown, also at substantial output power of 150 W and 100 W, respectively, pushing the frontier of the whole TDL oscillator domain.

6.3. THz generation

The properties of mode-locked TDL oscillators also benefit frequency conversion toward long wavelength in the THz range. This potential has been recognized and discussed in detail in a review article in 2018 [110]. Analogically to HHG, THz generation typically suffer from low conversion efficiency ranging from 10^{-5} up to a few percent. Therefore, increasing the THz power available for the experiment also requires an increase in the driving laser power. In addition to the high average power, the short pulse duration of TDL oscillators provides a broad optical spectrum in the THz domain relevant for broadband spectroscopy applications.

Optical rectification in nonlinear crystals is particularly suitable for this purpose since it supports the high average powers delivered by TDLs. The first THz generation driven by a mode-locked TDL was published in 2018 [58]. The original demonstration used one of the simplest approaches of optical rectification in GaP in a collinear geometry. The generated THz radiation featured a broad spectrum extending up to 7 THz with an average power around 10 μW. The same concept has been power-scaled to 300 μW in 2019 [59] and to 1.3 mW later the same year [60]. In a narrowband regime, average terahertz power has been increased even further. Up to 66 mW was generated in lithium niobate driven by a TDL oscillator [61].

6.4. Dual-comb oscillators

Dual-comb spectroscopy is an extremely powerful tool for applications simultaneously requiring fast acquisition time and high spectral resolution [111]. Conventionally, the technology requires two optical frequency combs with slightly different line spacing, such as two fully stabilized mode-locked lasers operating at slightly different repetition rates. The spectroscopic information is obtained through heterodyne beating between the two combs.

A simplified alternative to fully-stabilized lasers is based on generating the two optical frequency combs from the same laser cavity in a free-running operation. Here, the noise of the unstabilized f_{CEO} and repetition rate of the two pulse trains is highly correlated and the common part of the noise cancels out in the beating process. This allows for short-term measurements within a time frame where the two pulse trains remain mutually stable, without the requirement for active stabilization. TDL oscillators are promising sources for this purpose since their high peak power allows for efficient nonlinear conversion toward MIR or UV wavelengths, which are of high interest for many spectroscopy applications [111,112].

The first steps on this path were made in 2019 [64] by the demonstration of the highest average power dual-comb laser based on a KLM TDL oscillator. The dual-comb cavity was based on splitting both end mirrors while the rest of the cavity components remained shared. The second demonstration of this concept came in 2020 based on polarization splitting [65]. The study showed that the stability of the free-running KLM TDL oscillator is sufficient for performing dual-comb spectroscopy within a 1-ms window in a proof-of-principle experiment measuring the absorption spectrum of acetylene gas. The acquisition time was limited by the uncorrelated noise in the laser mostly originating from water cooling of the disk. Longer acquisition times would likely require the development of a passive cooling of the thin disk. The suitability for high resolution measurements after nonlinear frequency conversion still needs to be demonstrated.

6.5. Field resolved spectroscopy

An advanced application utilizing a TDL oscillator as a driving source building upon the recent advances in this technology is a field-resolved MIR spectroscopy [57], published in 2020. The study uses a nonlinearly compressed TDL oscillator delivering 16 fs pulses at 60 W of average and 28 MHz repetition rate for driving intra-pulse difference frequency generation (DFG) toward MIR. The few-cycle pulse duration of the laser enables detection of the MIR light through electro-optic sampling (EOS) in the time domain, providing information directly about the electric field rather than its intensity. The measurement in the time domain allows for starting the acquisition after the passage of the MIR excitation pulse and sampling only the response of the sample. This endows the field-resolved spectroscopy with unique sensitivity and resolution and also broad tunability in the MIR range. The technology was shown to be highly suitable for fingerprinting of complex molecular ensembles such as human blood serum or in vivo transmission spectroscopy of intact strongly absorptive biological samples such as living cell cultures or even plant leaves. The unprecedented sensitivity and repeatability of the presented experiments proves the suitability of the TDL oscillators for driving demanding applications requiring short pulse durations high average powers and also stable long-term operation.

7. Conclusion

We have reviewed the recent development of ultrafast TDL oscillators. Over the last decade, we have observed a strong push toward short pulse duration. A lot of effort was focused on the development of broadband gain materials suitable for the thin-disk geometry. However, against expectations, the industrial standard of Yb:YAG has still remained the most successful candidate even for very short sub-100-fs pulses. It will be very interesting to see if this trend will continue in future or if Yb:YAG will be replaced by another candidate, since the development of broadband gain materials is still ongoing. Concerning power-scaling of TDL oscillators, a significant progress has been recently made by systems operated in vacuum. It will be equally interesting to see if these systems will be replaced by simpler approaches such as those based on helium atmosphere. Hand in hand with the improving performance of TDL oscillators came the development of nonlinear pulse compression techniques suitable for the high average powers and low pulse energies of these lasers. Nowadays few-cycle pulses are already routinely available from nonlinearly compressed TDL oscillators. With the fast development of both technologies, we will likely observe these sources entering the

single-cycle regime in the near future. In combination with CEO-frequency stabilization, this will likely allow TDL oscillators becoming reliable waveform-stable single-cycle sources with GW-level peak powers and megahertz repetition rates. Such sources will benefit many scientific applications particularly in the attosecond domain. Another important potential of ultrafast TDLs is driving extreme nonlinear processes such as HHG directly inside the laser oscillator, offering a way toward compact coherent XUV sources based on the commercially available and well-developed TDL technology.

Acknowledgements
Schweizerischer Nationalfonds zur Förderung der Wissenschaftlichen Forschung (200020_179146, 200020_200774, 206021_144970, 206021_170772, 206021_198176). H2020 European Research Council (ERC) "Efficient megahertz XUV light source" (279545), Starting Grant 2011.

References

[1] A. Giesen, H. Hügel, A. Voss, K. Wittig, U. Brauch, H. Opower, *Appl Phys B* **1994**, *58*, 365–372.
[2] S. Nagel, B. Metzger, D. Bauer, J. Dominik, T. Gottwald, V. Kuhn, A. Killi, T. Dekorsy, S.-S. Schad, *Opt. Lett.* **2021**, *46*, 965–968.
[3] T. Dietz, M. Jenne, D. Bauer, M. Scharun, D. Sutter, A. Killi, *Opt. Express* **2020**, *28*, 11415–11423.
[4] D. Petring, F. Schneider, N. Wolf, V. Nazery, in *Int. Congr. Appl. Lasers Electro-Opt.*, Laser Institute of America, Temecula, California, USA, **2008**, p. 206.
[5] K. Löffler, in *Handb. Laser Weld. Technol.*, (Eds: S. Katayama), Woodhead Publishing, **2013**, pp. 73–102.
[6] S.-S. Schad, C. Stolzenburg, K. Michel, D. Sutter, *Laser Tech. J.* **2014**, *11*, 49–53.
[7] T. Nubbemeyer, M. Kaumanns, M. Ueffing, M. Gorjan, A. Alismail, H. Fattahi, J. Brons, O. Pronin, H. G. Barros, Z. Major, T. Metzger, D. Sutter, F. Krausz, *Opt. Lett.* **2017**, *42*, 1381–1384.
[8] J. Aus der Au, G. J. Spühler, T. Südmeyer, R. Paschotta, R. Hövel, M. Moser, S. Erhard, M. Karszewski, A. Giesen, U. Keller, *Opt. Lett.* **2000**, *25*, 859–861.
[9] F. Brunner, T. Südmeyer, E. Innerhofer, F. Morier-Genoud, R. Paschotta, V. E. Kisel, V. G. Shcherbitsky, N. V. Kuleshov, J. Gao, K. Contag, A. Giesen, U. Keller, *Opt. Lett.* **2002**, *27*, 1162–1164.
[10] E. Innerhofer, T. Südmeyer, F. Brunner, R. Häring, A. Aschwanden, R. Paschotta, C. Hönninger, M. Kumkar, U. Keller, *Opt. Lett.* **2003**, *28*, 367–369.
[11] S. V. Marchese, T. Südmeyer, M. Golling, R. Grange, U. Keller, *Opt. Lett.* **2006**, *31*, 2728–2730.
[12] G. Palmer, M. Siegel, A. Steinmann, U. Morgner, *Opt. Lett.* **2007**, *32*, 1593–1595.
[13] S. V. Marchese, C. R. E. Baer, R. Peters, C. Kränkel, A. G. Engqvist, M. Golling, D. J. H. C. Maas, K. Petermann, T. Südmeyer, G. Huber, U. Keller, *Opt. Express* **2007**, *15*, 16966–16971.
[14] S. V. Marchese, C. R. E. Baer, A. G. Engqvist, S. Hashimoto, D. Maas, M. Golling, T. Südmeyer, U. Keller, *Opt. Express* **2008**, *16*, 6397–6407.

[15] G. Palmer, M. Schultze, M. Siegel, M. Emons, U. Bünting, U. Morgner, *Opt. Lett.* **2008**, *33*, 1608–1610.
[16] C. R. Baer, C. Kränkel, C. J. Saraceno, O. H. Heckl, M. Golling, T. Südmeyer, R. Peters, K. Petermann, G. Huber, U. Keller, *Opt. Lett.* **2009**, *34*, 2823–2825.
[17] C. R. E. Baer, C. Kränkel, C. J. Saraceno, O. H. Heckl, M. Golling, R. Peters, K. Petermann, T. Südmeyer, G. Huber, U. Keller, *Opt. Lett.* **2010**, *35*, 2302–2304.
[18] O. Pronin, J. Brons, C. Grasse, V. Pervak, G. Boehm, M.-C. Amann, V. L. Kalashnikov, A. Apolonski, F. Krausz, *Opt. Lett.* **2011**, *36*, 4746–4748.
[19] D. Bauer, I. Zawischa, D. H. Sutter, A. Killi, T. Dekorsy, *Opt. Express* **2012**, *20*, 9698–9704.
[20] C. J. Saraceno, O. H. Heckl, C. R. E. Baer, C. Schriber, M. Golling, K. Beil, C. Kränkel, T. Südmeyer, G. Huber, U. Keller, *Appl. Phys. B* **2012**, *106*, 559–562.
[21] S. Ricaud, A. Jaffres, K. Wentsch, A. Suganuma, B. Viana, P. Loiseau, B. Weichelt, M. Abdou-Ahmed, A. Voss, T. Graf, D. Rytz, C. Hönninger, E. Mottay, P. Georges, F. Druon, *Opt. Lett.* **2012**, *37*, 3984–3986.
[22] C. Saraceno, S. Pekarek, O. Heckl, C. Baer, C. Schriber, M. Golling, T. Südmeyer, K. Beil, C. Krankel, G. Huber, others, in *Adv. Solid-State Photonics*, Optical Society of America, **2012**, pp. AM2A-3.
[23] A. Diebold, F. Emaury, C. Schriber, M. Golling, C. J. Saraceno, T. Südmeyer, U. Keller, *Opt. Lett.* **2013**, *38*, 3842–3845.
[24] A. Klenner, F. Emaury, C. Schriber, A. Diebold, C. J. Saraceno, S. Schilt, U. Keller, T. Südmeyer, *Opt. Express* **2013**, *21*, 24770–24780.
[25] N. Kanda, A. A. Eilanlou, T. Imahoko, T. Sumiyoshi, Y. Nabekawa, M. Kuwata-Gonokami, K. Midorikawa, in *Adv. Solid State Lasers Congr.*, Optical Society of America, **2013**, pp. AF3A-8.
[26] J. Brons, V. Pervak, E. Fedulova, D. Bauer, D. Sutter, V. Kalashnikov, A. Apolonskiy, O. Pronin, F. Krausz, *Opt. Lett.* **2014**, *39*, 6442–6445.
[27] C. Schriber, L. Merceron, A. Diebold, F. Emaury, M. Golling, K. Beil, C. Kränkel, C. J. Saraceno, T. Südmeyer, U. Keller, in *Adv. Solid State Lasers*, Optical Society of America, **2014**, p. AF1A.4.
[28] C. Schriber, F. Emaury, A. Diebold, S. Link, M. Golling, K. Beil, C. Kränkel, C. J. Saraceno, T. Südmeyer, U. Keller, *Opt. Express* **2014**, *22*, 18979–18986.
[29] C. J. Saraceno, F. Emaury, C. Schriber, M. Hoffmann, M. Golling, T. Südmeyer, U. Keller, *Opt. Lett.* **2014**, *39*, 9–12.
[30] C. J. Saraceno, F. Emaury, O. H. Heckl, C. R. E. Baer, M. Hoffmann, C. Schriber, M. Golling, T. Südmeyer, U. Keller, *Opt. Express* **2012**, *20*, 23535–23541.
[31] A. A. Eilanlou, Y. Nabekawa, M. Kuwata-Gonokami, K. Midorikawa, *Jpn. J. Appl. Phys.* **2014**, *53*, 082701.
[32] J. Zhang, J. Brons, M. Seidel, V. Pervak, V. Kalashnikov, Z. Wei, A. Apolonski, F. Krausz, O. Pronin, in *Eur. Quantum Electron. Conf.*, Optical Society of America, **2015**, p. PD_A_1.
[33] J. Zhang, J. Brons, N. Lilienfein, E. Fedulova, V. Pervak, D. Bauer, D. Sutter, Z. Wei, A. Apolonski, O. Pronin, F. Krausz, *Opt. Lett.* **2015**, *40*, 1627–1630.
[34] O. Pronin, M. Seidel, F. Lücking, J. Brons, E. Fedulova, M. Trubetskov, V. Pervak, A. Apolonski, T. Udem, F. Krausz, *Nat. Commun.* **2015**, *6*, 6988.
[35] B. Borchers, C. Schäfer, C. Fries, M. Larionov, R. Knappe, in *Adv. Solid State Lasers*, Optical Society of America, **2015**, p. ATh4A.9.
[36] J. Brons, V. Pervak, D. Bauer, D. Sutter, O. Pronin, F. Krausz, *Opt. Lett.* **2016**, *41*, 3567–3570.

[37] B. Kreipe, J. Andrade, B. Deppe, C. Kränkel, U. Morgner, in *Conf. Lasers Electro-Opt.*, Optical Society of America, **2016**, p. SM1I.4.
[38] I. Graumann, A. Diebold, F. Emaury, B. Deppe, C. Kraenkel, C. Saraceno, U. Keller, in *Lasers Congr. 2016 ASSL LSC LAC*, Optical Society of America, **2016**, pp. ATu1A-3.
[39] C. Paradis, N. Modsching, V. J. Wittwer, B. Deppe, C. Kränkel, T. Südmeyer, *Opt. Express* **2017**, *25*, 14918–14925.
[40] I. J. Graumann, A. Diebold, C. G. E. Alfieri, F. Emaury, B. Deppe, M. Golling, D. Bauer, D. Sutter, C. Kränkel, C. J. Saraceno, C. R. Phillips, U. Keller, *Opt. Express* **2017**, *25*, 22519–22536.
[41] F. Saltarelli, A. Diebold, I. J. Graumann, C. R. Phillips, U. Keller, *Opt. Express* **2017**, *25*, 23254–23265.
[42] N. Modsching, C. Paradis, F. Labaye, M. Gaponenko, I. J. Graumann, A. Diebold, F. Emaury, V. J. Wittwer, T. Südmeyer, *Opt. Lett.* **2018**, *43*, 879–882.
[43] S. Kitajima, A. Shirakawa, H. Yagi, T. Yanagitani, *Opt. Lett.* **2018**, *43*, 5451–5454.
[44] J. Zhang, K. F. Mak, O. Pronin, *IEEE J. Sel. Top. Quantum Electron.* **2018**, *24*, 1–11.
[45] F. Saltarelli, A. Diebold, I. J. Graumann, C. R. Phillips, U. Keller, *Optica* **2018**, *5*, 1603.
[46] I. J. Graumann, F. Saltarelli, L. Lang, V. J. Wittwer, T. Südmeyer, C. R. Phillips, U. Keller, *Opt. Express* **2019**, *27*, 37349–37363.
[47] F. Saltarelli, I. J. Graumann, L. Lang, D. Bauer, C. R. Phillips, U. Keller, *Opt. Express* **2019**, *27*, 31465–31474.
[48] M. Poetzlberger, J. Zhang, S. Gröbmeyer, D. Bauer, D. Sutter, J. Brons, O. Pronin, *Opt. Lett.* **2019**, *44*, 4227–4230.
[49] S. Gröbmeyer, J. Brons, M. Seidel, O. Pronin, *Laser Photonics Rev.* **2019**, *13*, 1800256.
[50] N. Modsching, J. Drs, J. Fischer, C. Paradis, F. Labaye, M. Gaponenko, C. Kränkel, V. J. Wittwer, T. Südmeyer, *Opt. Express* **2019**, *27*, 16111–16120.
[51] S. Goncharov, K. Fritsch, O. Pronin, in *2021 Conf. Lasers Electro-Opt. Eur. Eur. Quantum Electron. Conf. OSA Tech. Dig. Opt. Soc. Am. 2021*, Munich, Germany, **2021**, p. cf_4_1.
[52] J. Drs, J. Fischer, N. Modsching, F. Labaye, V. J. Wittwer, T. Südmeyer, *Opt. Express* **2021**, *29*, 35929–35937.
[53] J. Fischer, J. Drs, N. Modsching, F. Labaye, V. J. Wittwer, T. Südmeyer, *Opt. Express* **2021**, *29*, 42075–42081.
[54] S. Tomilov, M. Hoffmann, J. Heidrich, B. Ö. Alaydin, M. Golling, Y. Wang, U. Keller, C. J. Saraceno, in *2021 Conf. Lasers Electro-Opt. Eur. Eur. Quantum Electron. Conf. CLEOEurope-EQEC*, **2021**, pp. 1–1.
[55] J. Zhang, M. Pötzlberger, Q. Wang, J. Brons, M. Seidel, D. Bauer, D. Sutter, V. Pervak, A. Apolonski, K. F. Mak, V. Kalashnikov, Z. Wei, F. Krausz, O. Pronin, *Ultrafast Sci.* **2022**, *2022*.
[56] T. Südmeyer, C. Kränkel, C. R. E. Baer, O. H. Heckl, C. J. Saraceno, M. Golling, R. Peters, K. Petermann, G. Huber, U. Keller, *Appl. Phys. B* **2009**, *97*, 281–295.
[57] I. Pupeza, M. Huber, M. Trubetskov, W. Schweinberger, S. A. Hussain, C. Hofer, K. Fritsch, M. Poetzlberger, L. Vamos, E. Fill, T. Amotchkina, K. V. Kepesidis, A. Apolonski, N. Karpowicz, V. Pervak, O. Pronin, F. Fleischmann, A. Azzeer, M. Žigman, F. Krausz, *Nature* **2020**, *577*, 52–59.

[58] C. Paradis, J. Drs, N. Modsching, O. Razskazovskaya, F. Meyer, C. Kränkel, C. J. Saraceno, V. J. Wittwer, T. Südmeyer, *Opt. Express* **2018**, *26*, 26377–26384.
[59] J. Drs, N. Modsching, C. Paradis, C. Kränkel, V. J. Wittwer, O. Razskazovskaya, T. Südmeyer, *JOSA B* **2019**, *36*, 3039–3045.
[60] F. Meyer, N. Hekmat, T. Vogel, A. Omar, S. Mansourzadeh, F. Fobbe, M. Hoffmann, Y. Wang, C. J. Saraceno, *Opt. Express* **2019**, *27*, 30340–30349.
[61] F. Meyer, T. Vogel, S. Ahmed, C. J. Saraceno, *Opt. Lett.* **2020**, *45*, 2494–2497.
[62] G. Barbiero, H. Wang, J. Brons, B.-H. Chen, V. Pervak, H. Fattahi, *J. Phys. B At. Mol. Opt. Phys.* **2020**, *53*, 6.
[63] F. Emaury, A. Diebold, C. J. Saraceno, U. Keller, *Optica* **2015**, *2*, 980–984.
[64] K. Fritsch, J. Brons, M. Iandulskii, K. F. Mak, Z. Chen, F. Krausz, N. Picqué, O. Pronin, in *Eur. Quantum Electron. Conf.*, **2019**, p. CA.5-2.
[65] N. Modsching, J. Drs, P. Brochard, J. Fischer, S. Schilt, V. J. Wittwer, T. Südmeyer, *Opt. Express* **2021**, *29*, 15104–15113.
[66] F. Labaye, M. Gaponenko, V. J. Wittwer, A. Diebold, C. Paradis, N. Modsching, L. Merceron, F. Emaury, I. J. Graumann, C. R. Phillips, C. J. Saraceno, C. Kränkel, U. Keller, T. Südmeyer, *Opt. Lett.* **2017**, *42*, 5170–5173.
[67] N. Kanda, T. Imahoko, K. Yoshida, A. Tanabashi, A. Amani Eilanlou, Y. Nabekawa, T. Sumiyoshi, M. Kuwata-Gonokami, K. Midorikawa, *Light Sci. Appl.* **2020**, *9*, 168.
[68] J. Fischer, J. Drs, F. Labaye, N. Modsching, V. Wittwer, T. Südmeyer, *Opt. Express* **2021**, *29*, 5833–5839.
[69] Y. Wang, S. Tomilov, C. J. Saraceno, *Adv. Opt. Technol.* **2021**, *10*, 247–261.
[70] R. Peters, C. Kränkel, S. T. Fredrich-Thornton, K. Beil, K. Petermann, G. Huber, O. H. Heckl, C. R. E. Baer, C. J. Saraceno, T. Südmeyer, U. Keller, *Appl. Phys. B* **2011**, *102*, 509–514.
[71] M. Larionov, J. Gao, S. Erhard, A. Giesen, K. Contag, V. Peters, E. Mix, L. Fornasiero, K. Petermann, G. Huber, J. A. der Au, G. J. Spühler, F. Brunner, R. Paschotta, U. Keller, A. A. Lagatsky, A. Abdolvand, N. V. Kuleshov, in *Adv. Solid-State Lasers*, Optica Publishing Group, **2001**, p. WC4.
[72] R. Peters, C. Kränkel, K. Petermann, G. Huber, *Opt. Express* **2007**, *15*, 7075.
[73] C. Kränkel, *IEEE J. Sel. Top. Quantum Electron.* **2015**, *21*, 250–262.
[74] C. Kränkel, A. Uvarova, É. Haurat, L. Hülshoff, M. Brützam, C. Guguschev, S. Kalusniak, D. Klimm, *Acta Crystallogr. Sect. B Struct. Sci. Cryst. Eng. Mater.* **2021**, *77*, 550–558.
[75] C. Kränkel, A. Uvarova, C. Guguschev, S. Kalusniak, L. Hülshoff, H. Tanaka, D. Klimm, *Opt. Mater. Express* **2022**, *12*, 1074–1091.
[76] S. Ricaud, A. Jaffres, P. Loiseau, B. Viana, B. Weichelt, M. Abdou-Ahmed, A. Voss, T. Graf, D. Rytz, M. Delaigue, E. Mottay, P. Georges, F. Druon, *Opt. Lett.* **2011**, *36*, 4134–4136.
[77] K. Hasse, T. Calmano, B. Deppe, C. Liebald, C. Kränkel, *Opt. Lett.* **2015**, *40*, 3552–3555.
[78] A. Greborio, A. Guandalini, J. Aus der Au, in *Proc SPIE*, (Eds: W. A. Clarkson, R. K. Shori), 8235, **2012**, p. 823511.
[79] F. Labaye, V. J. Wittwer, M. Hamrouni, N. Modsching, E. Cormier, E. Cormier, T. Südmeyer, *Opt. Express* **2022**, *30*, 2528–2538.
[80] U. Keller, *Appl. Phys. B* **2010**, *100*, 15–28.
[81] U. Keller, D. A. B. Miller, G. D. Boyd, T. H. Chiu, J. F. Ferguson, M. T. Asom, *Opt. Lett.* **1992**, *17*, 505.

[82] U. Keller, K. J. Weingarten, F. X. Kärtner, D. Kopf, B. Braun, I. D. Jung, R. Fluck, C. Hönninger, N. Matuschek, J. Aus der Au, *IEEE J. Sel. Top. Quantum Electron.* **1996**, *2*, 435–453.
[83] C. J. Saraceno, C. Schriber, M. Mangold, M. Hoffmann, O. H. Heckl, C. R. Baer, M. Golling, T. Südmeyer, U. Keller, *IEEE J. Sel. Top. Quantum Electron.* **2012**, *18*, 29–41.
[84] C. G. E. Alfieri, A. Diebold, F. Emaury, E. Gini, C. J. Saraceno, U. Keller, *Opt. Express* **2016**, *24*, 27587.
[85] A. Diebold, T. Zengerle, C. G. E. Alfieri, C. Schriber, F. Emaury, M. Mangold, M. Hoffmann, C. J. Saraceno, M. Golling, D. Follman, G. D. Cole, M. Aspelmeyer, T. Südmeyer, U. Keller, *Opt. Express* **2016**, *24*, 10512.
[86] D. E. Spence, P. N. Kean, W. Sibbett, *Opt. Lett.* **1991**, *16*, 42–44.
[87] P. F. Moulton, *J. Opt. Soc. Am. B* **1986**, *3*, 125–133.
[88] U. Keller, *Nature* **2003**, *424*, 831–838.
[89] A. Diebold, F. Saltarelli, I. J. Graumann, C. J. Saraceno, C. R. Phillips, U. Keller, *Opt. Express* **2018**, *26*, 12648–12659.
[90] T. Südmeyer, F. Brunner, E. Innerhofer, R. Paschotta, K. Furusawa, J. C. Baggett, T. M. Monro, D. J. Richardson, U. Keller, *Opt. Lett.* **2003**, *28*, 1951.
[91] E. Innerhofer, F. Brunner, S. V. Marchese, R. Paschotta, U. Keller, K. Furusawa, J. C. Baggett, T. M. Monro, D. J. Richardson, in *Adv. Solid-State Photonics*, Optical Society of America, **2005**, p. TuA3.
[92] C. J. Saraceno, O. H. Heckl, C. R. E. Baer, T. Südmeyer, U. Keller, *Opt. Express* **2011**, *19*, 1395.
[93] O. H. Heckl, C. J. Saraceno, C. R. E. Baer, T. Südmeyer, Y. Y. Wang, Y. Cheng, F. Benabid, U. Keller, *Opt. Express* **2011**, *19*, 19142–19149.
[94] K. Fritsch, M. Poetzlberger, V. Pervak, J. Brons, O. Pronin, *Opt. Lett.* **2018**, *43*, 4643.
[95] S. Gröbmeyer, K. Fritsch, B. Schneider, M. Poetzlberger, V. Pervak, J. Brons, O. Pronin, *Appl. Phys. B* **2020**, *126*, 159.
[96] C.-L. Tsai, F. Meyer, A. Omar, Y. Wang, A.-Y. Liang, C.-H. Lu, M. Hoffmann, S.-D. Yang, C. J. Saraceno, *Opt. Lett.* **2019**, *44*, 4115–4118.
[97] G. Barbiero, H. Wang, M. Graßl, S. Gröbmeyer, D. Kimbaras, M. Neuhaus, V. Pervak, T. Nubbemeyer, H. Fattahi, M. F. Kling, *Opt. Lett.* **2021**, *46*, 5304–5307.
[98] M. Müller, J. Buldt, H. Stark, C. Grebing, J. Limpert, *Opt. Lett.* **2021**, *46*, 2678–2681.
[99] S. Hädrich, E. Shestaev, M. Tschernajew, F. Stutzki, N. Walther, F. Just, M. Kienel, I. Seres, P. Jójárt, Z. Bengery, B. Gilicze, Z. Várallyay, Á. Börzsönyi, M. Müller, C. Grebing, A. Klenke, D. Hoff, G. G. Paulus, T. Eidam, J. Limpert, *Opt. Lett.* **2022**, *47*, 1537–1540.
[100] H. R. Telle, G. Steinmeyer, A. E. Dunlop, J. Stenger, D. H. Sutter, U. Keller, *Appl. Phys. B* **1999**, *69*, 327–332.
[101] M. Seidel, J. Brons, F. Lücking, V. Pervak, A. Apolonski, T. Udem, O. Pronin, *Opt. Lett.* **2016**, *41*, 1853–1856.
[102] N. Modsching, C. Paradis, P. Brochard, N. Jornod, K. Gürel, C. Kränkel, S. Schilt, V. J. Wittwer, T. Südmeyer, *Opt. Express* **2018**, *26*, 28461–28467.
[103] J. R. C. Andrade, N. Modsching, A. Tajalli, C. M. Dietrich, S. Kleinert, F. Placzek, B. Kreipe, S. Schilt, V. J. Wittwer, T. Sudmeyer, U. Morgner, *IEEE Photonics J.* **2020**, *12*, 1–9.
[104] I. Pupeza, C. Zhang, M. Högner, J. Ye, *Nat. Photonics* **2021**, 1–12.

[105] S. Hädrich, M. Krebs, A. Hoffmann, A. Klenke, J. Rothhardt, J. Limpert, A. Tünnermann, *Light Sci. Appl.* **2015**, *4*, e320.
[106] F. Krausz, M. Ivanov, *Rev. Mod. Phys.* **2009**, *81*, 163–234.
[107] A. K. Mills, T. J. Hammond, M. H. C. Lam, D. J. Jones, *J. Phys. B At. Mol. Opt. Phys.* **2012**, *45*, 142001.
[108] S. Hädrich, J. Rothhardt, M. Krebs, S. Demmler, A. Klenke, A. Tünnermann, J. Limpert, *J. Phys. B At. Mol. Opt. Phys.* **2016**, *49*, 172002.
[109] J. Drs, J. Fischer, F. Labaye, N. Modsching, V. J. Wittwer, T. Südmeyer, in *Adv. Solid State Lasers*, Optical Society of America, **2021**, p. ATh3A.2.
[110] C. J. Saraceno, *J. Opt.* **2018**, *20*, 044010.
[111] N. Picqué, T. W. Hänsch, *Nat. Photonics* **2019**, *13*, 146–157.
[112] V. Schuster, C. Liu, R. Klas, P. Dominguez, J. Rothhardt, J. Rothhardt, J. Limpert, B. Bernhardt, *Opt. Express* **2021**, *29*, 21859–21875.

2 TDL development and intra-oscillator HHG

The main motivation for the development of TDL oscillators in our group has been the project of driving HHG directly inside the laser oscillator. This approach involves building a laser inside a vacuum chamber and placing a gas target for the nonlinear interaction directly inside the laser cavity. The most important parameters for the HHG process are the peak power as well as the pulse duration of the driving laser. Intra-oscillator HHG inside a TDL has been first demonstrated in our group shortly before the start of my thesis. However, the driving laser parameters had to be strongly improved in order to drive HHG efficiently. We have, thus, invested significant effort into improving the driving laser source itself.

In order to achieve the shortest pulse duration, two development directions were explored. Firstly, it was important to switch from originally used SESAM mode-locking to KLM. Secondly, broadband gain materials, such as Yb:LuO and Yb:CALGO, were explored in the TDL configuration. These efforts resulted in a publication of a 20 W 95 fs KLM TDL oscillator based on Yb:LuO, reproduced with permission from Optics Express [1].

The next step was building a similar laser inside a vacuum chamber for driving intra-oscillator HHG. However, during these efforts we damaged two of our LuO disks, which forced us to switch to the commercially available gain material of Yb:YAG. Despite all expectation, this switch to a less broadband gain material allowed us to dramatically improve the performance of the laser in the sub-100-fs domain by operation in a strongly self-phase modulation broadened regime. In a first study focused on decreasing the pulse duration, we have achieved the record short pulse duration for TDL oscillators of 27 fs, reproduced with permission from Optics Express [2]. In a second study focused on high average power, we have pushed our laser to 100 W output power at 50 fs pulse duration and 26% optical-to-optical efficiency, reproduced with permission from Optics Express [3].

Finally, the improved laser performance allowed for significant progress in intra-oscillator HHG. Compared to our initial result from 2017, reaching 0.5 nW of XUV flux at 11 eV driven by a SESAM mode-locked Yb:LuO TDL oscillator,

the newly developed KLM Yb:YAG laser resulted in a more than four orders of magnitude improvement in terms of XUV flux. At an intracavity peak power of 375 MW and 105 fs pulse duration, the laser generated 0.4 µW of XUV flux in a single harmonic at 30 eV [4], reproduced with permission from Optics Express. Later, we have further increased the XUV flux to 10 µW by scaling the intracavity peak power to 550 MW [5].

References

1. Modsching, N., Drs, J., Fischer, J., Paradis, C., Labaye, F., Gaponenko, M., Kränkel, C., Wittwer, V. J. & Südmeyer, T. Sub-100-fs Kerr lens mode-locked Yb:Lu_2O_3 thin-disk laser oscillator operating at 21 W average power. *Optics Express* **27**, 16111 (2019).

2. Drs, J., Fischer, J., Modsching, N., Labaye, F., Wittwer, V. J. & Südmeyer, T. Sub-30-fs Yb:YAG thin-disk laser oscillator operating in the strongly self-phase modulation broadened regime. *Optics Express* **29**. Publisher: Optical Society of America, 35929 (2021).

3. Fischer, J., Drs, J., Modsching, N., Labaye, F., Wittwer, V. J. & Südmeyer, T. Efficient 100-MW, 100-W, 50-fs-class Yb:YAG thin-disk laser oscillator. *Optics Express* **29**. Publisher: Optical Society of America, 42075 (2021).

4. Fischer, J., Drs, J., Labaye, F., Modsching, N., Wittwer, V. & Südmeyer, T. Intra-oscillator high harmonic generation in a thin-disk laser operating in the 100-fs regime. *Optics Express* **29**, 5833 (2021).

5. Drs, J., Fischer, J., Labaye, F., Modsching, N., Wittwer, V. J. & Südmeyer, T. *10-µW, 30-eV High Harmonic Generation inside an Yb:YAG Thin-Disk Laser Oscillator* in *Advanced Solid State Lasers (2021)* (Optical Society of America, 2021), ATh3A.2.

Research Article | Vol. 27, No. 11 | 27 May 2019 | OPTICS EXPRESS 16111
Optics EXPRESS

Sub-100-fs Kerr lens mode-locked Yb:Lu_2O_3 thin-disk laser oscillator operating at 21 W average power

NORBERT MODSCHING,[1,*] JAKUB DRS,[1] JULIAN FISCHER,[1] CLÉMENT PARADIS,[1] FRANÇOIS LABAYE,[1] MAXIM GAPONENKO,[1] CHRISTIAN KRÄNKEL,[2] VALENTIN J. WITTWER,[1] AND THOMAS SÜDMEYER[1]

[1]*Laboratoire Temps-Fréquence (LTF), Institut de Physique, Université de Neuchâtel, Avenue de Bellevaux 51, 2000 Neuchâtel, Switzerland*
[2]*Center for Laser Materials, Leibniz-Institut für Kristallzüchtung, Max-Born-Str. 2, 12489 Berlin, Germany*
**norbert.modsching@unine.ch*

Abstract: We investigate power-scaling of a Kerr lens mode-locked (KLM) Yb:Lu_2O_3 thin-disk laser (TDL) oscillator operating in the sub-100-fs pulse duration regime. Employing a scheme with higher round-trip gain by increasing the number of passes through the thin-disk gain element, we increase the average power by a factor of two and the optical-to-optical efficiency by a factor of almost three compared to our previous sub-100-fs mode-locking results. The oscillator generates pulses with a duration of 95 fs at 21.1 W average power and 47.9 MHz repetition rate. We discuss the cavity design for continuous-wave and mode-locked operation and the estimation of the focal length of the Kerr lens. Unlike to usual KLM TDL oscillators, an operation at the edge of the stability zone in continuous-wave operation is not required. This work shows that KLM TDL oscillators based on the gain material Yb:Lu_2O_3 are an excellent choice for power-scaling of laser oscillators in the sub-100-fs regime, and we expect that such lasers will soon operate at power levels in excess of hundred watts.

1. Introduction

High-power ultrafast laser systems operating at MHz repetition rates are a versatile tool for numerous applications in science and industry [1]. Compared to amplifiers, oscillators generate usually close to transform-limited pulses in fundamental TEM_{00} mode operation without pre- or post-pulses and feature low noise levels, suitable for carrier-envelope-offset frequency stabilization. However, the currently achieved power levels decrease strongly as function of the minimum achieved pulse duration. In the last decade, numerous studies have been targeting to increase the achievable power levels of ultrafast laser oscillators operating in the sub-100-fs regime [2–4]. Sub-100-fs bulk oscillators based on Ti:sapphire are currently limited to 3.5 W of average power [5] (Fig. 1). In comparison, sub-100-fs oscillators based on Yb-doped bulk gain materials operate at a reduced quantum defect, enabling up to 12.5 W of average power [6]. However, even in this case thermal effects in the bulk gain material are the most severe challenge for further increase of the average power.

The thin-disk geometry is advantageous for further power increase of sub-100-fs laser oscillators, because it reduces the thermal effects in the gain material during laser operation [7]. Various techniques have been applied for efficient mode-locking of thin-disk laser (TDL) oscillators, e.g. by saturable absorber mirrors (SESAMs) [8], nonlinear polarization rotation [9], nonlinear mirror mode-locking [10] and Kerr lens mode-locking [11]. Among those techniques, the shortest pulse duration of a TDL oscillator was achieved by Kerr lens mode-locking [12].

#362282 https://doi.org/10.1364/OE.27.016111
Journal © 2019 Received 14 Mar 2019; revised 4 May 2019; accepted 6 May 2019; published 22 May 2019

Optics EXPRESS

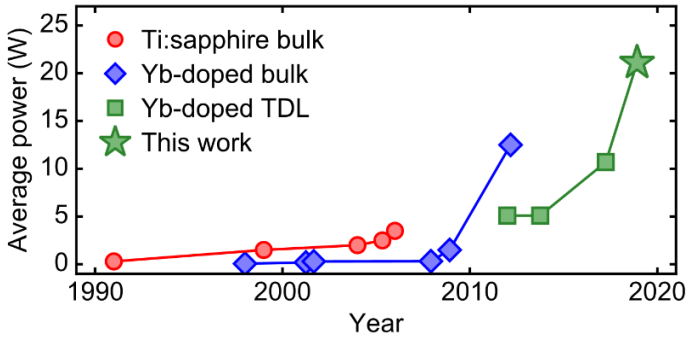

Fig. 1. Progress of the average power of ultrafast solid-state laser oscillators operating in the sub-100-fs pulse duration regime (Ti:sapphire [5,13], Yb-doped bulk [6,13–15], Yb-doped thin-disk laser (TDL) [16–18]).

In order to expand high-power operation of ultrafast TDL oscillators into the sub-100-fs regime [2], mode-locking of various broadband Yb-doped gain materials was investigated by several research groups [19–24]. The first TDL oscillators achieving sub-100-fs pulse durations were based on the broadband gain materials Yb:$LuScO_3$ and Yb:CALGO. Up to 5.1 W average power were demonstrated with an optical-to-optical efficiency amounting to 11% [16,17] (Table 1). Although their distorted crystalline structure is beneficial for a broad gain bandwidth, the resulting reduced thermal conductivity as well as the crystal quality of the available disks are limiting factors for achieving higher average powers. Currently, the highest average power of any ultrafast TDL oscillator based on disordered gain materials is limited to 28 W with 300-fs pulses [24].

Table 1. Selection of state-of-the-art ultrafast Yb-based laser oscillators.[a]

Type	Gain material	P_{ave}	τ_{pulse}	η_{eff}	Reference
Bulk	Yb:CALGO	12.5 W	94 fs	20%	[6]
Bulk	Yb:CALGO	3.3 W	45 fs	16%	[25]
TDL	Yb:$LuScO_3$	5.1 W	96 fs	11%	[16]
TDL	Yb:CALGO	5.1 W	62 fs	7%	[17]
TDL	Yb:YAG	155 W	140 fs	29%	[26]
TDL	Yb:YAG	3.5 W	49 fs	3.5%	[27,28]
TDL	Yb:Lu_2O_3	10.7 W	88 fs	5.8%	[18]
TDL	Yb:Lu_2O_3	21.1 W	95 fs	16.2%	This work

[a]P_{ave}: average power; τ_{pulse}: pulse duration; η_{eff}: optical-to-optical efficiency; TDL, thin-disk laser.

Ultrafast TDL oscillators based on the most mature gain material Yb:YAG have already reached average powers of 275 W, but operating at several hundred femtoseconds of pulse duration [29,30]. Kerr lens mode-locked (KLM) TDL oscillators demonstrated laser operation with 140-fs pulses at 155 W of average power and an optical-to-optical efficiency of 29% by fully exploiting the emission bandwidth of Yb:YAG [26]. Even shorter pulse durations of 49 fs were achieved by inserting nonlinear crystals for the generation of additional spectral components by self-phase modulation (SPM) in the cavity of a KLM Yb:YAG TDL oscillators. However, in this case the laser performance was limited to 3.5 W of average power at an optical-to-optical efficiency of 3.5% [27,28]. A gain material for high-power laser operation, which directly supports sub-100-fs pulse durations is Yb:Lu_2O_3. Yb:Lu_2O_3 provides a 60% broader emission bandwidth than Yb:YAG supporting the generation of 86-fs pulses at an even better thermal conductivity [2]. Although the gain material is still at an early stage of development, its suitability for high-power laser operation was already demonstrated by an ultrafast SESAM mode-locked TDL oscillator reaching 141 W of average power, albeit at pulse durations of several hundred femtoseconds [31]. In 2017, we demonstrated a KLM TDL oscillator fully

Optics EXPRESS

exploiting the emission bandwidth of Yb:Lu_2O_3. The laser operated at 10.7 W of average power in 88-fs pulses with a modest optical-to-optical efficiency of 5.8% [18].

In this work, we investigate the impact of higher round-trip gain on the average power and the optical-to-optical efficiency of a sub-100-fs KLM Yb:Lu_2O_3 TDL oscillator. Folding the standing-wave cavity two times on the disk enabled an increase of the average output power by a factor of two and the optical-to-optical efficiency by a factor of three compared to our previous result [18]. We demonstrate that using this approach TDL oscillators based on the gain material Yb:Lu_2O_3 are suitable for the generation of sub-100-fs pulses at high average power with optical-to-optical efficiencies that are comparable to Yb-doped bulk oscillators (Table 1).

2. Cavity design

The performance of the Yb:Lu_2O_3 disk in continuous-wave (CW) operation and previous mode-locking results are published in [18]. Compared to these results, the presented cavity is modified by folding the standing-wave cavity a second time on the disk (Fig. 2). A second folding of the cavity on the disk is commonly used in high-power KLM TDL oscillators [26,30]. In this configuration, the gain propagation length of the laser beam per cavity round-trip amounts to the eightfold of the gain crystal thickness, resulting in a higher round-trip gain.

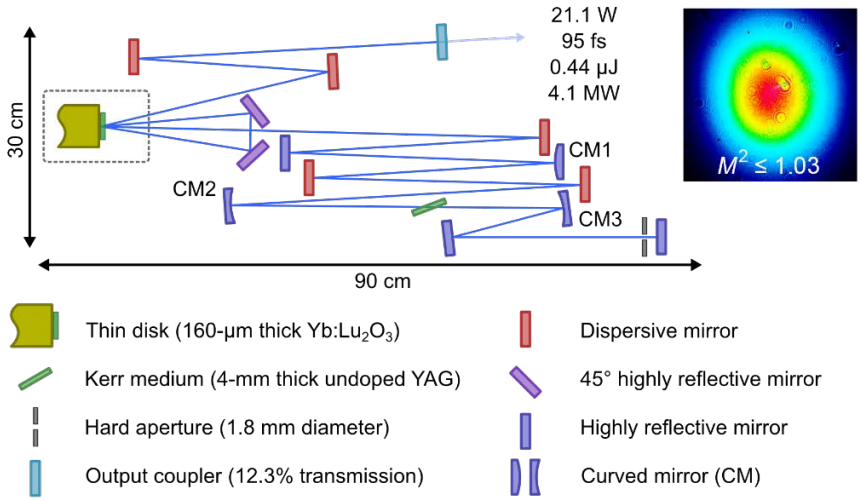

Fig. 2. Schematic of the Kerr lens mode-locked Yb:Lu_2O_3 thin-disk laser oscillator. (inset) Beam profile in mode-locked operation and M^2 beam quality factor. CM1, convex radius of curvature (ROC) of 2 m; CM2 and CM3, concave ROC of 250 mm.

Higher round-trip gain in the oscillator cavity enables laser operation at higher total cavity losses and, thus, the operation at a higher output coupler transmission (T_{OC}). Considering a constant intracavity performance, an increase in the T_{OC} should result in an increase of the output performance. However, higher round-trip gain also causes stronger gain narrowing which can reduce the spectral bandwidth and might prevent an exploitation of the gain bandwidth. The gain spectrum of Yb:Lu_2O_3 features a peak at a central wavelength of around 1033 nm with a full width at half maximum (FWHM) bandwidth of around 13 nm [Fig. 5(a)] [2,32]. Both parameters are nearly constant with the inversion level. Therefore, effects on the spectral gain properties for laser operation at a different inversion level can be neglected.

The mode radius in the cavity is calculated based on a formalism of ray transfer matrices for Gaussian beams (Fig. 3). We restrict the discussion to the sagittal plane which experiences a stronger Kerr lens due to the smaller beam radius in the Kerr medium (KM). The different mode radii in tangential and sagittal plane originate from the Brewster's angle under which the

Optics EXPRESS

KM is placed. In mode-locked operation, the additional Kerr lens changes the mode radius compared to the CW operation.

The focal length of the Kerr lens (f_{KM}) is estimated for a given intracavity peak power by an iterative optimization routine. In the simplified model, f_{KM} is considered as a single lens in the center of the KM. In the routine, the cavity is calculated for an initially guessed focal length $f_{KM,guess}$. For a stable cavity, the mode radius in the KM (w_{KM}) is retrieved and a resulting averaged focal length of the lens in the Kerr medium ($f_{KM,calc}$) is calculated based on

$$f_{KM,calc}^{-1} = \frac{4n_2 d_{KM,eff}}{\pi w_{KM}^4} \cdot P_{peak,IC} \quad ,$$

where n_2 is the nonlinear refractive index of the KM, $d_{KM,eff}$ is the effective thickness of the KM under Brewster's angle, and $P_{peak,IC}$ is the intracavity peak power [33]. A stable solution for f_{KM} can be found by an iterative optimization routine minimizing the difference between $f_{KM,guess}$ and $f_{KM,calc}$ for a given intracavity peak power. Once a stable solution is found, it enables an estimation of the mode radius in mode-locked operation (Fig. 3). In the presented cavity are two design aspects considered. First, the mode radius has to decrease at the position of the hard aperture (HA) to form a fast saturable absorber for self-amplitude modulation. Second, the mode radii at the position of the disk (DISK1, DISK2), have to increase for an optimized overlap with the pump spot. This increase affects the optical-to-optical efficiency and creates an additional soft-aperture self-amplitude modulation.

For efficient laser operation, the mode radius on the disk in mode-locked operation has to fit to the pump spot on the disk. An 80% overlap with the pump spot diameter of 2.8 mm was evaluated for highest optical-to-optical efficiency of the fundamental-mode in CW operation [18] (Fig. 3). The different mode radii on the disk originate from the concave 2.1 m radius of curvature of the disk. For improved overlap of both mode radii on the disk (DISK1, DISK2) the free space propagation distance between them (length b) was minimized, using two highly reflective mirrors optimized for 45° angle of incidence (Fig. 2). In contrast to our previous mode-locking results, a slightly elliptical beam profile is observed (inset of Fig. 2). We attributed the ellipticity to the larger angle of incidence on the disk of 9°.

Unlike to usual KLM TDL oscillators [11,34], an operation at the edge of the stability zone in CW operation is not required. Typically, KLM TDL oscillators are first optimized for fundamental-mode CW laser operation in the center of the stability zone and adjusted mode radius on the disk. Then, a 4-*f* imaging section is introduced into the cavity via two curved mirrors to create an intracavity focus without influencing the behavior of the laser in CW operation. The Kerr medium is placed in the vicinity of the intracavity focus for the formation of the Kerr lens in mode-locked operation. By increasing the distance between the curved mirrors, the cavity is shifted towards the edge of the stability zone in CW operation to promote Kerr lens mode-locking. In contrast, our cavity design has not been optimized for CW operation. The curved mirrors CM2 and CM3 form an intracavity focus without serving the purpose of a 4-*f* imaging section leading to different cavity dynamics. This allows for tailoring the mode size on the disk by adjusting the length e between CM2 and CM3 (Fig. 4). During the experimental optimization of the mode-locking performance for highest average power at sub-100-fs pulse durations the length e, the position and thickness of the KM, the HA diameter, the T_{OC} and the introduced group delay dispersion (GDD) were adapted.

Optics EXPRESS

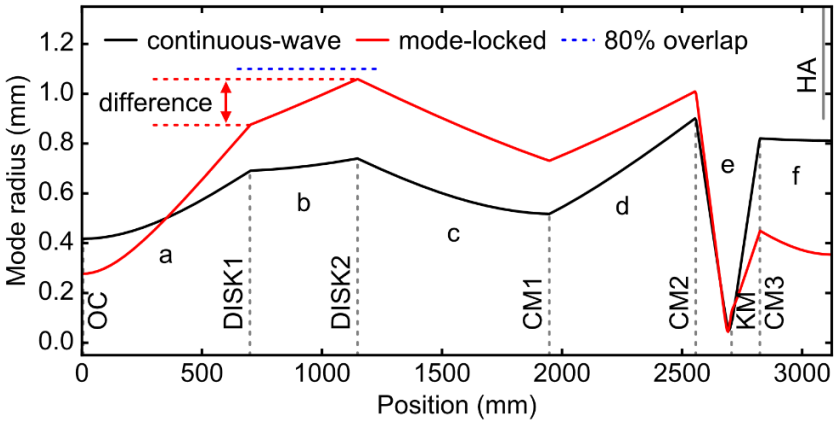

Fig. 3. Cavity design in continuous-wave and mode-locked operation shown for the sagittal plane. The mode radius is defined as the $1/e^2$ decay of the maximal intensity. In mode-locked operation, the effect of the Kerr lens in the Kerr medium (KM) is estimated for an intracavity peak power of 33 MW. Gray dotted lines indicate the position of the cavity components. In mode-locked operation, the mode radius on the disk (DISK1, DISK2) targets an 80% overlap with the pump spot (blue dotted). The different mode radii on the disk (red dotted) originate from the ROC of the disk. Cavity lengths in the simulation are a = 700 mm; b = 448 mm; c = 799 mm; d = 610 mm; e = 267mm; f = 300 mm. The distance between curved mirror CM2 and the KM is 149 mm. The hard aperture (HA, gray solid) is placed 30 mm before the cavity end mirror. In the experimental setup, the uncertainty of each length measurement towards the disk is ± 3 mm. The uncertainty of each length measurement between all other cavity components is ± 1 mm. OC, output coupler.

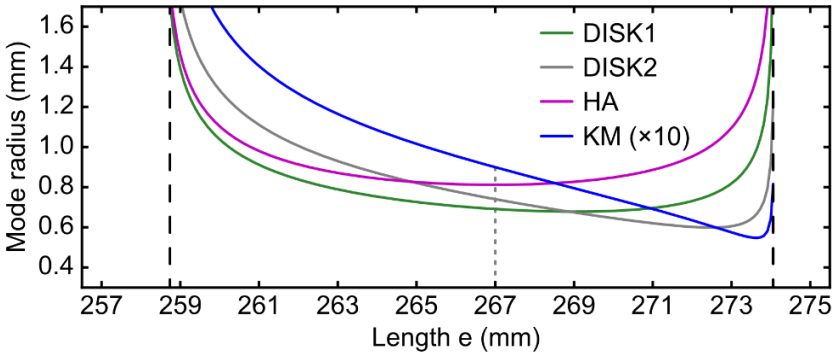

Fig. 4. Impact of the distance between the curved mirrors CM2 and CM3 in CW operation on the mode radii on the disk (DISK1; DISK2), in the Kerr medium (KM) and on the hard aperture (HA). Vertical black dashed lines indicate the edge of the stability zone for a stable cavity. The gray dotted line indicates the length e after the cavity optimization.

3. Performance in mode-locked operation

For mode-locked operation, −5400 fs^2 of GDD per cavity roundtrip are introduced by five dispersive mirrors (Fig. 2) at a T_{OC} of 12.3%. A 4 mm thick undoped YAG plate acts as KM and the diameter of the HA is 1.8 mm. The mode radii in the KM in CW operation were estimated by the cavity calculation to be 90 µm × 165 µm in sagittal and tangential plane, respectively. The start-up of the mode-locked operation follows the same procedure utilized in our initial laser result [18]. In the presented configuration, the formation of a single soliton in the cavity is achieved by setting the pump power to 160 W and knocking on the laser table. Afterwards, the pump power is reduced to 130 W to suppress a CW breakthrough visible in the

Optics EXPRESS

optical spectrum. As Kerr lens mode-locking features discrete stable solutions for the pulse formation, residual energy is often extracted by CW lasing.

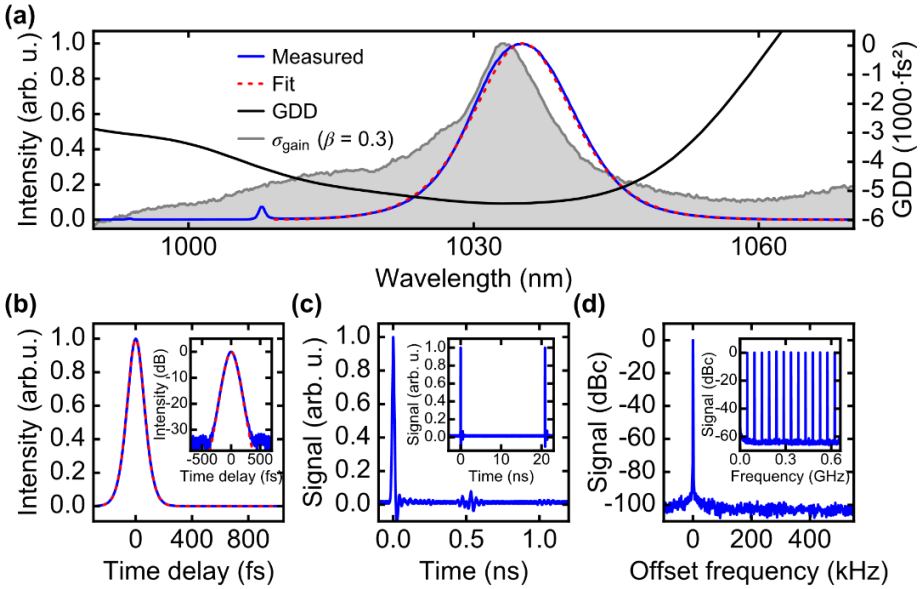

Fig. 5. (a) Optical spectrum of the laser output with sech^2 fit for soliton pulses, introduced group delay dispersion (GDD) per cavity roundtrip, and normalized gain cross-section of Yb:Lu_2O_3 for an inversion level β of 0.3 as reference (data taken from [2]). (b) Autocorrelation trace of the 95-fs pulses with sech^2 fit (measured in blue solid line and fit in red dotted line) in linear and (inset) logarithmic scale. (c) Sampling oscilloscope trace for 1 ns and (inset) 20 ns. (d) Radio-frequency spectrum of the fundamental repetition-rate frequency at 47.9 MHz and (inset) its harmonics at 100 Hz and 1 kHz resolution bandwidth, respectively.

In this configuration, the oscillator generates 95-fs pulses at an average output power of 21.1 W. The generated peak power is estimated to be 4.1 MW for soliton pulses at 0.44 µJ of pulse energy. The optical spectrum of the generated pulses [Fig. 5(a)] is centered at a wavelength of 1035.1 nm with a FWHM bandwidth of 12.3 nm. It is in good agreement with the sech^2 fit for soliton pulses. In comparison, the normalized spectrum of the gain cross-sections of Yb:Lu_2O_3 is plotted for an inversion level β of 0.3. Compared to the gain cross-sections, the central wavelength of the optical spectrum is shifted by 2 nm towards longer wavelengths. The shift is a result of the reflectivity and dispersion of the cavity components.

The pulse duration of 95 fs is measured by intensity autocorrelation [Fig. 5(b)] and has an ideal sech^2 shape for soliton pulses down to the measurement noise floor of –32 dB. The time-bandwidth product of 0.325 is close to the transform limit and 1.04 times the ideal value for sech^2 pulses. Single pulse operation was proven by a 180-ps scan with the autocorrelator and by observing the pulse train with an 18.5-ps-rise-time photodetector on a 40-GHz sampling oscilloscope [Fig. 5(c)]. Fluctuations at 0.5 ns and 1.0 ns are electronic reflections. The radio-frequency spectrum measured at the fundamental repetition frequency of 47.9 MHz shows no side peaks down to the measurement noise floor of –100 dBc and modulation-free higher harmonics confirm clean mode-locking [Fig. 5(d)]. The beam quality factor M^2 was measured to be ≤ 1.03. A summary of the parameters in mode-locked operation is given in Table 2.

For long-term operation, the pump power was slightly reduced to 126 W, decreasing the average power by 5% to 20.0 W. This suppressed a CW breakthrough that appeared during the warm-up of the system after several minutes. During a one-hour measurement in this condition, the average power and pulse duration showed no drift and fluctuated by less than 0.3% rms (Fig. 6).

Optics EXPRESS

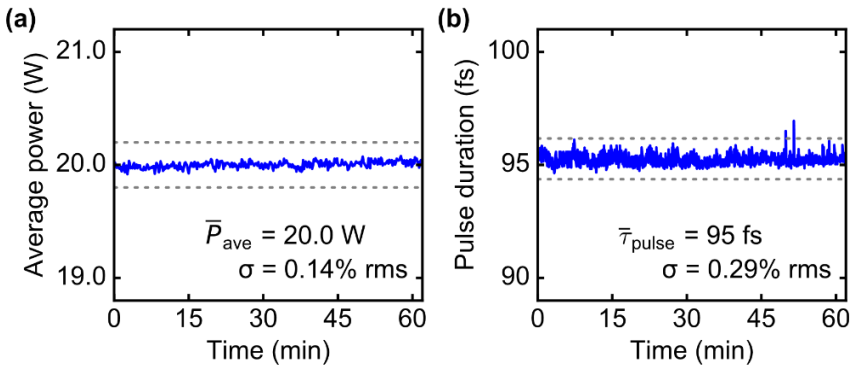

Fig. 6. (a) Average power and (b) pulse duration during a stability measurement of one hour. Corresponding averaged values are given with the root mean square (rms) error (σ). Gray dotted lines indicate the ± 1% margins of the average value.

Table 2. Summary of the mode-locking performance of the KLM Yb:Lu_2O_3 TDL oscillator for a single and double folding of the cavity on the disk.[a]

	Single folding	Double folding	Com-parison		Single folding	Double folding	Com-parison
$w_{KM,CW}$	90 µm × 150 µm	90 µm × 165 µm	≈	E_{pulse}	0.18 µJ	0.44 µJ	2 × ↑
τ_{FWHM}	88 fs	95 fs	≈	$P_{peak,\,IC}$	39 MW	33 MW	≈
$N_{Disk,RT}$	4	8	2 × ↑	$E_{pulse,\,IC}$	3.9 µJ	3.6 µJ	≈
P_{ave}	10.7 W	21.1 W	2 × ↑	$P_{ave,\,IC}$	233 W	172 W	26% ↓
η_{eff}	5.8%	16.2%	3 × ↑	f_{rep}	61 MHz	47.9 MHz	21% ↓
T_{OC}	4.6%	12.3%	3 × ↑	GDD_{RT}	–2200 fs^2	–5400 fs^2	2 × ↑
P_{peak}	1.8 MW	4.1 MW	2 × ↑	d_{KM}	2 mm	4 mm	2 × ↑
				$\lambda_{central}$	1037.6 nm	1035.1 nm	

[a]$w_{KM,CW}$: mode radius in the Kerr medium in continuous-wave operation; τ_{FWHM}: FWHM pulse duration; N_{Disk}: number of passes through the disk per cavity round-trip; P_{ave}: average power; η_{eff}: optical-to-optical efficiency; T_{OC}: output coupler transmission; P_{peak}: peak power; E_{pulse}: pulse energy; IC: intracavity; f_{rep}: repetition rate; GDD_{RT}: introduced group delay dispersion per cavity round-trip; d_{KM}: thickness of the Kerr medium; $\lambda_{central}$: central wavelength; ≈: comparable; ↑: increase; ↓: decrease.

The performance of the oscillator is compared to previous mode-locking results achieved with folding the cavity once on the disk (Table 2) [18]. In both configurations, the mode size in the KM in CW operation and the pulse duration are similar.

Doubling the number of passes through the disk per cavity round-trip enabled an increase of the average output power by a factor of two. Optical-to-optical efficiency and output coupler transmission were increased by a factor of almost three to 16.2% and 12.3%, respectively. Although peak power and pulse energy increased, the corresponding intracavity values remained comparable. This observation agrees with the geometrical scaling law of KLM TDLs [30] which relates the achievable intracavity peak power to the mode size in the KM in CW operation. As consequence of a similar intracavity peak power ($P_{peak,IC} \approx 0.88 \cdot E_{pulse,IC} / \tau_{FWHM}$), the 26% decrease in intracavity average power can be attributed to the reduced repetition rate ($E_{pulse,IC} = P_{ave} / T_{OC} \cdot f_{rep}$). The two times larger amount of introduced GDD per round-trip compensates for the stronger SPM (γ_{SPM}) in the two times thicker YAG KM plate ($E_{pulse,IC} \approx 2 \cdot 1.76 \cdot |GDD| / \gamma_{SPM} \cdot \tau_{FWHM}$). The stronger SPM is attributed to be required for the compensation of the gain narrowing caused by the increased T_{OC} to maintain the spectral bandwidth. The central wavelength is slightly shifted by 2 nm towards the gain peak in the cross sections of Yb:Lu_2O_3 at 1033 nm, which may contribute to the increased laser efficiency. We suggest that the different central wavelengths originate from the slightly different dispersion profiles of the dispersive mirrors used in both lasers.

Optics EXPRESS

4. Conclusion and outlook

We demonstrated a KLM Yb:Lu_2O_3 TDL oscillator generating 95-fs pulses at 21.1 W average power. By folding the cavity two times on the disk, the average power was increased by a factor of two with an almost three times higher optical-to-optical efficiency of 16.2%, compared to our previous result [18]. We showed that KLM TDL oscillators based on the gain material Yb:Lu_2O_3 are suitable for the generation of sub-100-fs pulses at high average power with optical-to-optical efficiencies that are comparable to Yb-doped bulk oscillators. The presented TDL oscillator has been used as single-stage driving laser for broadband THz generation via optical rectification in GaP [35]. In this case, high-power laser operation with sub-100-fs pulse duration was beneficial for the generated THz spectral bandwidth that expanded up to 5 THz at 0.3 mW of THz average power.

The average power of SESAM mode-locked Yb:Lu_2O_3 TDL oscillators was scaled from initially 20 W up to 141 W [31,36]. We anticipate that similar power-scaling should be feasible for sub-100-fs KLM Yb:Lu_2O_3 TDL oscillators. We expect that further power-scaling of sub-100-fs KLM Yb:Lu_2O_3 TDL oscillators can be achieved by scaling the intracavity peak power via adapting the mode size in the Kerr medium [30], enlarging the pump spot diameter on the disk [7] and by further increasing the number of passes through the disk. By this, we anticipate that sub-100-fs KLM Yb:Lu_2O_3 TDL oscillators operating at more than hundred watt of average power are within reach.

Funding

Swiss National Science Foundation (SNSF) (179146, 170772, 144970); German Ministry of Education and Research (BMBF) (13N14192).

Acknowledgements

The authors thank Olga Razskazovskaya (Université de Neuchâtel, Switzerland) for the fabrication of optical coatings and helpful discussions.

Experimental results presented in this work are open-access available under DOI: http://doi.org/10.23728/b2share.b5900f02cd3147cfa9f23c51f539f1d8

References

1. D. T. Reid, C. M. Heyl, R. R. Thomson, R. Trebino, G. Steinmeyer, H. H. Fielding, R. Holzwarth, Z. Zhang, P. Del'Haye, T. Südmeyer, G. Mourou, T. Tajima, D. Faccio, F. J. M. Harren, and G. Cerullo, "Roadmap on ultrafast optics," J. Opt. **18**(9), 093006 (2016).
2. T. Südmeyer, C. Kränkel, C. R. E. Baer, O. H. Heckl, C. J. Saraceno, M. Golling, R. Peters, K. Petermann, G. Huber, and U. Keller, "High-power ultrafast thin disk laser oscillators and their potential for sub-100-femtosecond pulse generation," Appl. Phys. B **97**(2), 281–295 (2009).
3. H. Zhao and A. Major, "Megawatt peak power level sub-100 fs Yb:KGW oscillators," Opt. Express **22**(25), 30425–30431 (2014).
4. U. Keller, "Ultrafast solid-state laser oscillators: a success story for the last 20 years with no end in sight," Appl. Phys. B **100**(1), 15–28 (2010).
5. S. Dewald, T. Lang, C. D. Schröter, R. Moshammer, J. Ullrich, M. Siegel, and U. Morgner, "Ionization of noble gases with pulses directly from a laser oscillator," Opt. Lett. **31**(13), 2072–2074 (2006).
6. A. Greborio, A. Guandalini, and J. Aus der Au, "Sub-100 fs pulses with 12.5-W from Yb:CALGO based oscillators," in Proc. SPIE, (2012), paper 823511.
7. A. Giesen, H. Hügel, A. Voss, K. Wittig, U. Brauch, and H. Opower, "Scalable concept for diode-pumped high-power solid-state lasers," Appl. Phys. B. **58**(5), 365–372 (1994).
8. J. Aus der Au, G. J. Spühler, T. Südmeyer, R. Paschotta, R. Hövel, M. Moser, S. Erhard, M. Karszewski, A. Giesen, and U. Keller, "16.2-W average power from a diode-pumped femtosecond Yb:YAG thin disk laser," Opt. Lett. **25**(11), 859–861 (2000).
9. B. Borchers, C. Schäfer, C. Fries, M. Larionov, and R. Knappe, "Nonlinear polarization rotation mode-locking via phase-mismatched type I SHG of a thin disk femtosecond laser," in Advanced Solid State Lasers (Optical Society of America, 2015), paper ATh4A.9.
10. F. Saltarelli, A. Diebold, I. J. Graumann, C. R. Phillips, and U. Keller, "Modelocking of a thin-disk laser with the frequency-doubling nonlinear-mirror technique," Opt. Express **25**(19), 23254–23266 (2017).

Optics EXPRESS

11. O. Pronin, J. Brons, C. Grasse, V. Pervak, G. Boehm, M.-C. Amann, V. L. Kalashnikov, A. Apolonski, and F. Krausz, "High-power 200 fs Kerr-lens mode-locked Yb:YAG thin-disk oscillator," Opt. Lett. **36**(24), 4746–4748 (2011).
12. N. Modsching, C. Paradis, F. Labaye, M. Gaponenko, I. J. Graumann, A. Diebold, F. Emaury, V. J. Wittwer, and T. Südmeyer, "Kerr lens mode-locked Yb:CALGO thin-disk laser," Opt. Lett. **43**(4), 879–882 (2018).
13. U. Keller, *Ultrafast Solid-State Lasers*, Landolt-Börnstein. Laser Physics and Applications. Subvolume B: Laser Systems. Part I (Springer, 2007).
14. M. Tokurakawa, A. Shirakawa, K. Ueda, H. Yagi, S. Hosokawa, T. Yanagitani, and A. A. Kaminskii, "Diode-pumped 65 fs Kerr-lens mode-locked Yb^{3+}:Lu_2O_3 and nondoped Y_2O_3 combined ceramic laser," Opt. Lett. **33**(12), 1380–1382 (2008).
15. M. Tokurakawa, A. Shirakawa, K. Ueda, H. Yagi, M. Noriyuki, T. Yanagitani, and A. A. Kaminskii, "Diode-pumped ultrashort-pulse generation based on Yb^{3+}:Sc_2O_3 and Yb^{3+}:Y_2O_3 ceramic multi-gain-media oscillator," Opt. Express **17**(5), 3353–3361 (2009).
16. C. J. Saraceno, O. H. Heckl, C. R. E. Baer, C. Schriber, M. Golling, K. Beil, C. Kränkel, T. Südmeyer, G. Huber, and U. Keller, "Sub-100 femtosecond pulses from a SESAM modelocked thin disk laser," Appl. Phys. B **106**(3), 559–562 (2012).
17. A. Diebold, F. Emaury, C. Schriber, M. Golling, C. J. Saraceno, T. Südmeyer, and U. Keller, "SESAM mode-locked Yb:$CaGdAlO_4$ thin disk laser with 62 fs pulse generation," Opt. Lett. **38**(19), 3842–3845 (2013).
18. C. Paradis, N. Modsching, V. J. Wittwer, B. Deppe, C. Kränkel, and T. Südmeyer, "Generation of 35-fs pulses from a Kerr lens mode-locked Yb:Lu_2O_3 thin-disk laser," Opt. Express **25**(13), 14918–14925 (2017).
19. C. R. E. Baer, C. Kränkel, O. H. Heckl, M. Golling, T. Südmeyer, R. Peters, K. Petermann, G. Huber, and U. Keller, "227-fs pulses from a mode-locked Yb:$LuScO_3$ thin disk laser," Opt. Express **17**(13), 10725–10730 (2009).
20. G. Palmer, M. Schultze, M. Siegel, M. Emons, U. Bünting, and U. Morgner, "Passively mode-locked Yb:KLu(WO_4)_2 thin-disk oscillator operated in the positive and negative dispersion regime," Opt. Lett. **33**(14), 1608–1610 (2008).
21. F. Brunner, T. Südmeyer, E. Innerhofer, F. Morier-Genoud, R. Paschotta, V. E. Kisel, V. G. Shcherbitsky, N. V. Kuleshov, J. Gao, K. Contag, A. Giesen, and U. Keller, "240-fs pulses with 22-W average power from a mode-locked thin-disk Yb:$KY(WO_4)_2$ laser," Opt. Lett. **27**(13), 1162–1164 (2002).
22. O. H. Heckl, C. Kränkel, C. R. E. Baer, C. J. Saraceno, T. Südmeyer, K. Petermann, G. Huber, and U. Keller, "Continuous-wave and modelocked Yb:YCOB thin disk laser: first demonstration and future prospects," Opt. Express **18**(18), 19201–19208 (2010).
23. C. J. Saraceno, O. H. Heckl, C. R. E. Baer, M. Golling, T. Südmeyer, K. Beil, C. Kränkel, K. Petermann, G. Huber, and U. Keller, "CW and Modelocked Operation of an Yb:(Sc,Y,Lu)2O3 Thin-disk Laser," in CLEO:2011 - Laser Applications to Photonic Applications (Optical Society of America, 2011), paper CWP1.
24. S. Ricaud, A. Jaffres, K. Wentsch, A. Suganuma, B. Viana, P. Loiseau, B. Weichelt, M. Abdou-Ahmed, A. Voss, T. Graf, D. Rytz, C. Hönninger, E. Mottay, P. Georges, and F. Druon, "Femtosecond Yb:$CaGdAlO_4$ thin-disk oscillator," Opt. Lett. **37**(19), 3984–3986 (2012).
25. S. Manjooran and A. Major, "Diode-pumped 45 fs Yb:CALGO laser oscillator with 1.7 MW of peak power," Opt. Lett. **43**(10), 2324–2327 (2018).
26. J. Brons, V. Pervak, D. Bauer, D. Sutter, O. Pronin, and F. Krausz, "Powerful 100-fs-scale Kerr-lens mode-locked thin-disk oscillator," Opt. Lett. **41**(15), 3567–3570 (2016).
27. J. Zhang, J. Brons, M. Seidel, V. Pervak, V. Kalashnikov, Z. Wei, A. Apolonski, F. Krausz, and O. Pronin, "49-fs Yb:YAG thin-disk oscillator with distributed Kerr-lens mode-locking," in European Quantum Electronics Conference (Optical Society of America, 2015), paper PD_A_1.
28. J. Brons, "High-power femtosecond laser-oscillators for applications in high-field physics," Dissertation, Ludwig-Maximilians-Universität München (2017).
29. C. J. Saraceno, F. Emaury, O. H. Heckl, C. R. E. Baer, M. Hoffmann, C. Schriber, M. Golling, T. Südmeyer, and U. Keller, "275 W average output power from a femtosecond thin disk oscillator operated in a vacuum environment," Opt. Express **20**(21), 23535–23541 (2012).
30. J. Brons, V. Pervak, E. Fedulova, D. Bauer, D. Sutter, V. Kalashnikov, A. Apolonskiy, O. Pronin, and F. Krausz, "Energy scaling of Kerr-lens mode-locked thin-disk oscillators," Opt. Lett. **39**(22), 6442–6445 (2014).
31. C. R. E. Baer, C. Kränkel, C. J. Saraceno, O. H. Heckl, M. Golling, R. Peters, K. Petermann, T. Südmeyer, G. Huber, and U. Keller, "Femtosecond thin-disk laser with 141 W of average power," Opt. Lett. **35**(13), 2302–2304 (2010).
32. C. Kränkel, "Rare-earth-doped sesquioxides for diode-pumped high-power lasers in the 1-, 2-, and 3-µm spectral range," IEEE J. Sel. Top. Quantum Electron. **21**(1), 250–262 (2015).
33. S. Yefet and A. Pe'er, "A Review of Cavity Design for Kerr Lens Mode-Locked Solid-State Lasers," Appl. Sci. (Basel) **3**(4), 1–31 (2015).
34. J. Brons, O. Pronin, M. Seidel, V. Pervak, D. Bauer, D. Sutter, V. L. Kalashnikov, A. Apolonskiy, and F. Krausz, "120 W, 4 µJ from a purely Kerr-lens mode-locked Yb:YAG thin-disk oscillator," in Advanced Solid-State Lasers Congress (Advanced Solid-State Lasers Congress, G. Huber and P. Moulton, eds., OSA Technical Digest (online), 2013), paper AF3A.4.

Optics EXPRESS

35. J. Drs, N. Modsching, C. Paradis, C. Kränkel, V. Wittwer, O. Razskazovskaya, and T. Südmeyer, "Optical rectification of ultrafast Yb-lasers: Pushing power and bandwidth of THz generation in GaP," Opt. Express. submitted.
36. S. V. Marchese, C. R. E. Baer, R. Peters, C. Kränkel, A. G. Engqvist, M. Golling, D. J. H. C. Maas, K. Petermann, T. Südmeyer, G. Huber, and U. Keller, "Efficient femtosecond high power Yb:Lu_2O_3 thin disk laser," Opt. Express **15**(25), 16966–16971 (2007).

Research Article | Vol. 29, No. 25 / 6 Dec 2021 / Optics Express 42075
Optics EXPRESS

Efficient 100-MW, 100-W, 50-fs-class Yb:YAG thin-disk laser oscillator

JULIAN FISCHER,* JAKUB DRS, NORBERT MODSCHING, FRANÇOIS LABAYE, VALENTIN J. WITTWER, AND THOMAS SÜDMEYER

Laboratoire Temps-Fréquence (LTF), Institut de Physique, Université de Neuchâtel, Avenue de Bellevaux 51, 2000 Neuchâtel, Switzerland
julian.fischer@unine.ch

Abstract: We demonstrate an efficient 102-MW peak power, 103-W average power, Kerr-lens mode-locked thin-disk laser (TDL) oscillator generating 52-fs pulses at 17.1-MHz repetition rate. The TDL is based on an Yb:YAG disk and operates in the strongly self-phase-modulation (SPM) broadened regime. In this regime, the spectral bandwidth of the oscillating pulse exceeds the available gain bandwidth by generating additional frequency components via SPM in the Kerr medium inside the laser cavity. At an optical-to-optical efficiency of 26%, our oscillator delivers a more than six times higher average power compared to any 50-fs-class laser oscillator. Compared to previous 100-W-class high-power laser oscillators, we reach this performance in a more than two times shorter pulse duration at a comparable optical-to-optical efficiency. Our TDL delivers the highest peak power of any ultrafast laser oscillator. The short pulse duration combined with high average power and peak power makes the presented TDL oscillator an attractive source for high field science and nonlinear optics.

1. Introduction

Ultrafast lasers have enabled nonlinear frequency conversion processes such as high harmonic generation (HHG), optical parametric amplification (OPA), or THz generation, providing coherent light at a wide range of photon energies [1,2]. Many experiments relying on these technologies such as multidimensional spectroscopy or pump probe measurements strongly benefit from high repetition rates allowing for shorter acquisition times. This has stimulated the development of megahertz-repetition-rate laser systems over the last decade. The resulting need for higher average powers has caused a shift from a Ti:sapphire to an Yb-based laser technology. Due to the low quantum defect and availability of efficient diode pumping, ultrafast Yb-based laser amplifier systems can reach kilowatts of average power at sub-picosecond pulse durations and megahertz repetition rates. Up to 10.4 kW at 254 fs and 80 MHz have already been demonstrated using twelve coherently combined fiber laser amplifiers [3], 620 W at 640 fs and 20 MHz using an Innoslab amplifier [4], and 1.9 kW at 1 ps and 400 kHz based on a multi-pass thin-disk amplifier [5]. The high average power, however, comes at the expense of a longer pulse duration, typically >200 fs, due to the gain bandwidth of most common Yb-doped gain materials.

Another successful approach allowing for short pulses from Yb-based gain materials is ultrafast thin-disk laser (TDL) oscillators. Thanks to the thin-disk geometry, they can operate at high peak and average powers, while keeping the favorable properties inherent to laser oscillators. TDL oscillators provide transform-limited soliton pulses without temporal pre or post features and excellent beam quality at megahertz repetition rates and can thus be used as a single-stage alternative to laser amplifier systems. The output pulses are directly suited for nonlinear frequency conversion [6] as well as for few-cycle pulse compression [7,8]. Figure 1 shows an overview of ultrafast TDL oscillators with respect to peak power and pulse duration based on the two most common mode-locking techniques. While semiconductor saturable absorber mirror (SESAM)

#442833 https://doi.org/10.1364/OE.442833
Journal © 2021 Received 27 Sep 2021; revised 18 Nov 2021; accepted 18 Nov 2021; published 2 Dec 2021

Optics EXPRESS

mode-locked TDLs have been historically well-suited for delivering the highest average powers (currently up to 350 W), they only provide these power levels at >500-fs pulse durations, limiting the achievable peak power [9–11]. On the other hand, Kerr-lens mode-locked (KLM) TDLs have been particularly successful in delivering shorter pulse durations at high average power, enabling a higher peak power. Recently, 90 MW of peak power were presented in 140-fs pulses and 220 W of average power [12]. However, even for KLM TDLs, a clear trade-off between peak power and pulse duration can be observed for sub-100-fs pulse durations [Fig. 1].

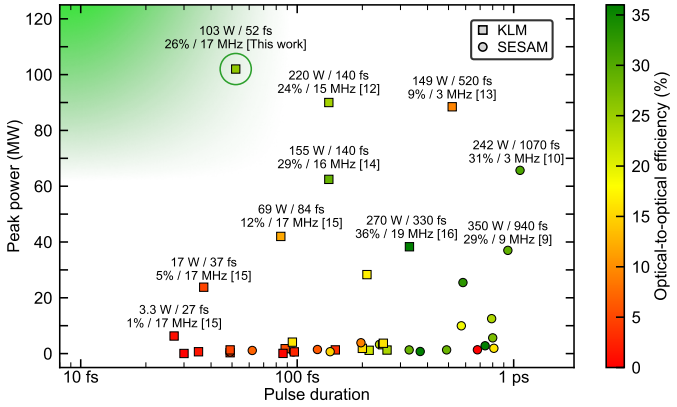

Fig. 1. Overview of sub-ps KLM and SESAM mode-locked thin-disk laser oscillators based on Yb-doped gain materials. Mode-locking techniques are distinguished by the symbol. KLM: Kerr-lens mode-locking; SESAM: semiconductor saturable absorber mirror. The most outstanding performances are labeled with average power, pulse duration, optical-to-optical efficiency, and repetition rate. The result presented in this manuscript is highlighted with the green circle. The green shaded area represents the favored region of laser operation at shortest pulse duration and highest peak power. References: [9,10,12–16].

As we have recently shown in [15], so far the most promising direction towards sub-100-fs pulse durations at high peak powers is based on operating a KLM Yb:YAG TDL oscillator in the strongly self-phase modulation (SPM) broadened regime. In this regime, additional frequency components outside of the gain bandwidth are generated by excessive SPM in the Kerr medium inside the laser cavity. We have demonstrated the shortest pulse duration of a TDL oscillator corresponding to 27 fs at 3.3-W average power and 6-MW peak power, but only with 1% of optical-to-optical efficiency ("efficiency" in the following). We have also shown 84-fs pulses at 69 W and 42 MW, however, even here the efficiency was still only 12%, limiting the achievable average and peak power.

Whereas our previous result was optimized for shortest pulse duration, in this work, we optimized our KLM Yb:YAG TDL operating in the SPM-broadened regime towards increased output performance, i.e. highest peak power, and efficiency. At 103 W of average output power with 52-fs pulses, our TDL delivers 102 MW of peak power at 26% efficiency. The peak power is the highest delivered by any ultrafast laser oscillator [12,13]. Compared to previous 100-W-class ultrafast TDL oscillators, we reach this performance range in a more than two times shorter pulse duration while maintaining a comparable efficiency [9–12,14].

2. Experimental setup

The setup of the KLM TDL oscillator is shown in Fig. 2. The oscillator is housed in a vacuum chamber with a footprint of 0.8×1.6 m^2 and operates at a pressure of around 1 mbar. The laser

Optics EXPRESS

is built using a commercially available TDL head (Trumpf GmbH) designed for 36 passes of the pump. An Yb:YAG disk with a thickness of ~100-µm and ~20-m concave radius of curvature (RoC) is used. The disk is optically pumped on a 2.9-mm diameter pump spot at a wavelength of 969 nm with a fiber-coupled wavelength-stabilized pump diode (Dilas Diodenlaser GmbH). The pump system is capable of delivering up to 2 kW of pump average power, but we limited ourselves to a maximum pump power of 400 W, resulting in a pump intensity of ~6 kW/cm^2 on the disk, to prevent the risk of damaging the disk.

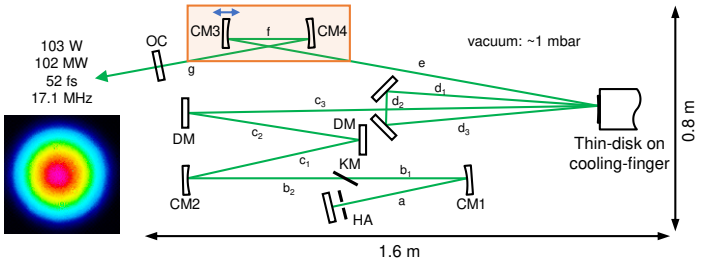

Fig. 2. Schematic of the Kerr-lens mode-locked Yb:YAG thin-disk laser oscillator with double pass over the disk. The orange box highlights the tight focus created between two curved mirrors, CM3 and CM4, which has been implemented for intra-oscillator high harmonic generation. As indicated by the double arrow, CM3 is mounted on a translation stage used for fine-tuning of the laser cavity during mode-locked operation. The inset shows the beam profile of the laser output in mode-locked operation when the laser generates 52-fs pulses at 103-W average power. HA: hard aperture; CM1 and CM2: concave mirror with 1-m radius of curvature (RoC); KM: Kerr medium; DM: dispersive mirror; CM3 and CM4: concave mirror with 150-mm and 250-mm RoC; OC: output coupler. Cavity lengths: a = 520 mm; b_1 = 475 mm; b_2 = 550 mm; c_1+c_2+c_3 = 3455 mm; d_1+d_2+d_3 = 1545 mm; e = 1780mm; f = ~200 mm; g = 250 mm.

The laser cavity is folded twice over the disk for higher roundtrip gain. Following the standard scheme of Kerr-lens mode-locking for TDLs [17], a wedged (30 arcmin) 1-mm-thick *c*-cut sapphire plate acts as the Kerr medium which is placed under Brewster's angle in the vicinity of a first intracavity focus created by two concave mirrors, CM1 and CM2, with 1-m RoC. A water-cooled copper plate with a 4.4-mm diameter hole serves as a hard aperture for the fast-saturable loss. The Kerr medium is purged with oxygen from both sides to prevent contamination during laser operation, for example through carbon deposition in vacuum. Two -500-fs^2 dispersive mirrors (DM) in folding configuration introduce a total negative group delay dispersion (GDD) of -2000 fs^2 per cavity roundtrip. The corresponding spectral profile of the GDD is shown in Fig. 3(a), which was obtained by measuring the GDD of the DMs with an in-house developed white-light interferometer and multiplied by the number of bounces per cavity roundtrip. The TDL setup has been originally designed for intra-oscillator HHG [18] and the output coupling arm of the oscillator thus contains an extension intended to create a tight focus for HHG. It consists of two concave mirrors with a RoC of 150 mm (CM3) and 250 mm (CM4) leading to an estimated tight focus of ~20-µm radius in mode-locked operation. Due to the tight focus, operation of the TDL strictly requires vacuum. In ambient air, the intensity in the focus would exceed the air ionization level and the plasma formation would prevent mode-locking. CM3 is placed on a motorized linear stage, allowing to tune the laser cavity from a position where it is easy to start the mode-locking operation to a position of improved intracavity and output performance. Before mode-locking can be initialized, the distance between CM3 and CM4 is slightly increased in order to decrease the beam size on the aperture, facilitating the onset of mode-locking. Mode-locked operation is initiated by shaking one of the cavity mirrors

Optics EXPRESS

through a piezo actuator. After mode-locking is started, the pump power is decreased until the continuous-wave (cw) breakthrough otherwise visible in the optical spectrum disappears. Then, the pump power is again slowly increased while at the same time the distance between CM3 and CM4 is decreased, increasing the beam size on the hard aperture. This procedure allows operation of the TDL at maximum pump power without the appearance of a cw-breakthrough. Between the mode-locking starting position and the final, high-power operation position, the linear stage is moved by less than 1 mm, resulting in a ~20% decrease in pulse duration and a peak power increase by a factor of ~2 while the pump power is also increased by a factor of ~2. The cavity remains stable for cw-operation in all configurations. Further details about the optimization of the TDL regarding, e.g., the hard aperture size or the thickness of the Kerr medium are given in our recent publication [15]. The cavity end mirror after the tight focus serves as an output coupler with a transmission (T_{OC}) of 8.5%.

To increase the thermal stability of the laser system in vacuum, the cavity is built on a water-cooled breadboard and most of the mirror mounts are water-cooled. The optical coatings of the dispersive and highly reflective mirrors have been designed inhouse and grown in our ion-beam sputtering coating facility.

3. Experimental results

Table 1 summarizes the laser parameters and mode-locking performance of our TDL. The oscillator delivers an output power of 103 W, a peak power of 102 MW, and pulse energy of 5.5 µJ at a pulse duration of 52 fs. These parameters correspond to an intracavity peak and intracavity average power of 1.2 GW and 1.2 kW, respectively. The pump power of 400 W leads to an efficiency of 26%. This efficiency is for the first time comparable to the efficiency of other 100-W-class high-power TDLs operating with significantly longer pulses [9–12,14].

Table 1. Laser parameters and corresponding mode-locking performance of our TDL oscillator.

Laser parameter	Value	Laser parameter	Value
Output coupler transmission	8.5%	Pulse energy	5.5 µJ
Introduced roundtrip GDD	-2000 fs^2	Intracavity peak power	1.2 GW
Hard aperture diameter	4.4 mm	Intracavity average power	1.2 kW
Pump power	400 W	Pulse duration	52 fs
Output power	103 W	Central wavelength	1027.3 nm
Optical-to-optical efficiency	26%	FWHM bandwidth	21.4 nm
Peak power	102 MW	Repetition rate	17.1 MHz

Figure 3(a) shows the optical spectrum of the output pulses together with the normalized gain cross-section of Yb:YAG at an inversion level of 0.3. The optical spectrum is centered at a wavelength of 1027.3 nm. The central wavelength is blue-shifted by ~2 nm, away from the gain peak of Yb:YAG at 1030 nm. With a full width at half maximum (FWHM) bandwidth of 21.4 nm, the optical spectrum exceeds the ~8-nm FHWM gain bandwidth of Yb:YAG more than twice, indicating operation of the TDL in the strongly SPM-broadened regime [15,19,20]. Despite a small shoulder at the longer wavelength side, a feature that is commonly observed for TDL oscillators operating in the SPM-broadened regime [15,19,20], the $sech^2$ fit agrees well with the shape expected for soliton pulses. Also, the intensity autocorrelation of the 52-fs pulses is in excellent agreement with the fit for soliton pulses [Fig. 3(b)]. We achieve an ideal time-bandwidth product of 0.315, indicating the generation of transform-limited soliton pulses. The radio-frequency spectrum measured at the fundamental repetition frequency of 17.1 MHz shows no side peaks [Fig. 3(c)]. Modulation-free higher harmonics confirm clean mode-locking [inset of Fig. 3(c)]. We confirmed single pulse operation by a 180-ps scan in the autocorrelator

Optics EXPRESS

and by observing the pulse train with an 18.5-ps-rise-time photodetector on a 40-GHz sampling oscilloscope [Fig. 3(d)]. The output pulses feature an excellent fundamental mode Gaussian beam profile [inset of Fig. 2].

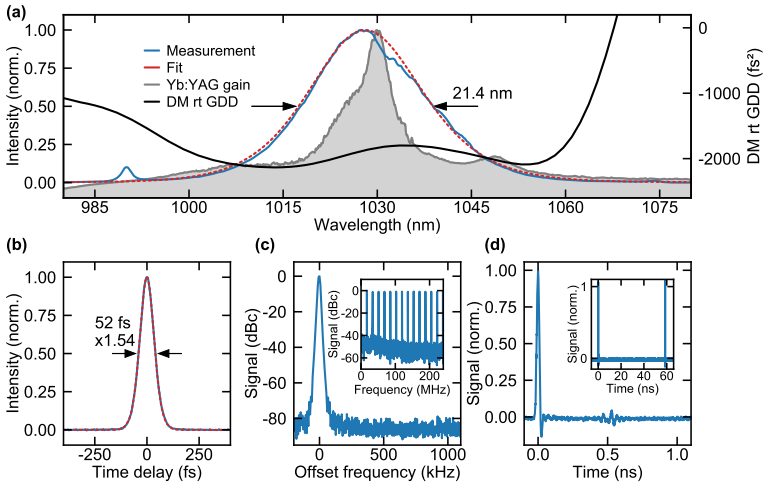

Fig. 3. Characterization of the Kerr-lens mode-locked Yb:YAG thin-disk laser oscillator. (a) Normalized optical spectrum of the laser output with sech^2 fit. In addition, the normalized Yb:YAG gain cross section at an inversion level of 0.3 (data taken from [22]) and the total group delay dispersion (GDD) introduced by the dispersive mirrors (DM) per cavity round-trip (rt) are shown. (b) Intensity autocorrelation trace with fit for soliton pulses. (c) Radio-frequency (RF) spectrum of the fundamental repetition rate (f_{rep}) at 17.1 MHz measured with 10-kHz resolution bandwidth (RBW). The inset shows the RF-spectrum of the higher f_{rep} harmonics measured with 30-kHz RBW. (d) Sampling oscilloscope trace for 1-ns and 70-ns (inset) time window.

Within our pump power restriction of 400 W (~6 kW/cm^2) set to prevent damage of the disk, we were not able to mode-lock the laser at a T_{OC} higher than 8.5%. We expect that higher pump intensities of ~10 kW/cm^2 [16,21] should allow for mode-locking at a T_{OC} above 10% and a corresponding performance improvement. High-power operation of our TDL is currently limited to a few minutes by the overheating of the non-water-cooled connector of the pump-delivery fiber in the vacuum environment. After changing to a water-cooled fiber, we expect long-term operability.

4. Conclusion and outlook

We have demonstrated an efficient 102-MW peak power, 103-W average power KLM TDL oscillator generating 52-fs pulses at 17.1-MHz repetition rate. The TDL oscillator is based on Yb:YAG gain material and operates in the strongly SPM-broadened regime at an efficiency of 26%. Our average output power is more than six times higher than any previous 50-fs-class laser oscillator [15,19,20]. Furthermore, we achieve the highest peak power delivered by any ultrafast laser oscillator [12,13]. Compared to previous 100-W-class high-power TDL oscillators, we reach this performance range in a more than two times shorter pulse duration while maintaining a comparable efficiency [9–12,14]. The clean soliton pulses with excellent beam quality and high peak power are well suited for broadband THz generation [23] or oscillator-driven HHG [24].

Additionally, the output of our TDL oscillator is very suitable for consecutive temporal pulse compression. Whereas efficient compression starting from several hundred femtoseconds down

Optics EXPRESS

to few-cycle pulses is already feasible [7,25–27], the compression often comes with reduced pulse contrast as well as limited beam quality and thus remains a challenging task. Thanks to our clean 52-fs soliton pulses and assuming a compression ratio of ten for a single compression stage [8,28,29], we expect being able to reach few-cycle pulse durations within a single instead of the typically at least two required cascaded temporal compression stages. This would make our source an excellent choice for applications requiring few-cycle pulses at high pulse contrast, excellent beam quality, and MHz repetition rates. After carrier-envelope phase stabilization of the TDL operating in the SPM-broadened regime [30], even applications in the single-cycle regime could be addressed.

Since the thin-disk concept is power scalable and we have not encountered any physical limitation, we expect that further power-scaling is feasible and that 50-fs-class TDL oscillators operating at several hundred megawatts of peak power are within reach.

Funding. Schweizerischer Nationalfonds zur Förderung der Wissenschaftlichen Forschung (200020_179146, 200020_200774, 206021_144970, 206021_170772, 206021_198176).

Disclosures. The authors declare that there are no conflicts of interest related to this article.

Data availability. Data underlying the results presented in this paper are available in Ref. [31].

References

1. D. T. Reid, C. M. Heyl, R. R. Thomson, R. Trebino, G. Steinmeyer, H. H. Fielding, R. Holzwarth, Z. Zhang, P. Del'Haye, T. Südmeyer, G. Mourou, T. Tajima, D. Faccio, F. J. M. Harren, and G. Cerullo, "Roadmap on ultrafast optics," J. Opt. **18**(9), 093006 (2016).
2. P. U. Jepsen, D. G. Cooke, and M. Koch, "Terahertz spectroscopy and imaging – Modern techniques and applications," Laser Photonics Rev. **5**(1), 124–166 (2011).
3. M. Müller, C. Aleshire, A. Klenke, E. Haddad, F. Légaré, A. Tünnermann, and J. Limpert, "10.4 kW coherently combined ultrafast fiber laser," Opt. Lett. **45**(11), 3083–3086 (2020).
4. P. Russbueldt, T. Mans, J. Weitenberg, H. D. Hoffmann, and R. Poprawe, "Compact diode-pumped 1.1 kW Yb:YAG Innoslab femtosecond amplifier," Opt. Lett. **35**(24), 4169–4171 (2010).
5. T. Dietz, M. Jenne, D. Bauer, M. Scharun, D. Sutter, and A. Killi, "Ultrafast thin-disk multi-pass amplifier system providing 1.9 kW of average output power and pulse energies in the 10 mJ range at 1 ps of pulse duration for glass-cleaving applications," Opt. Express **28**(8), 11415–11423 (2020).
6. C. Paradis, J. Drs, N. Modsching, O. Razskazovskaya, F. Meyer, C. Kränkel, C. J. Saraceno, V. J. Wittwer, and T. Südmeyer, "Broadband terahertz pulse generation driven by an ultrafast thin-disk laser oscillator," Opt. Express **26**(20), 26377–26384 (2018).
7. C.-L. Tsai, F. Meyer, A. Omar, Y. Wang, A.-Y. Liang, C.-H. Lu, M. Hoffmann, S.-D. Yang, and C. J. Saraceno, "Efficient nonlinear compression of a mode-locked thin-disk oscillator to 27 fs at 98 W average power," Opt. Lett. **44**(17), 4115–4118 (2019).
8. O. Pronin, M. Seidel, F. Lücking, J. Brons, E. Fedulova, M. Trubetskov, V. Pervak, A. Apolonski, T. Udem, and F. Krausz, "High-power multi-megahertz source of waveform-stabilized few-cycle light," Nat. Commun. **6**(1), 6988 (2015).
9. F. Saltarelli, I. J. Graumann, L. Lang, D. Bauer, C. R. Phillips, and U. Keller, "Power scaling of ultrafast oscillators: 350-W average-power sub-picosecond thin-disk laser," Opt. Express **27**(22), 31465–31474 (2019).
10. C. J. Saraceno, F. Emaury, C. Schriber, M. Hoffmann, M. Golling, T. Südmeyer, and U. Keller, "Ultrafast thin-disk laser with 80 µJ pulse energy and 242 W of average power," Opt. Lett. **39**(1), 9–12 (2014).
11. C. J. Saraceno, F. Emaury, O. H. Heckl, C. R. E. Baer, M. Hoffmann, C. Schriber, M. Golling, T. Südmeyer, and U. Keller, "275 W average output power from a femtosecond thin disk oscillator operated in a vacuum environment," Opt. Express **20**(21), 23535–23541 (2012).
12. S. Goncharov, K. Fritsch, and O. Pronin, "100 MW Thin-Disk Oscillator," in 2021 *Conference on Lasers and Electro-Optics Europe and European Quantum Electronics Conference, OSA Technical Digest* (Optical Society of America, 2021), paper cf_4_1.
13. N. Kanda, A. A. Eilanlou, T. Imahoko, T. Sumiyoshi, Y. Nabekawa, M. Kuwata-Gonokami, and K. Midorikawa, "High-Pulse-Energy Yb:YAG Thin Disk Mode-Locked Oscillator for Intra-Cavity High Harmonic Generation," in Advanced Solid State Lasers Congress (Optical Society of America, 2013), paper AF3A-8.
14. J. Brons, V. Pervak, D. Bauer, D. Sutter, O. Pronin, and F. Krausz, "Powerful 100-fs-scale Kerr-lens mode-locked thin-disk oscillator," Opt. Lett. **41**(15), 3567–3570 (2016).
15. J. Drs, J. Fischer, N. Modsching, F. Labaye, V. J. Wittwer, and T. Südmeyer, "Sub-30-fs Yb:YAG thin-disk laser oscillator operating in the strongly self-phase modulation broadened regime," Opt. Express **29**(22), 35929–35937 (2021).
16. J. Brons, V. Pervak, E. Fedulova, D. Bauer, D. Sutter, V. Kalashnikov, A. Apolonskiy, O. Pronin, and F. Krausz, "Energy scaling of Kerr-lens mode-locked thin-disk oscillators," Opt. Lett. **39**(22), 6442–6445 (2014).

Optics EXPRESS

17. O. Pronin, J. Brons, C. Grasse, V. Pervak, G. Boehm, M.-C. Amann, V. L. Kalashnikov, A. Apolonski, and F. Krausz, "High-power 200 fs Kerr-lens mode-locked Yb:YAG thin-disk oscillator," Opt. Lett. **36**(24), 4746–4748 (2011).
18. J. Fischer, J. Drs, F. Labaye, N. Modsching, V. Wittwer, and T. Südmeyer, "Intra-oscillator high harmonic generation in a thin-disk laser operating in the 100-fs regime," Opt. Express **29**(4), 5833–5839 (2021).
19. C. Paradis, N. Modsching, V. J. Wittwer, B. Deppe, C. Kränkel, and T. Südmeyer, "Generation of 35-fs pulses from a Kerr lens mode-locked Yb:Lu_2O_3 thin-disk laser," Opt. Express **25**(13), 14918–14925 (2017).
20. J. Zhang, J. Brons, M. Seidel, V. Pervak, V. Kalashnikov, Z. Wei, A. Apolonski, F. Krausz, and O. Pronin, "49-fs Yb:YAG thin-disk oscillator with distributed Kerr-lens mode-locking," in *European Quantum Electronics Conference* (Optical Society of America, 2015), paper PD_A_1.
21. J. Brons, "High-power femtosecond laser-oscillators for applications in high-field physics," Dissertation, Ludwig-Maximilians-Universität München (2017).
22. T. Südmeyer, C. Kränkel, C. R. E. Baer, O. H. Heckl, C. J. Saraceno, M. Golling, R. Peters, K. Petermann, G. Huber, and U. Keller, "High-power ultrafast thin disk laser oscillators and their potential for sub-100-femtosecond pulse generation," Appl. Phys. B **97**(2), 281–295 (2009).
23. C. J. Saraceno, "Mode-locked thin-disk lasers and their potential application for high-power terahertz generation," J. Opt. **20**(4), 044010 (2018).
24. S. Hädrich, J. Rothhardt, M. Krebs, S. Demmler, A. Klenke, A. Tünnermann, and J. Limpert, "Single-pass high harmonic generation at high repetition rate and photon flux," J. Phys. B At. Mol. Opt. Phys. **49**(17), 172002 (2016).
25. C. Grebing, M. Müller, J. Buldt, H. Stark, and J. Limpert, "Kilowatt-average-power compression of millijoule pulses in a gas-filled multi-pass cell," Opt. Lett. **45**(22), 6250–6253 (2020).
26. Y.-G. Jeong, R. Piccoli, D. Ferachou, V. Cardin, M. Chini, S. Hädrich, J. Limpert, R. Morandotti, F. Légaré, B. E. Schmidt, and L. Razzari, "Direct compression of 170-fs 50-cycle pulses down to 1.5 cycles with 70% transmission," Sci. Rep. **8**(1), 11794 (2018).
27. G. Barbiero, H. Wang, M. Graßl, S. Gröbmeyer, D. Kimbaras, M. Neuhaus, V. Pervak, T. Nubbemeyer, H. Fattahi, and M. F. Kling, "Efficient nonlinear compression of a thin-disk oscillator to 8.5 fs at 55 W average power," Opt. Lett. **46**(21), 5304–5307 (2021).
28. K. F. Mak, M. Seidel, O. Pronin, M. H. Frosz, A. Abdolvand, V. Pervak, A. Apolonski, F. Krausz, J. C. Travers, and P. St. J. Russell, "Compressing μJ-level pulses from 250 fs to sub-10 fs at 38-MHz repetition rate using two gas-filled hollow-core photonic crystal fiber stages," Opt. Lett. **40**(7), 1238–1241 (2015).
29. R. Klas, A. Kirsche, M. Gebhardt, J. Buldt, H. Stark, S. Hädrich, J. Rothhardt, and J. Limpert, "Ultra-short-pulse high-average-power megahertz-repetition-rate coherent extreme-ultraviolet light source," PhotoniX **2**, 4 (2021).
30. N. Modsching, C. Paradis, P. Brochard, N. Jornod, K. Gürel, C. Kränkel, S. Schilt, V. J. Wittwer, and T. Südmeyer, "Carrier-envelope offset frequency stabilization of a thin-disk laser oscillator operating in the strongly self-phase modulation broadened regime," Opt. Express **26**(22), 28461–28467 (2018).
31. J. Fischer, "Efficient 100-MW, 100-W, 50-fs-class Yb:YAG thin-disk laser oscillator,"*EUDAT* (2021).

Research Article | Vol. 29, No. 22 / 25 Oct 2021 / Optics Express 35929
Optics EXPRESS

Sub-30-fs Yb:YAG thin-disk laser oscillator operating in the strongly self-phase modulation broadened regime

JAKUB DRS,* JULIAN FISCHER, NORBERT MODSCHING, FRANÇOIS LABAYE, VALENTIN J. WITTWER, AND THOMAS SÜDMEYER

Laboratoire Temps-Fréquence (LTF), Institut de Physique, Université de Neuchâtel, Avenue de Bellevaux 51, 2000 Neuchâtel, Switzerland
*jakub.drs@unine.ch

Abstract: We experimentally investigate the limits of pulse duration in a Kerr-lens mode-locked Yb:YAG thin-disk laser (TDL) oscillator. Thanks to its excellent mechanical and optical properties, Yb:YAG is one of the most used gain materials for continuous-wave and pulsed TDLs. In mode-locked operation, its 8-nm wide gain bandwidth only directly supports pulses with a minimum duration of approximately 140 fs. For achieving shorter pulses, a Kerr-lens mode-locked TDL oscillator can be operated in the strongly self-phase modulation (SPM) broadened regime. Here, the spectral bandwidth of the oscillating pulse exceeds the available gain bandwidth by generating additional frequencies via SPM inside the Kerr medium. In this work, we study and compare different laser configurations in the strongly SPM-broadened regime. Starting with a configuration providing 84-fs pulses at 69 W average power at 17 MHz repetition rate, we reduce the pulse duration by optimizing various mode-locking parameters. One crucial parameter is the dispersion control which was provided by in-house-developed dispersive mirrors produced by ion-beam sputtering (IBS). We discuss trade-offs in average power, pulse duration, efficiency, and intra-cavity peak power. For the configuration operating at the highest SPM-broadening, we achieve a minimum pulse duration of 27 fs, which represents the shortest pulse duration directly generated by any ultrafast TDL oscillator. The corresponding full width at half maximum (FWHM) spectral bandwidth exceeds more than five times the FWHM gain bandwidth. The average output power of 3.3 W is moderate for ultrafast TDL oscillators, but higher than other Yb-based laser oscillators operating at this pulse duration. Additionally, the corresponding intra-cavity peak power of 0.8 GW is highly attractive for implementing intra-cavity extreme nonlinear optical interactions such as high harmonic generation.

1. Introduction

Ultrafast lasers have revolutionized many scientific fields [1]. For applications relying on few-cycle pulses, Ti:sapphire lasers have been the workhorse. But since the last decade, also Yb-based lasers have started entering this domain, gradually reaching shorter and shorter pulse durations. Currently, pulses below 18 fs have been demonstrated directly generated by an Yb-based bulk laser oscillator [2,3]. The properties of Yb-doped gain materials, in particular, the low quantum defect and the pumping wavelength compatible with efficient laser diodes, make these lasers much better suited for high-power applications otherwise inaccessible to the Ti:sapphire technology. On the other hand, decreasing the pulse duration of Yb-based lasers is much more challenging because of the narrower gain bandwidth compared to Ti:sapphire.

A successful laser technology specifically designed for Yb-doped materials is the thin-disk laser (TDL) [4]. Thanks to the thin-disk geometry allowing for extremely efficient cooling and very large beam sizes in the gain material, ultrafast TDL oscillators [5] can handle the highest

#440196 https://doi.org/10.1364/OE.440196
Journal © 2021 Received 11 Aug 2021; revised 4 Oct 2021; accepted 6 Oct 2021; published 18 Oct 2021

Optics EXPRESS

average and peak intra-cavity powers among all mode-locked laser oscillator technologies [6]. As such, they can serve as a single-stage alternative to laser amplifier systems directly delivering clean transform limited soliton pulses at excellent beam quality and megahertz repetition rates. Ultrafast TDL oscillators have demonstrated output powers up to 350 W in 1-ps pulses [7] or 150 W in 140-fs pulses [8]. Moreover, the high intra-cavity performance of TDL oscillators makes this technology an excellent candidate for driving nonlinear frequency conversion directly inside the laser cavity such as intra-oscillator high harmonic generation (HHG) [9].

Decreasing the pulse duration of the TDL oscillators has been an important goal since more than a decade [10]. Up to nowadays, it has been mostly believed that short pulse durations (<100 fs) require broadband gain materials. A lot of effort has been, thus, invested into mode-locking studies using disks based on various broadband Yb-doped gain materials such as Yb:$LuScO_3$ [11], Yb:Sc_2O_3 [12], Yb:CALGO [13,14], and Yb:Lu_2O_3 [15,16]. Unfortunately, despite the fact that most of these materials have been very useful in the bulk geometry, in the thin-disk, they have not yet been particularly successful. The main limitation seems to be either the not yet sufficient crystal growth quality required for production of high-quality disks, or the inferior thermal properties and the lower gain of these materials, which did not yet allow to fully harness their potential in the thin-disk geometry for high-power operation. The highest average power achieved by a TDL oscillator using these materials in the sub-100-fs regime has been so far limited to ~20 W [16]. This can be also identified from Fig. 1 showing an overview of state-of-the-art TDL oscillators based on different Yb-doped materials. Here, the broadband, but much less commonly available gain materials depicted in red, clearly dominate the left part of the graph corresponding to short pulse durations. But one can also clearly identify the trade-off between pulse duration and average power which is strongly decreasing for shorter pulses. On the other hand, the Yb:YAG gain material depicted by the green markers represents the well-developed industrial standard for high-power applications. High-quality disks are commercially available and are suitable for several hundred watts of output power. Unfortunately, its moderate gain bandwidth of ~8-nm full width at half maximum (FWHM) directly supports only a pulse duration down to ~140 fs. In 2015, it has been shown that the pulse duration of an Yb:YAG TDL oscillator can be decreased beyond this limit by utilizing a distributed Kerr-lens mode-locking (KLM) scheme [17]. The laser emitted 49-fs pulses at 3.5 W of average power and 3.5% optical-to-optical efficiency. Here the shorter pulse duration was achieved by operating the laser oscillator in the self-phase modulation (SPM) broadened regime, where the frequencies outside of the gain bandwidth are generated by intra-cavity SPM inside the Kerr medium, as also shown in [18]. The operation in the SPM-broadened regime, however, still follows the standard soliton mode-locking scheme, where the phase shift induced by SPM is compensated by the one from anomalous dispersion and combined with saturable losses resulting in a stable roundtrip soliton solution.

In our study, we further exploit the strongly SPM-broadened regime using a KLM Yb:YAG TDL oscillator. We show three laser configurations operating at 84 fs with 69 W of average power, 37 fs with 17 W, and 27 fs with 3.3 W, by far exceeding the performance achieved with broadband Yb-doped gain materials as shown by the star markers in Fig. 1. We further discuss the trade-off between different parameters of our laser operating in the strongly SPM-broadened regime in a comprehensive table and show the dispersion profile introduced by our in-house developed dispersive mirrors. The 27-fs configuration represents the shortest pulse duration of any TDL oscillator [14] and the corresponding intra-cavity peak power of ~0.8 GW is extremely promising for intra-oscillator HHG. This demonstrates that at the current state of development, the most promising direction toward high-power short-pulse TDL oscillators is still using commercially available Yb:YAG disks, while operating the KLM laser in the strongly SPM-broadened regime.

We expect being able to further increase the output power of our laser toward the 100-W level at a few tens of femtoseconds. This together with the clean $sech^2$-shaped optical spectrum and excellent beam quality, inherent to laser oscillators, should make our TDL oscillator an excellent

Optics EXPRESS

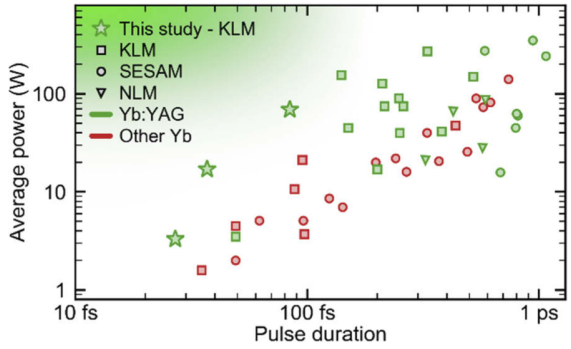

Fig. 1. Overview of various Yb-based TDL oscillators operating at >1 W of average power and <1-ps pulse duration. The color code depicts Yb:YAG in green and other more broadband Yb-doped gain materials in red. Different mode-locking mechanisms are indicated by the markers: squares - Kerr-lens mode-locking (KLM), circles - semiconductor saturable absorber mirror (SESAM) mode-locking, triangles - nonlinear mirror mode-locking (NLM). The targeted area of shortest pulse duration and highest average power is highlighted by the green shaded area. The references for the graph can be found in [9].

candidate for subsequent nonlinear pulse compression toward single-cycle pulses. This will highly benefit various experiments, particularly in the domain of attosecond science.

2. Experimental setup

The TDL oscillator setup is depicted in Fig. 2. The whole system, originally designed for driving intra-oscillator HHG [19], is housed in a vacuum chamber with a footprint of 0.8×1.6 m^2 and operates at ~100 mbar of pressure. The cavity design is inspired by the power-scaling approach for KLM TDLs presented in [20]. The laser cavity is built around a commercial TDL head from TRUMPF GmbH designed for 36 passes of the pump through a ~100-µm-thick Yb:YAG disk. The disk is optically pumped by a 2-kW, 969-nm volume-Bragg-grating-stabilized fiber-coupled diode from DILAS Diodenlaser GmbH. The cavity is folded twice over the disk, increasing the gain per cavity roundtrip. For KLM of the TDL oscillator [21], a sapphire plate at the Brewster's angle is placed in the vicinity of an intra-cavity focus created by two concave mirrors (CM1, CM2) with 1-m radius of curvature (RoC). A water-cooled copper hard aperture is placed close to one laser end mirror. Several dispersive mirrors (DM) introduce a negative group delay dispersion (GDD), balancing the positive dispersion of the Kerr and gain medium and the SPM. The optical coatings of the mirrors have been designed and grown inhouse in our ion-beam sputtering coating facility. Mode-locked operation in vacuum is initialized by shaking one of the cavity mirrors mounted on a piezo stage. The second cavity end mirror serves as an output coupler. An imaging cavity extension consisting of two focusing mirrors (CM3, CM4) is introduced into the output coupling arm of the laser, originally intended for creating a tight focus at an HHG gas target. One of the tight focus mirrors (CM3) is placed on a motorized linear stage, allowing for fine-tuning of the laser cavity during the mode-locked operation. The stage can be moved within ~1-mm travel range between a position where the laser easily mode-locks to a position of highest laser performance. The cavity, however, remains stable for all positions even with negligible Kerr effect in the case of continuous-wave operation.

Due to the presence of the tight focus, our laser requires vacuum environment for its operation. In ambient air, the intensity in the focus would exceed the air ionization level and the plasma formation would prevent stable mode-locked operation. On the other hand, a common issue of

Optics EXPRESS

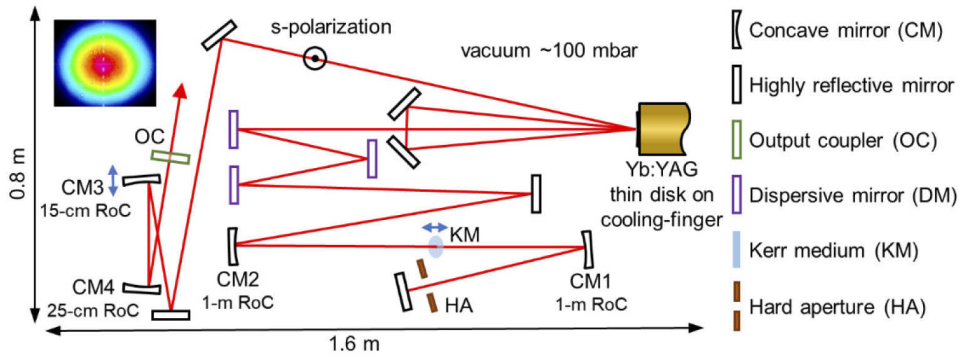

Fig. 2. Schematic of the Kerr-lens mode-locked Yb:YAG TDL oscillator with a double pass on the disk. An imaging cavity extension with concave 15-cm and 25-cm RoC mirrors creates a tight-focus which can be used for an HHG gas target. CM3 is mounted on a translation stage that allows for fine tuning of the cavity during laser operation from a position where it is easy to mode-lock to a position of highest laser performance. The inset shows the beam profile of the 27-fs laser configuration during mode-locked operation.

optical systems operated in vacuum is the deposition of carbon on the optics experiencing high intensities such as the Kerr medium inside the laser [22]. As a compromise between both effects, we selected a vacuum level of 100 mbar. At this pressure, the SPM and dispersion induced by air are still negligible compared to the other cavity components.

3. Experimental results

The here presented results correspond to two individual experiments. The first one, performed in 2020, was focused on increasing the average power in the sub-100-fs regime, yielding 69 W of average power at 84-fs pulse duration. Unfortunately, during this experiment, our fiber for pump power delivery suffered a damage due to insufficient cooling of the collimation unit in the vacuum environment. Since we have not yet fully resolved this issue with the pump delivery, we have decreased the pump spot diameter on the disk in order to reduce the required pump power for the second experiment targeting for shortest pulse duration. Additionally, we have optimized the dispersion in the detection line to compensate for the transmissive elements (output coupler, vacuum window, telescope lenses). We have also switched from p- to s-polarization by turning the Brewster's angle Kerr medium by 90° in order to benefit from the flatter dispersion profile of our 45° angle of incidence cavity mirrors in s-polarization. For all experiments, we have limited ourselves to a pump intensity of ~6 kW/cm^2 to prevent damage of the disk.

Each of the presented laser configuration was individually experimentally optimized. The degrees of freedom for the optimization included the GDD introduced by the DMs, thickness and position of the sapphire plate used as a Kerr medium, the size of the hard aperture, output-coupling rate, the position of the detuning stage of the CM3, and the pump power. A set of semi-empirical scaling rules can be formulated to aid with the optimization process:

- The pulse duration scales approximately linearly with the introduced GDD down to the point where the laser does not mode-lock anymore.
- Decreasing the thickness of the Kerr medium increases the intra-cavity peak power, but also leads to an increased pulse duration.

Optics EXPRESS

- Moving the Kerr medium further away from the intra-cavity focus towards the CM2 improves the intra-cavity peak power but increases the difficulty to initiate mode-locking of the laser.

The position of CM3 is initially adjusted for easiest mode-locking and later allows for elimination of the continuous-wave lasing break-through which otherwise appears at higher pump powers, preventing a further pump increase. The size of the hard aperture has a minor influence, since the size of the beam can be tuned using the position of the CM3, but typically has a weak optimum depending on the laser configuration.

The experimental results of the laser configurations are summarized in Fig. 3 and Table 1. The 84-fs and 37-fs configuration were optimized for highest output power at an introduced total negative GDD per cavity roundtrip of -6000 fs^2 and -1500 fs^2, respectively. The 84-fs configuration allows for stable mode-locking up to an output coupling rate of 12% and the 37-fs configuration up to 5%, resulting in an average power of 69 W and 17 W, respectively. The required pump power of 580 W and 350 W leads to optical-to-optical efficiencies of 12% and 4.9%. Both configurations feature relatively clean $sech^2$ soliton spectra with FWHM bandwidths of 16.5 nm and 29.5 nm, clearly exceeding the 8-nm gain bandwidth of Yb:YAG. The bump in the optical spectra at 1030 nm corresponds to the position of the peak of the Yb:YAG gain profile and is a commonly seen feature in TDL oscillators operating in the strongly SPM-broadened regime [15,17].

Table 1. Mode-locking performance and parameters for the presented laser configurations at pulse durations of 84 fs, 37 fs, 29 fs, and 27 fs.

Configuration	84 fs	37 fs	29 fs	27 fs
Output power (W)	69	17.1	2.5	3.3
Peak power (MW)	42	23.8	4.5	6.3
Pulse energy (µJ)	3.6	0.91	0.13	0.18
Central wavelength (nm)	1029.0	1029.4	1028.4	1028.0
FWHM bandwidth (nm)	16.5	29.5	34.2	39.8
Time-bandwidth product	0.392	0.309	0.281	0.307
Relative deviation of TBP from $sech^2$	1.25	0.98	0.89	0.97
Introduced GDD per roundtrip (fs^2)	-6000	-1500	-900	-900
Intra cavity peak power (MW)	350	477	587	820
Kerr medium distance from CM2 (mm)	560	545	545	548
Repetition rate (MHz)	17.3	17.1	17.1	17.1
Output coupling rate (%)	12	5.0	0.77	0.77
Pump power (W)	580	350	150	315
Pump-spot diameter (mm)	4.0	2.9	2.9	2.9
Optical-to-optical efficiency (%)	12	4.9	1.7	1.1
Hard aperture diameter (mm)	3.6	4.0	4.2	4.2
Sapphire plate thickness (mm)	4	2	2	2
Laser polarization	p	s	s	s

The 27-fs and 29-fs configurations are optimized for the shortest pulse duration. For this purpose, we selected a low output-coupling rate of 0.77% and further reduced the introduced total roundtrip GDD to -900 fs^2. The 27-fs is a rather extreme configuration of the laser. It requires a pump power of 350 W, which is more than 2 × higher compared to the 29-fs one [Table 1]. The only other difference between both configurations is the slightly different position of the Kerr medium, which was moved during the mode-locked operation by ~3 mm out of the

Optics EXPRESS

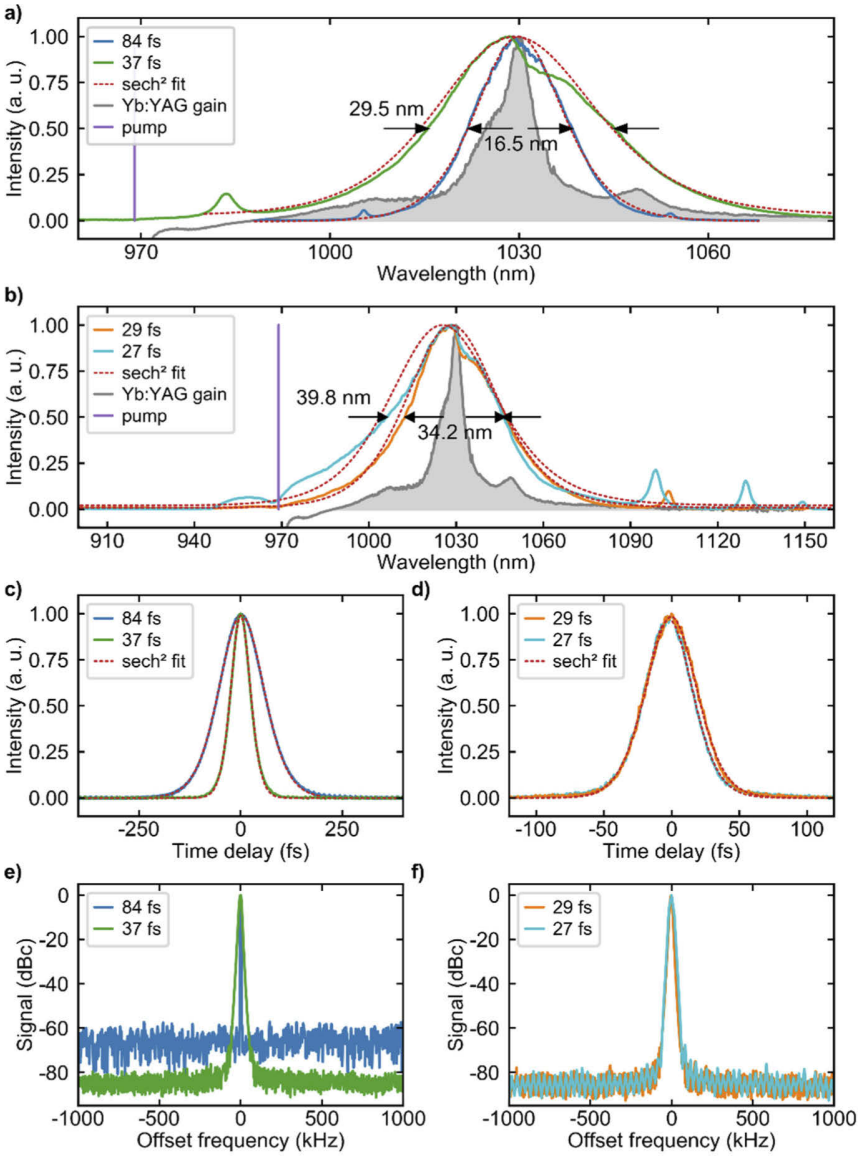

Fig. 3. a) and b) Optical spectra of the laser output with least-squares fits of sech^2 soliton pulses and normalized gain cross-section of Yb:YAG at an inversion level of 0.3. The pump wavelength of 969 nm is depicted by the purple line. c) and d) Intensity autocorrelation traces with fits for sech^2 soliton pulses. e) and f) Radio-frequency (RF) spectrum of the fundamental repetition-rate at 17.1 MHz measured at 10-kHz resolution bandwidth. The 84-fs laser configuration was characterized using a different RF analyzer at 3-kHz resolution bandwidth using a higher-bandwidth photodiode, thus, the noise level of this measurement is slightly higher than the others.

Optics EXPRESS

focus. At this extreme performance, the 39.8-nm FWHM optical spectrum deviates from the ideal sech^2 shape and clearly extends towards shorter wavelength even beyond the 969-nm pump wavelength [Fig. 3(b)]. The dip at the pump wavelength can be attributed to the reabsorption of the spectral components, originally generated by the SPM in the Kerr medium, inside the Yb:YAG gain material. On the other hand, the 29-fs configuration is much more relaxed. It requires only 150 W of pump power leading to an optical-to-optical efficiency of 1.7%. The 34.2-nm FWHM optical spectrum follows closer the ideal sech^2 shape. Nevertheless, we achieve a slightly too low time-bandwidth-product (TBP) of 0.281 (0.89× ideal sech^2). We attribute this deviation to the gain bump in the optical spectrum artificially narrowing its FWHM.

Single-pulse operation was verified for each configuration by a 180-ps autocorrelator scan and by observing the pulse train on a 40-GHz sampling oscilloscope with an 18.5-ps-rise-time photodetector. The radio-frequency spectra [Fig. 3(e), (f)] measured at the fundamental repetition frequency of 17.1 MHz show no side peaks down to the measurement noise floor indicating stable mode-locking.

4. Introduced group delay dispersion

One of the key challenges in shortening the pulse duration is the optimization of the introduced GDD for a flat profile over a broad spectral range. For the results presented here, the introduced GDD per cavity roundtrip by the DMs is shown in Fig. 4 in comparison to the corresponding optical spectra in shaded colors. The coatings of the dispersive mirrors were designed and

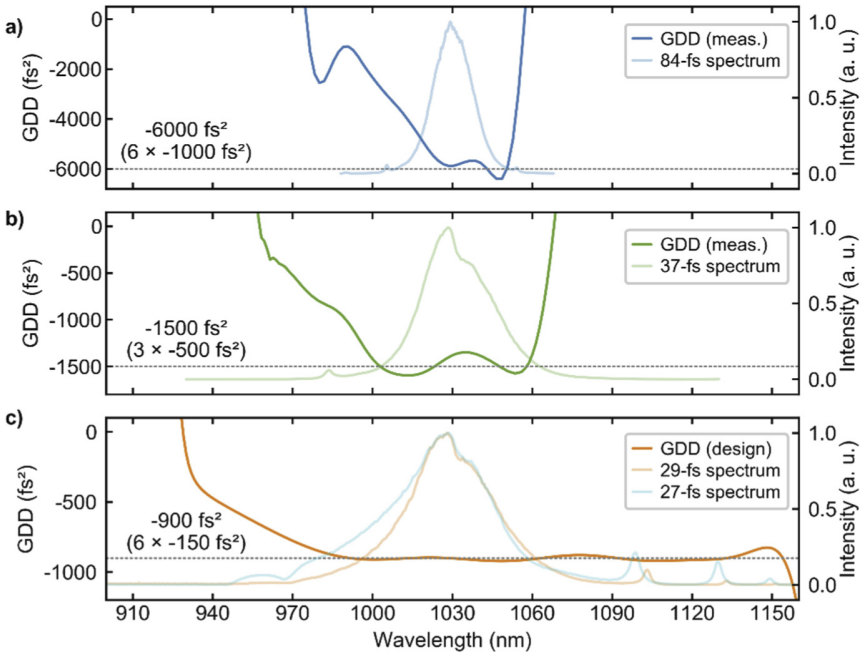

Fig. 4. Total introduced GDD of the DMs per cavity roundtrip for the four presented laser configurations in comparison to the corresponding optical spectrum. The nominal values are indicated by the horizontal dotted lines. For a) and b) the dispersion profile of the dispersive mirrors used in the 84-fs and 37-fs laser configuration was obtained by measuring the single-bounce GDD of a DM with an in-house developed white-light interferometer and multiplied by the number of bounces per cavity roundtrip. c) The introduced GDD of the 29-fs and 27-fs laser configuration is based on the design of the DMs.

Optics EXPRESS

manufactured inhouse in our ion-beam sputtering coating facility. For the 84-fs and 37-fs configuration, the dispersion profile of the DMs was measured utilizing a home-build white-light interferometer and multiplied by the number of bounces per cavity roundtrip. In the shortest-pulse configurations, the flat dispersion range of the DMs exceeded the spectral coverage of the white-light interferometer restricting us to rely on the design parameters. As can be seen exemplarily in the 84-fs configuration, the flat dispersion range is truncated by a gradually rising edge towards shorter wavelengths and a steep edge towards longer wavelengths, a common feature in the here applied double-resonant Gires-Tournois- Interferometer (GTI) type dispersive mirror design. While towards shorter pulse durations, the total amount of introduced negative GDD was decreased, the flat dispersion profile had to be extended over a broader spectral range to support a broader optical spectrum. This was realized in a chirped-mirror-type dispersive mirror design. In the trade-off between the GDD per bounce and the spectral width of the flat dispersion profile, the GDD per bounce had to be reduced. It amounted for the 84-fs configuration to $6 \times$ -1000 fs^2, for the 37-fs configuration to $3 \times$ -500 fs^2, and for the 27-fs / 29-fs configuration to $6 \times$ -150 fs^2. A further reduction of the introduced GDD to -750 fs^2 ($5 \times$ -150 fs^2) resulted repeatably in strong Q-switching and a damage in the Kerr medium.

Towards shorter pulse durations, we observe the expansion of the optical spectrum only towards shorter wavelengths. We attribute the limitation at the longer wavelength side to the unknown optical coatings of the thin disk. We expect shorter pulse durations within reach by optimization of all optical coatings including the coatings of the thin disk.

5. Conclusion

We have presented the experimental investigation of a KLM TDL oscillator based on commercially available Yb:YAG gain material operating in the strongly SPM-broadened regime. We have discussed the optimization of the introduced negative group delay dispersion that enabled generating pulses as short as 27 fs, corresponding to the shortest pulse duration of any ultrafast TDL oscillator [14]. Independent of the gain material, we considerably exceed the average power in comparison to previous sub-100-fs TDL oscillators of similar pulse duration [14–17]. This result is particularly important for the original purpose of our laser of driving intra-oscillator HHG [23], where short pulse durations strongly benefit the phase-matching of the XUV light [24]. We also expect being able to increase the output power of the laser well above the 100-W level at a few tens of femtoseconds pulse duration. Thanks to the clean soliton spectrum and excellent beam quality, the laser output should be ideally suited for further nonlinear pulse compression into the single-cycle regime within a single compression stage [25–27]. The ultrashort megahertz-repetition-rate pulses will be beneficial for experiments in the attosecond domain. Additionally, the laser output should be simultaneously available with the intra-oscillator HHG generated XUV light, offering a compact solution for pump-probe experiments. We expect even shorter pulse durations within reach by the optimization of the optical coatings including the coatings of the thin disk.

Funding. Schweizerischer Nationalfonds zur Förderung der Wissenschaftlichen Forschung (200020_179146, 200020_200774, 206021_144970, 206021_170772, 206021_198176).

Disclosures. The authors declare that there are no conflicts of interest related to this article.

Data availability. Data underlying the results presented in this paper are available in Ref. [28]

References

1. D. T. Reid, C. M. Heyl, R. R. Thomson, R. Trebino, G. Steinmeyer, H. H. Fielding, R. Holzwarth, Z. Zhang, P. Del'Haye, T. Südmeyer, G. Mourou, T. Tajima, D. Faccio, F. J. M. Harren, and G. Cerullo, "Roadmap on ultrafast optics," J. Opt. **18**(9), 093006 (2016).
2. Y. Wang, X. Su, Y. Xie, F. Gao, S. Kumar, Q. Wang, C. Liu, B. Zhang, B. Zhang, and J. He, "17.8 fs broadband Kerr-lens mode-locked Yb:CALGO oscillator," Opt. Lett. **46**(8), 1892–1895 (2021).

Optics EXPRESS

3. J. Ma, F. Yang, W. Gao, X. Xiaodong, X. Jun, D. Shen, and D. Tang, "Sub-five-optical-cycle pulse generation from a Kerr-lens mode-locked Yb:$CaYAlO_4$ laser," Opt. Lett. **46**(10), 2328 (2021).
4. A. Giesen, H. Hügel, A. Voss, K. Wittig, U. Brauch, and H. Opower, "Scalable concept for diode-pumped high-power solid-state lasers," Appl. Phys. B **58**(5), 365–372 (1994).
5. J. Aus der Au, G. J. Spühler, T. Südmeyer, R. Paschotta, R. Hövel, M. Moser, S. Erhard, M. Karszewski, A. Giesen, and U. Keller, "16.2-W average power from a diode-pumped femtosecond Yb:YAG thin disk laser," Opt. Lett. **25**(11), 859–861 (2000).
6. C. J. Saraceno, D. Sutter, T. Metzger, and M. Abdou Ahmed, "The amazing progress of high-power ultrafast thin-disk lasers," J. Eur. Opt. Soc.-Rapid Publ. **15**(1), 15 (2019).
7. F. Saltarelli, I. J. Graumann, L. Lang, D. Bauer, C. R. Phillips, and U. Keller, "Power scaling of ultrafast oscillators: 350-W average-power sub-picosecond thin-disk laser," Opt. Express **27**(22), 31465–31474 (2019).
8. J. Brons, V. Pervak, D. Bauer, D. Sutter, O. Pronin, and F. Krausz, "Powerful 100-fs-scale Kerr-lens mode-locked thin-disk oscillator," Opt. Lett. **41**(15), 3567–3570 (2016).
9. F. Labaye, M. Gaponenko, N. Modsching, P. Brochard, C. Paradis, S. Schilt, V. J. Wittwer, and T. Südmeyer, "XUV sources based on intra-oscillator high harmonic generation with thin-disk lasers: Current status and prospects," IEEE J. Sel. Top. Quantum Electron. **25**(4), 1–19 (2019).
10. T. Südmeyer, C. Kränkel, C. R. E. Baer, O. H. Heckl, C. J. Saraceno, M. Golling, R. Peters, K. Petermann, G. Huber, and U. Keller, "High-power ultrafast thin disk laser oscillators and their potential for sub-100-femtosecond pulse generation," Appl. Phys. B **97**(2), 281–295 (2009).
11. C. J. Saraceno, O. H. Heckl, C. R. E. Baer, C. Schriber, M. Golling, K. Beil, C. Kränkel, T. Südmeyer, G. Huber, and U. Keller, "Sub-100 femtosecond pulses from a SESAM modelocked thin disk laser," Appl. Phys. B **106**(3), 559–562 (2012).
12. C. Schriber, F. Emaury, A. Diebold, S. Link, M. Golling, K. Beil, C. Kränkel, C. J. Saraceno, T. Südmeyer, and U. Keller, "Dual-gain SESAM modelocked thin disk laser based on Yb:Lu_2O_3 and Yb:Sc_2O_3," Opt. Express **22**(16), 18979–18986 (2014).
13. A. Diebold, F. Emaury, C. Schriber, M. Golling, C. J. Saraceno, T. Südmeyer, and U. Keller, "SESAM mode-locked Yb:$CaGdAlO_4$ thin disk laser with 62 fs pulse generation," Opt. Lett. **38**(19), 3842–3845 (2013).
14. N. Modsching, C. Paradis, F. Labaye, M. Gaponenko, I. J. Graumann, A. Diebold, F. Emaury, V. J. Wittwer, and T. Südmeyer, "Kerr lens mode-locked Yb:CALGO thin-disk laser," Opt. Lett. **43**(4), 879–882 (2018).
15. C. Paradis, N. Modsching, V. J. Wittwer, B. Deppe, C. Kränkel, and T. Südmeyer, "Generation of 35-fs pulses from a Kerr lens mode-locked Yb:Lu_2O_3 thin-disk laser," Opt. Express **25**(13), 14918–14925 (2017).
16. N. Modsching, J. Drs, J. Fischer, C. Paradis, F. Labaye, M. Gaponenko, C. Kränkel, V. J. Wittwer, and T. Südmeyer, "Sub-100-fs Kerr lens mode-locked Yb:Lu_2O_3 thin-disk laser oscillator operating at 21 W average power," Opt. Express **27**(11), 16111–16120 (2019).
17. J. Zhang, J. Brons, M. Seidel, V. Pervak, V. Kalashnikov, Z. Wei, A. Apolonski, F. Krausz, and O. Pronin, "49-fs Yb:YAG thin-disk oscillator with distributed Kerr-lens mode-locking," in *European Quantum Electronics Conference* (Optical Society of America, 2015), paper PD_A_1.
18. M. Tokurakawa, A. Shirakawa, K. Ueda, H. Yagi, S. Hosokawa, T. Yanagitani, and A. A. Kaminskii, "Diode-pumped 65 fs Kerr-lens mode-locked Yb^{3+}:Lu_2O_3 and nondoped Y_2O_3 combined ceramic laser," Opt. Lett. **33**(12), 1380–1382 (2008).
19. J. Fischer, J. Drs, F. Labaye, N. Modsching, V. Wittwer, and T. Südmeyer, "Intra-oscillator high harmonic generation in a thin-disk laser operating in the 100-fs regime," Opt. Express **29**(4), 5833–5839 (2021).
20. J. Brons, V. Pervak, E. Fedulova, D. Bauer, D. Sutter, V. Kalashnikov, A. Apolonskiy, O. Pronin, and F. Krausz, "Energy scaling of Kerr-lens mode-locked thin-disk oscillators," Opt. Lett. **39**(22), 6442–6445 (2014).
21. O. Pronin, J. Brons, C. Grasse, V. Pervak, G. Boehm, M.-C. Amann, V. L. Kalashnikov, A. Apolonski, and F. Krausz, "High-power 200 fs Kerr-lens mode-locked Yb:YAG thin-disk oscillator," Opt. Lett. **36**(24), 4746–4748 (2011).
22. A. A. Eilanlou, Y. Nabekawa, M. Kuwata-Gonokami, and K. Midorikawa, "Femtosecond laser pulses in a Kerr lens mode-locked thin-disk ring oscillator with an intra-cavity peak power beyond 100 MW," Jpn. J. Appl. Phys. **53**(8), 082701 (2014).
23. F. Labaye, M. Gaponenko, V. J. Wittwer, A. Diebold, C. Paradis, N. Modsching, L. Merceron, F. Emaury, I. J. Graumann, C. R. Phillips, C. J. Saraceno, C. Kränkel, U. Keller, and T. Südmeyer, "Extreme ultraviolet light source at a megahertz repetition rate based on high-harmonic generation inside a mode-locked thin-disk laser oscillator," Opt. Lett. **42**(24), 5170–5173 (2017).
24. S. Hädrich, J. Rothhardt, M. Krebs, S. Demmler, A. Klenke, A. Tünnermann, and J. Limpert, "Single-pass high harmonic generation at high repetition rate and photon flux," J. Phys. B: At., Mol. Opt. Phys. **49**(17), 172002 (2016).
25. M. Müller, J. Buldt, H. Stark, C. Grebing, and J. Limpert, "Multipass cell for high-power few-cycle compression," Opt. Lett. **46**(11), 2678–2681 (2021).
26. S. Gröbmeyer, K. Fritsch, B. Schneider, M. Poetzlberger, V. Pervak, J. Brons, and O. Pronin, "Self-compression at 1 µm wavelength in all-bulk multi-pass geometry," Appl. Phys. B **126**(10), 159 (2020).
27. C.-L. Tsai, F. Meyer, A. Omar, Y. Wang, A.-Y. Liang, C.-H. Lu, M. Hoffmann, S.-D. Yang, and C. J. Saraceno, "Efficient nonlinear compression of a mode-locked thin-disk oscillator to 27 fs at 98 W average power," Opt. Lett. **44**(17), 4115–4118 (2019).
28. J. Drs, Sub-30-fs Yb:YAG thin-disk laser oscillator operating in the strongly self-phase modulation broadened regime, EUDAT (2021), http://doi.org/10.23728/b2share.42d04391fbcf47f7b0ddde764f18f270.

Research Article | Vol. 29, No. 4 / 15 February 2021 / Optics Express 5833
Optics EXPRESS

Intra-oscillator high harmonic generation in a thin-disk laser operating in the 100-fs regime

JULIAN FISCHER,* JAKUB DRS, FRANÇOIS LABAYE, NORBERT MODSCHING, VALENTIN J. WITTWER, AND THOMAS SÜDMEYER

Laboratoire Temps-Fréquence (LTF), Institut de Physique, Université de Neuchâtel, Avenue de Bellevaux 51, 2000 Neuchâtel, Switzerland
julian.fischer@unine.ch

Abstract: We demonstrate that Kerr lens modelocking is well-suited for operating an ultrafast thin-disk laser with intra-oscillator high harmonic generation (HHG) in the 100-fs pulse duration regime. Exploiting nearly the full emission bandwidth of the gain material Yb:YAG, we generate 105-fs pulses with an intracavity peak power of 365 MW and an intracavity average power of 470 W. We drive HHG in argon with a peak intensity of ~$7{\cdot}10^{13}$ W/cm^2 at a repetition rate of 11 MHz. Extreme-ultraviolet (XUV) light is generated up to the 31st harmonic order (H31) at 37 eV, with an average power of ~0.4 µW in H25 at 30 eV. This work presents a considerable increase in performance of XUV sources based on intra-oscillator HHG and confirms that this approach is a promising technology for simple and portable XUV sources at MHz repetition rates.

1. Introduction

High harmonic generation (HHG) driven by ultrafast laser pulses in a noble gas target is the most common method for tabletop coherent extreme-ultraviolet (XUV) light sources. Driving this highly nonlinear process requires peak intensities in the range of 10^{13} - 10^{15} W/cm^2. Such high intensities are traditionally achieved using chirped pulse amplifier (CPA) systems based on Ti:sapphire bulk lasers. Due to thermal effects in the bulk gain material, these systems are limited in average power and typically operate with low kilohertz repetition rates in a single-pass configuration. The progress towards megahertz repetition rate XUV sources is of high scientific and technical interest, because it can strongly reduce acquisition times in imaging and pump-probe experiments, overcome limiting space-charge effects in photoelectron spectroscopy [1–4], and enable XUV frequency combs for spectroscopy applications [5,6].

Compared to Ti:sapphire based systems, Yb-based solid-state laser systems are much better suited for reaching the high pulse energies necessary for HHG combined with high repetition rates due to the lower quantum defect, the therefore lower thermal effects, and the more efficient direct diode pumping scheme. High-power fiber CPA systems have been achieving considerable success in this domain [7–9]. In 2015, an average power level of 50 µW in a single harmonic order at 28 eV and 10.7-MHz repetition rate was demonstrated [8]. This performance was reached with a driving laser that was based on the coherent combination of fiber chirped pulse amplification channels followed by a nonlinear temporal pulse compression in a gas filled photonic crystal fiber.

Another successful approach for HHG at megahertz repetition rates is based on placing the HHG gas target inside a passive femtosecond enhancement cavity (fsEC) [6,10], where the pulse enhancement provides sufficiently high intracavity peak power, even when operating at repetition rates of several hundred-megahertz. Because of the resonant enhancement, the power requirements of the driving laser are considerably reduced. Using this technology, XUV photon energies up to 94 eV with 1.3-nW average power in a single harmonic order at 250-MHz repetition

#414444 https://doi.org/10.1364/OE.414444
Journal © 2021 Received 12 Nov 2020; revised 11 Jan 2021; accepted 12 Jan 2021; published 9 Feb 2021

Optics EXPRESS

rate were demonstrated [11]. A record XUV average power of ~2 mW in a single harmonic at 13 eV and 77-MHz repetition rate was reported in 2018 [12]. However, the experimental realization of fsECs is challenging: coherent coupling of ultrafast pulses into a high-finesse optical resonator containing the HHG process is very demanding. For example, the system presented in [12] operated at an enhancement factor of ~200. In order to reach such enhancement factors, total cavity roundtrip losses have to be lower than 1%, making fsECs very sensitive to any kind of losses. This presents a constraint for the achievable enhancement and the implementation of efficient XUV output coupling methods, which often add further losses.

The high peak and average powers required for efficient HHG are also achievable inside ultrafast mode-locked thin-disk laser (TDL) oscillators, opening the potential for single-stage XUV sources. Placing the gas target directly inside the cavity of a TDL oscillator simplifies the overall experimental setup, requiring neither coherent coupling into an actively stabilized external fsEC nor temporal pulse compression. The available gain per cavity roundtrip strongly reduces the sensitivity to cavity losses compared to fsECs. In high-power TDL oscillators, the gain can be further increased with the number of passes over the disk. For instance, with a double pass on the disk, the roundtrip gain can compensate for output coupling rates of about 15%, while still exploiting the full available gain bandwidth [13,14]. This allows for the implementation of efficient XUV output coupling mechanisms that introduce significant losses for the circulating intracavity pulse, such as a pierced mirror with an increased diameter of the through hole [15,16].

In a proof-of-principle experiment in 2017, we demonstrated intra-oscillator HHG in xenon, driven inside a 255-fs semiconductor saturable absorber mirror (SESAM) mode-locked Yb:Lu_2O_3 TDL [17]. We generated XUV radiation up to the 17th harmonic (H17) at 20 eV with an average power of ~0.55 nW in H11 at 13 eV. In the same year, another demonstration of intra-oscillator HHG based on a Kerr lens mode-locked (KLM) Yb:YAG TDL was reported in [18] and recently published in more detail in [19]. The system operated with a pulse duration of 610 fs at a peak power of 445 MW and a repetition rate of 3.1 MHz. XUV light was generated in neon up to 52 eV (H43) and in argon with an average power of 47 nW in H17 at 20 eV.

In this work, we present intra-oscillator HHG at significantly improved performance. We use a 105-fs KLM Yb:YAG TDL operating at 365 MW of intracavity peak power and 11-MHz repetition rate. We generate XUV in argon with up to 37 eV (H31) with an average power of ~0.4 µW in H25 at 30 eV. Figure 1 shows a comparison of our system to other ultrafast high intracavity peak power TDLs together with the evolution of the intra-oscillator HHG driving systems. The desired parameter range for efficient HHG is depicted by the green shaded corner, corresponding to gigawatt level peak powers and tens of femtosecond pulse duration [4,25].

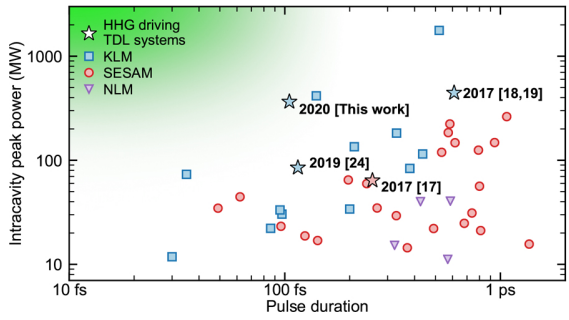

Fig. 1. Overview of ultrafast TDL oscillators based on SESAM, KLM, or nonlinear-mirror (NLM) modelocking with more than 10 MW of intracavity peak power. Stars with year show the evolution of HHG driving TDLs. The modelocking mechanism of HHG TDLs is indicated in the color code (blue for KLM; red for SESAM). References in [14,17–24].

Optics EXPRESS

However, a tradeoff between intracavity peak power and pulse duration for TDL oscillators utilizing different modelocking techniques can clearly be identified. The nearly instantaneous response of the Kerr effect and the high damage threshold of the components currently favor KLM for the combination of short pulse durations and high intracavity peak powers, making this approach most promising for intra-oscillator HHG.

2. Experimental setup

The TDL setup for intra-oscillator HHG is housed in a vacuum chamber with a footprint of 0.8×1.6 m^2 as shown in Fig. 2. The cavity design is based on the power-scaling approach for KLM TDLs presented in [26]. The laser is built using a commercially available TDL head designed for 36 passes of the pump through a ~100-µm thick Yb:YAG disk in order to achieve a high pump absorption. The disk is optically pumped at 969 nm with a fiber-coupled pump-diode on a 4.2-mm diameter pump spot. The diode delivers an average power up to 2 kW, but in the here described experiments, we only used a maximum pump power of 380 W. The cavity is folded twice over the disk, increasing the gain per cavity round trip. For KLM, an anti-reflection coated undoped 1-mm thick YAG plate is placed in the vicinity of an intracavity focus created by two concave mirrors (CM1, CM2) with 1-m radius of curvature (RoC). A water-cooled copper plate with a 3.6-mm diameter hole serves as hard aperture. Four dispersive mirrors introduce a total cavity roundtrip dispersion of -7000 fs^2. Mode-locked operation in vacuum is initialized by shaking one of the cavity mirrors mounted on a piezo stage. The cavity is extended by a telescope consisting of two concave mirrors (CM3, CM4) with RoC of 2 m and 3 m, respectively. One cavity end mirror serves as an output coupler with a transmission of 0.77%.

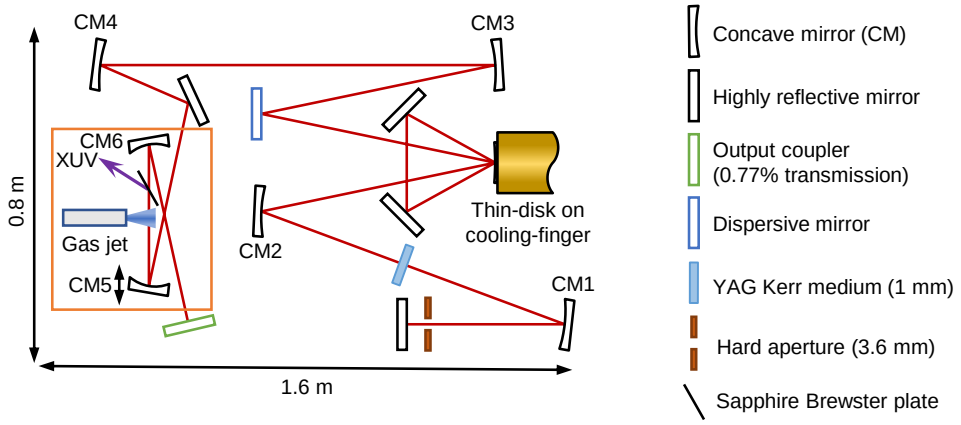

Fig. 2. Schematic of the Kerr lens mode-locked Yb:YAG thin-disk laser with a double pass on the disk and 4*f*-extension with tight-focus for HHG, which is indicated with an orange box. CM1 and CM2, RoC of 1 m; CM3, RoC of 2 m; CM4, RoC of 3 m; CM5 and CM6, RoC of 200 mm.

A 4*f*-extension consisting of two concave mirrors (CM5, CM6) with 200-mm RoC inserted in the output-coupling arm of the cavity creates a tight focus required to reach the high peak intensities for HHG. CM5 is placed on a piezo stage with a total travel range of 500 µm for fine-tuning of the cavity during mode-locked operation. Argon with a backing pressure of up to 10 bar can be injected into the cavity through a 50-µm opening diameter glass nozzle which is placed in the vicinity of the tight focus. A mass flow controller with a pressure sensor enables a precise delivery of the generation gas. A gas dump connected to the primary vacuum pump, placed on the opposite side of the tight focus than the nozzle, evacuates most of the gas, reducing

Optics EXPRESS

the gas load on the turbomolecular pumps [27]. The gas nozzle is mounted on a motorized xyz-stage for fine-adjustment of the XUV generation point. To extract the generated XUV light and to ensure p-polarized operation of the TDL, a 325-µm thick sapphire plate is placed under Brewster's angle for the fundamental laser wavelength at a distance of ~15 mm from the tight focus. Due to the simplicity of the aforementioned XUV out-coupling mechanism, the method has been routinely used in fsECs [28–30]. However, the maximum reflectivity of the sapphire plate is limited to 17% at a wavelength of 50 nm (25 eV) and decreases strongly for shorter and longer wavelengths (see, e.g., [31]). The generated XUV light is directed by an unprotected gold mirror towards a spectrometer (248/310 McPherson). The XUV flux is measured with an aluminum coated AXUV100Al photodiode. To suppress any residual infrared light from reaching the photodiode, an additional 200-nm thick aluminum filter is inserted in front.

Two turbomolecular pumps provide a vacuum level which prevents significant reabsorption of the generated XUV light within the distance of ~20 cm separating the detector from the generation point. The cavity components experiencing the highest intensities, the anti-reflection coated YAG plate and sapphire plate, are purged with oxygen from both sides to prevent contamination during laser operation. Optical coatings have been designed inhouse and grown in our ion-beam sputtering coating facility.

3. Experimental results

Without injection of gas into the tight focus, our laser runs with an intracavity average power of 640 W, an intracavity peak power of 520 MW, and an intracavity pulse energy of 55 µJ at a pump power of 285 W. This performance is reached after optimizing the distance between CM5 and CM6 with the piezo stage in mode-locked operation. Intensity autocorrelation trace, optical spectrum, and radiofrequency spectrum are shown in Figs. 3(a) to 3(c). The optical spectrum of the 99-fs soliton pulse is centered at 1027.8 nm with a full width at half maximum bandwidth (FWHM) of 14.0 nm. We confirmed single pulse operation by a 180-ps scan in the autocorrelator and by observing the pulse train with an 18.5-ps-rise-time photodetector on a 40-GHz sampling oscilloscope.

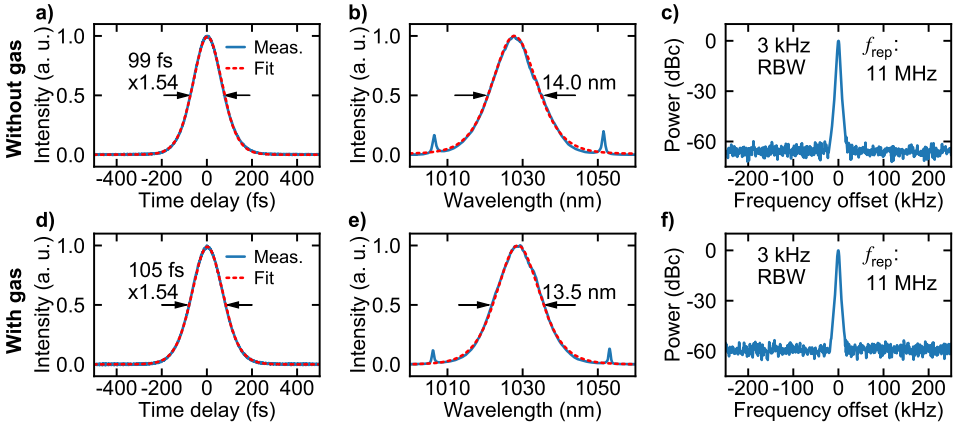

Fig. 3. Comparison of the thin-disk laser output parameters a) to c) without the injection of gas and d) to f) with injection of argon gas into the intracavity focus for HHG. a), d) Intensity autocorrelation traces with sech^2 fit. b), e) Optical spectra with spectral bandwidth and sech^2 fit. c), f) Radiofrequency spectra of the fundamental repetition rate (f_{rep}) with 3-kHz resolution bandwidth (RBW).

Optics EXPRESS

To initialize XUV generation, argon is injected into the tight focus of the laser cavity. In the current system, the gas plasma affects the laser: the position of CM5 has to be slightly shifted (< 500 µm) between operation with and without gas. We attribute this behavior to the lensing effect in the plasma since it can be compensated by this shift. With HHG, the laser operates with 105-fs pulse duration at an intracavity peak power of 365 MW and a pulse energy of 40 µJ. The intracavity average power is 470 W, which is obtained for a diode pump power of 180 W. Intensity autocorrelation trace, optical spectrum, and radiofrequency spectrum are shown in Figs. 3(d) to 3(f). Compared to operation without HHG, the optical spectrum shifts by 1 nm to a central wavelength of 1028.8 nm with a FWHM bandwidth of 13.5 nm.

The XUV optical spectrum attenuated by a 200-nm thick aluminum filter and generated in argon with a backing pressure of 3 bar is shown in Fig. 4. We generate up to H31 which corresponds to a wavelength of 33 nm and an energy of 37 eV. Utilizing the harmonic cut-off formula, the intracavity peak intensity in the tight focus is estimated to be $7{\cdot}10^{13}$ W/cm^2, corresponding to a focal radius of ~18 µm in mode-locked operation. A total generated XUV power of ~2 µW within the spectral range from H17 to H31 (20 - 37 eV) is conservatively estimated. We corrected by the tabulated values for the extraction efficiency of a sapphire plate (see, e.g. [31]), the reflectance of a gold mirror, and the transmission of a 200-nm thick aluminum filter. The absorption of XUV radiation in the gas background (oxygen: $\sim 9{\cdot}10^{-3}$ mbar; argon: $\sim 2.5{\cdot}10^{-3}$ mbar) to the detector is considerably small and therefore neglected. Assuming a flat spectral response of the XUV spectrometer, a generated average power of ~0.4 µW in H25 (30 eV) is estimated.

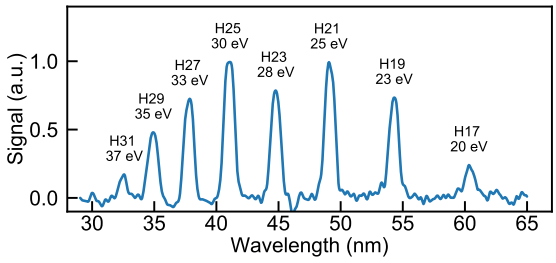

Fig. 4. Optical spectrum of XUV light generated in argon showing 17th to 31st harmonic. Peaks are labeled with harmonic order and corresponding photon energies. The XUV spectrum is attenuated by a 200-nm thick aluminum filter.

In the current study, thermal drift of uncooled cavity components limited operation to less than 15 minutes, which prevented a systematic optimization, especially with respect to the phase matching of the harmonics. Phase matching becomes increasingly difficult at repetition rates above ~10 MHz, due to a steady-state plasma accumulated in the generation volume [12]. Nevertheless, phase matching at even higher repetition rates has already been demonstrated, for instance, in single pass configuration at 10.7 MHz [8] and in a fsEC at 77 MHz [12]. After implementation of water-cooled mirror mounts in our cavity, which is currently in progress, we will investigate phase matching in detail. For this study, we plan to use an improved gas target similar to the system reported in [32].

4. Conclusion and outlook

We have demonstrated intra-oscillator HHG in a 105-fs KLM Yb:YAG TDL operating at 11-MHz repetition rate. In comparison to our previous result with XUV photon energies up to 20 eV (H17) and a total generated average power of ~0.55 nW in H11 (13 eV) in xenon [17], we now generate up to 37 eV (H31) with an average power of ~0.4 µW in H25 (30 eV) in argon, which

Optics EXPRESS

is an increase in XUV flux of three orders of magnitude. Combined with the decreased pulse duration of the TDL by a factor of more than two, our result presents a considerable advance in TDL based intra-oscillator XUV sources [17,19].

Following the intracavity peak power scaling concept for KLM TDLs introduced by Brons *et al.* [26] in combination with shorter pulse durations by operating the laser in the strongly SPM-broadened regime [33,34], we expect further advancement of our system towards sub-100-fs operation with gigawatt intracavity peak powers. Due to the strong dependency of the HHG efficiency on peak intensity and pulse duration, this should lead to a substantial improvement of the performance of the system [4,25]. Further advances are expected by more efficient XUV extraction. Instead of a sapphire plate under Brewster's angle for the fundamental wavelength, a grazing incidence plate or a pierced mirror can be employed. With a grazing incidence plate, an XUV reflectivity up to 70% can be reached at 80° angle of incidence and fused silica as top layer of the anti-reflection coating for the fundamental laser-wavelength [31]. The pierced mirror method is especially suited for the efficient extraction of highly energetic XUV light [11,15]. In addition to an improved XUV extraction efficiency, a further reduction of the pulse duration of the driving TDL, reducing the level of steady-state plasma adversely affecting the TDL and improving phase matching of the generated harmonics, is also desirable [8,15].

We believe that our approach of HHG inside a TDL oscillator will lead to a novel class of single-stage coherent XUV light sources operating at MHz repetition rate. As most of the volume in our vacuum chamber remains empty, we expect that the footprint of our system can be strongly reduced with sufficient engineering, leading to a more compact and transportable design. We expect that such systems will soon operate at a performance comparable to state-of-the-art megahertz repetition rate HHG systems.

Funding. H2020 European Research Council (279505); Schweizerischer Nationalfonds zur Förderung der Wissenschaftlichen Forschung (144970, 170772, 179146).

Acknowledgments. The authors acknowledge the support of the Ultrafast Laser Physics group of Ursula Keller (ETH Zürich) for lending the 248/310 McPherson spectrometer.

Disclosures. The authors declare that there are no conflicts of interest related to this article.

Data availability. Data underlying the results presented in this paper are available in Ref. [35].

References

1. C. M. Heyl, J. Güdde, A. L'Huillier, and U. Höfer, "High-order harmonic generation with μJ laser pulses at high repetition rates," J. Phys. B: At., Mol. Opt. Phys. **45**(7), 074020 (2012).
2. M. Keunecke, C. Möller, D. Schmitt, H. Nolte, G. S. M. Jansen, M. Reutzel, M. Gutberlet, G. Halasi, D. Steil, S. Steil, and S. Mathias, "Time-resolved momentum microscopy with a 1 MHz high-harmonic extreme ultraviolet beamline," Rev. Sci. Instrum. **91**(6), 063905 (2020).
3. S. Passlack, S. Mathias, O. Andreyev, D. Mittnacht, M. Aeschlimann, and M. Bauer, "Space charge effects in photoemission with a low repetition, high intensity femtosecond laser source," J. Appl. Phys. **100**(2), 024912 (2006).
4. C. M. Heyl, C. L. Arnold, A. Couairon, and A. L'Huillier, "Introduction to macroscopic power scaling principles for high-order harmonic generation," J. Phys. B: At., Mol. Opt. Phys. **50**(1), 013001 (2017).
5. A. K. Mills, T. J. Hammond, M. H. C. Lam, and D. J. Jones, "XUV frequency combs via femtosecond enhancement cavities," J. Phys. B: At., Mol. Opt. Phys. **45**(14), 142001 (2012).
6. C. Gohle, T. Udem, M. Herrmann, J. Rauschenberger, R. Holzwarth, H. A. Schuessler, F. Krausz, and T. W. Hänsch, "A frequency comb in the extreme ultraviolet," Nature **436**(7048), 234–237 (2005).
7. J. Boullet, Y. Zaouter, J. Limpert, S. Petit, Y. Mairesse, B. Fabre, J. Higuet, E. Mével, E. Constant, and E. Cormier, "High-order harmonic generation at a megahertz-level repetition rate directly driven by an ytterbium-doped-fiber chirped-pulse amplification system," Opt. Lett. **34**(9), 1489–1491 (2009).
8. S. Hädrich, M. Krebs, A. Hoffmann, A. Klenke, J. Rothhardt, J. Limpert, and A. Tünnermann, "Exploring new avenues in high repetition rate table-top coherent extreme ultraviolet sources," Light: Sci. Appl. **4**(8), e320 (2015).
9. S. Hädrich, A. Klenke, J. Rothhardt, M. Krebs, A. Hoffmann, O. Pronin, V. Pervak, J. Limpert, and A. Tünnermann, "High photon flux table-top coherent extreme-ultraviolet source," Nat. Photonics **8**(10), 779–783 (2014).
10. R. J. Jones, K. D. Moll, M. J. Thorpe, and J. Ye, "Phase-Coherent Frequency Combs in the Vacuum Ultraviolet via High-Harmonic Generation inside a Femtosecond Enhancement Cavity," Phys. Rev. Lett. **94**(19), 193201 (2005).

Optics EXPRESS

11. H. Carstens, M. Högner, T. Saule, S. Holzberger, N. Lilienfein, A. Guggenmos, C. Jocher, T. Eidam, D. Esser, V. Tosa, V. Pervak, J. Limpert, A. Tünnermann, U. Kleineberg, F. Krausz, and I. Pupeza, "High-harmonic generation at 250 MHz with photon energies exceeding 100 eV," Optica **3**(4), 366–369 (2016).
12. G. Porat, C. M. Heyl, S. B. Schoun, C. Benko, N. Dörre, K. L. Corwin, and J. Ye, "Phase-matched extreme-ultraviolet frequency-comb generation," Nat. Photonics **12**(7), 387–391 (2018).
13. J. Brons, V. Pervak, D. Bauer, D. Sutter, O. Pronin, and F. Krausz, "Powerful 100-fs-scale Kerr-lens mode-locked thin-disk oscillator," Opt. Lett. **41**(15), 3567–3570 (2016).
14. N. Modsching, J. Drs, J. Fischer, C. Paradis, F. Labaye, M. Gaponenko, C. Kränkel, V. J. Wittwer, and T. Südmeyer, "Sub-100-fs Kerr lens mode-locked Yb:Lu2O3 thin-disk laser oscillator operating at 21 W average power," Opt. Express **27**(11), 16111–16120 (2019).
15. I. Pupeza, S. Holzberger, T. Eidam, H. Carstens, D. Esser, J. Weitenberg, P. Rußbüldt, J. Rauschenberger, J. Limpert, T. Udem, A. Tünnermann, T. W. Hänsch, A. Apolonski, F. Krausz, and E. Fill, "Compact high-repetition-rate source of coherent 100 eV radiation," Nat. Photonics **7**(8), 608–612 (2013).
16. K. D. Moll, R. J. Jones, and J. Ye, "Output coupling methods for cavity-based high-harmonic generation," Opt. Express **14**(18), 8189–8197 (2006).
17. F. Labaye, M. Gaponenko, V. J. Wittwer, A. Diebold, C. Paradis, N. Modsching, L. Merceron, F. Emaury, I. J. Graumann, C. R. Phillips, C. J. Saraceno, C. Kränkel, U. Keller, and T. Südmeyer, "Extreme ultraviolet light source at a megahertz repetition rate based on high-harmonic generation inside a mode-locked thin-disk laser oscillator," Opt. Lett. **42**(24), 5170–5173 (2017).
18. N. Kanda, T. Imahoko, K. Yoshida, A. A. Eilanlou, Y. Nabekawa, T. Sumiyoshi, M. Kuwata-Gonokami, K. Midorikawa, K. Midorikawa, K. Midorikawa, and K. Midorikawa, "Multi-port Intra-Cavity High Harmonic Generation in a Yb:YAG Thin Disk Mode-Locked Oscillator with MHz Repetition Rate," in Frontiers in Optics 2017, OSA Technical Digest (Online) (Optical Society of America, 2017), paper LW5F.4.
19. N. Kanda, T. Imahoko, K. Yoshida, A. Tanabashi, A. Amani Eilanlou, Y. Nabekawa, T. Sumiyoshi, M. Kuwata-Gonokami, and K. Midorikawa, "Opening a new route to multiport coherent XUV sources via intracavity high-order harmonic generation," Light: Sci. Appl. **9**(1), 168 (2020).
20. F. Labaye, M. Gaponenko, N. Modsching, P. Brochard, C. Paradis, S. Schilt, V. J. Wittwer, and T. Sudmeyer, "XUV Sources Based on Intra-Oscillator High Harmonic Generation With Thin-Disk Lasers: Current Status and Prospects," IEEE J. Sel. Top. Quantum Electron. **25**(4), 1–19 (2019).
21. F. Saltarelli, I. J. Graumann, L. Lang, D. Bauer, C. R. Phillips, and U. Keller, "Power scaling of ultrafast oscillators: 350-W average-power sub-picosecond thin-disk laser," Opt. Express **27**(22), 31465–31474 (2019).
22. F. Saltarelli, A. Diebold, I. J. Graumann, C. R. Phillips, and U. Keller, "Modelocking of a thin-disk laser with the frequency-doubling nonlinear-mirror technique," Opt. Express **25**(19), 23254–23265 (2017).
23. I. J. Graumann, F. Saltarelli, L. Lang, V. J. Wittwer, T. Südmeyer, C. R. Phillips, and U. Keller, "Power-scaling of nonlinear-mirror modelocked thin-disk lasers," Opt. Express **27**(26), 37349–37363 (2019).
24. J. Fischer, J. Drs, F. Labaye, N. Modsching, C. Kränkel, V. J. Wittwer, and T. Südmeyer, "Intra-Oscillator High Harmonic Generation in a ~100-fs Kerr-Lens Mode-Locked Thin-Disk Laser," in *Conference on Lasers and Electro-Optics, OSA Technical Digest* (Optical Society of America, 2020), paper SF3H.3.
25. S. Hädrich, J. Rothhardt, M. Krebs, S. Demmler, A. Klenke, A. Tünnermann, and J. Limpert, "Single-pass high harmonic generation at high repetition rate and photon flux," J. Phys. B: At., Mol. Opt. Phys. **49**(17), 172002 (2016).
26. J. Brons, V. Pervak, E. Fedulova, D. Bauer, D. Sutter, V. Kalashnikov, A. Apolonskiy, O. Pronin, and F. Krausz, "Energy scaling of Kerr-lens mode-locked thin-disk oscillators," Opt. Lett. **39**(22), 6442–6445 (2014).
27. D. C. Yost, "Development of an Extreme Ultraviolet Frequency Comb for Precision Spectroscopy," PhD Thesis, University of Colorado (2011).
28. C. Benko, T. K. Allison, A. Cingöz, L. Hua, F. Labaye, D. C. Yost, and J. Ye, "Extreme ultraviolet radiation with coherence time greater than 1 s," Nat. Photonics **8**(7), 530–536 (2014).
29. C. Benko, L. Hua, T. K. Allison, F. Labaye, and J. Ye, "Cavity-Enhanced Field-Free Molecular Alignment at a High Repetition Rate," Phys. Rev. Lett. **114**(15), 153001 (2015).
30. A. Ozawa, Z. Zhao, M. Kuwata-Gonokami, and Y. Kobayashi, "High average power coherent vuv generation at 10 MHz repetition frequency by intracavity high harmonic generation," Opt. Express **23**(12), 15107–15118 (2015).
31. O. Pronin, V. Pervak, E. Fill, J. Rauschenberger, F. Krausz, and A. Apolonski, "Ultrabroadband efficient intracavity XUV output coupler," Opt. Express **19**(11), 10232–10240 (2011).
32. C. M. Heyl, S. B. Schoun, G. Porat, H. Green, and J. Ye, "A nozzle for high-density supersonic gas jets at elevated temperatures," Rev. Sci. Instrum. **89**(11), 113114 (2018).
33. J. Zhang, J. Brons, M. Seidel, V. Pervak, V. Kalashnikov, Z. Wei, A. Apolonski, F. Krausz, and O. Pronin, "49-fs Yb:YAG thin-disk oscillator with distributed Kerr-lens mode-locking," in *2015 European Conference on Lasers and Electro-Optics - European Quantum Electronics Conference* (Optical Society of America, 2015), paper PD_A_1.
34. C. Paradis, N. Modsching, V. J. Wittwer, B. Deppe, C. Kränkel, and T. Südmeyer, "Generation of 35-fs pulses from a Kerr lens mode-locked Yb:Lu2O3 thin-disk laser," Opt. Express **25**(13), 14918–14925 (2017).
35. J. Fischer, J. Drs, F. Labaye, N. Modsching, V. J. Wittwer, and T. Südmeyer, Data presented in this work are available on http://doi.org/10.23728/b2share.2c19736994b8437995c99aa48eb15da4 (2021).

3 Broadband THz generation

The high average power, short pulse duration and megahertz repetition rates of TDL oscillators is highly attractive for broadband high-power terahertz generation as described in detail in [1]. The first TDL driven THz generation source was demonstrated within the frame of this thesis. The system was based on one of the simplest approaches of optical rectification in collinear phase-matching geometry in a gallium phosphide (GaP) crystal. This first result, reproduced with permission from Optics Express [2], showed only a modest performance of $\tilde{1}0$ µW of average THz power, but at a relatively broad spectrum, extending to 7 THz, thanks to the short pulse duration of the driving laser. Although optical rectification in GaP is well-established in the 800-nm realm of Ti:sapphire lasers, surprisingly few attempts were made with 1 µm Yb-based lasers. Thus, we decided to use the tunability of our self-built TDL oscillator to systematically investigate the suitable parameter range for THz generation in GaP driven by 1 µm lasers. Since this study aligned with the development of the 20 W 100 fs laser [3], we also included this newly developed laser in the THz study, reaching 0.3 mW of generated THz average power with a spectrum extending to 5 THz, reproduced with permission from the Journal of the Optical Society of America B [4].

In the final part of this chapter, we inspired ourselves by the intra-oscillator HHG concept. Whereas the 20 W 100 fs TDL is a relatively complicated system requiring a >100 W pump diode, similar driving powers are routinely available inside small mode-locked bulk laser oscillators. By placing the GaP crystal directly inside the cavity of a KLM Yb:CALGO bulk oscillator, we have achieved comparable THz performance to our previous demonstration at a fraction of the pump power, complexity and cost of the components. The result is reproduced with permission from Optics Express [5].

References

1. Saraceno, C. J. Mode-locked thin-disk lasers and their potential application for high-power terahertz generation. *J. Opt.* **20**, 044010 (2018).
2. Paradis, C., Drs, J., Modsching, N., Razskazovskaya, O., Meyer, F., Kränkel, C., Saraceno, C. J., Wittwer, V. J. & Südmeyer, T. Broadband terahertz pulse generation driven by an ultrafast thin-disk laser oscillator. *Optics Express* **26**, 26377 (2018).
3. Modsching, N., Drs, J., Fischer, J., Paradis, C., Labaye, F., Gaponenko, M., Kränkel, C., Wittwer, V. J. & Südmeyer, T. Sub-100-fs Kerr lens mode-locked Yb:Lu_2O_3 thin-disk laser oscillator operating at 21 W average power. *Optics Express* **27**, 16111 (2019).
4. Drs, J., Modsching, N., Paradis, C., Kränkel, C., Wittwer, V. J., Razskazovskaya, O. & Südmeyer, T. Optical rectification of ultrafast Yb lasers: pushing power and bandwidth of terahertz generation in GaP. *JOSA B* **36**, 3039 (2019).
5. Hamrouni, M., Drs, J., Modsching, N., Wittwer, V. J., Labaye, F. & Südmeyer, T. Intra-oscillator broadband THz generation in a compact ultrafast diode-pumped solid-state laser. *Optics Express* **29**. Publisher: Optical Society of America, 23729 (2021).

Research Article | Vol. 26, No. 20 | 1 Oct 2018 | OPTICS EXPRESS 26377
Optics EXPRESS

Broadband terahertz pulse generation driven by an ultrafast thin-disk laser oscillator

CLÉMENT PARADIS,[1,*] JAKUB DRS,[1] NORBERT MODSCHING,[1] OLGA RAZSKAZOVSKAYA,[1] FRANK MEYER,[2] CHRISTIAN KRÄNKEL,[3] CLARA J. SARACENO,[2] VALENTIN J. WITTWER,[1] AND THOMAS SÜDMEYER[1]

[1]*Laboratoire Temps-Fréquence, Université de Neuchâtel 2000 Neuchâtel, Switzerland*
[2]*Photonics and Ultrafast Laser Science, Ruhr Universität Bochum 44801 Bochum, Germany*
[3]*Center for Laser Materials, Leibniz Institute for Crystal Growth 12489 Berlin, Germany*
**clement.paradis@unine.ch*

Abstract: We demonstrate broadband THz generation driven by an ultrafast thin-disk laser (TDL) oscillator. By optical rectification of 50-fs pulses at 61 MHz repetition rate in a collinear geometry in crystalline GaP, THz radiation with a central frequency at around 3.4 THz and a spectrum extending from below 1 THz to nearly 7 THz are generated. We realized a spectroscopic characterization of a GaP crystal and a benchmark measurement of the water-vapor absorption spectrum in the THz range. Sub-50-GHz resolution is achieved within a 5 THz bandwidth. Our experiments show the potential of ultrafast TDL oscillators for driving MHz-repetition-rate broadband THz systems.

1. Introduction

THz time-domain spectroscopy (THz-TDS) is a powerful tool to explore material properties and the dynamics of complex molecular systems through static and time-resolved investigations [1–5]. The employed THz source must fulfill a set of requirements including a spectral coverage in agreement with the studied system and a sufficient signal-to-noise ratio. Additionally, a compact system and a short acquisition time are often preferable. These criteria result in the demand for table-top high-power high-repetition-rate broadband THz sources.

Amongst other techniques, optical rectification of femtosecond pulses is a well-suited approach to produce high-power broadband THz radiation [6,7]. The development of THz sources based on optical rectification has been closely linked to the advances of sub-100-fs Ti:sapphire laser systems, which contributed to tremendous progress in this area. The efficiency of the optical rectification process is typically in the order of 10^{-7} to 10^{-2} [6,7]. Therefore, THz systems would benefit from power scalable laser technology. Recently developed diode-pumped ultrafast Yb-based lasers emitting at ~1 µm central wavelength demonstrated operation at average powers up to the kW level and high repetition rates with hundreds of femtosecond pulse duration [8–11]. In these lasers, detrimental thermal effects are significantly reduced due to alternative gain medium geometries (fibre, slab, thin disk) which allow for an efficient heat dissipation.

Most commonly, high-power ultrafast lasers rely on amplifier schemes based on complex multi-stage architecture (typically a seeding master oscillator, pulse stretching, multiple amplification stages and compression). In contrast, ultrafast thin-disk laser (TDL) oscillators offer a one-box solution for delivering nearly-ideal sech^2-shaped femtosecond pulses at MHz repetition rates, high average powers in diffraction-limited Gaussian beams. Nearly 300 W of average power have been achieved [12,13], but TDL oscillators typically operate at pulse durations longer than 100 fs [14]. However, sub-100-fs TDL oscillators based on broadband gain materials were recently demonstrated, albeit at moderate average power [15].

Despite appropriate laser parameters, Yb-based laser technology remains widely unexplored for THz generation [16]. Only few results have been reported attempting to use

#340332 https://doi.org/10.1364/OE.26.026377
Journal © 2018 Received 23 Jul 2018; revised 31 Aug 2018; accepted 10 Sep 2018; published 25 Sep 2018

Optics EXPRESS

Yb-based lasers to produce THz radiation. A high average power of 4 mW with a spectrum extending up to 1.2 THz has been demonstrated using tilted pulse front optical rectification in $LiNbO_3$ from 7 W average pump power and 1.3 ps pulse duration delivered by a 1 kHz repetition rate regenerative amplifier based on an Yb:YAG thin-disk crystal [17]. Compared to $LiNbO_3$, broader spectra are achieved in semiconductors such as ZnTe and GaP due to a broad collinear phase matching in the near infrared [18–20]. GaP has a large rectification bandwidth up to 40 THz, although it possesses a transverse optical phonon resonance at 11 THz [19]. Despite the associated dispersion, collinear phase matching up to 8 THz is achievable using crystal thicknesses in the order of hundreds of microns [21]. In 2006, the first experiments of optical rectification in GaP conducted with an Yb-based ultrafast pump laser yielded 6.5 µW THz average power from a 10-W 210-fs fiber amplifier operating at 120 MHz [22]. Later in 2013, 300 µW THz average power has been obtained with frequency content up to 2 THz using an Yb-doped fibre amplifier delivering 21 W of average power in 52-fs pulses at a repetition rate of 42 MHz [23]. Broad spectra with frequency content up 5 THz have been achieved both from a 3-W, 120-fs, 100-MHz Yb-doped fibre laser amplifier [24] and a 5-W, 20-fs, 78-MHz Yb-doped fibre laser amplifier [25].

Here, we report on MHz-repetition-rate broadband THz generation using the output of a mode-locked TDL. The 50-fs oscillator allows for a pulse-compression-free generation and detection of THz radiation up to 7 THz via optical rectification and electro-optic sampling (EOS) in crystalline GaP in a simple collinear geometry. Employing this THz source, we refine the Sellmeier coefficients of GaP in the THz range, enabling accurate phase matching calculations. Additionally, we benchmarked our system via THz spectroscopy of water vapor. Due to their power scalability and the high temporal resolution provided by sub-100-fs pump pulses, we believe that this result confirms the potential of ultrafast TDL oscillators to drive high-power broadband THz sources for static and time-resolved THz-TDS.

2. Broadband THz generation and detection

The experimental setup is depicted in Fig. 1. The driving laser source (described in [26]) is a Kerr lens mode-locked TDL oscillator based on the gain material $Yb:Lu_2O_3$ [27]. It delivers a diffraction limited beam ($M^2 = 1$) with 4 W of average power in 50-fs $sech^2$-shaped pulses at 61 MHz repetition rate. This leads to >60 nJ pulse energy and >1 MW peak power available directly at the output of the laser oscillator. The optical spectrum is centered at around 1031 nm with a FWHM of 20 nm (corresponding to 5 THz). THz radiation is generated via optical rectification of the femtosecond near-infrared pulses in a <110>-cut GaP crystal. The pump pulses are pre-chirped by three dispersive mirrors accounting for −1500 fs^2 of group delay dispersion to compensate for the propagation through the focusing lens and crystal. The pump beam is focused into the crystal to a 45 µm $1/e^2$ beam radius. Accounting for the 20% Fresnel reflection at the front interface of the uncoated GaP crystal, the peak intensity inside the crystal is estimated to be 27 GW/cm^2 and the fluence 1.7 mJ/cm^2. These values remain below the damage threshold of the material which has been measured to be 4.3 mJ/cm^2 (corresponding to 60 GW/cm^2 peak power) at 1040 nm with 61 fs pulses [28]. We used a ~5 mm diameter mirror to deflect the unconverted pump light. Due to the stronger divergence, only a small fraction of the THz radiation is reflected. An optical chopper running at 2.5 kHz modulates the pump beam for phase sensitive detection using a lock-in amplifier. The THz signal is then characterized via field-resolved detection using EOS in a second <110>-cut GaP [29,30]. The 50 fs gating probe pulses offer sufficient temporal resolution and do not require any additional temporal compression for a distortion-free broadband EOS measurement. The system is operated at room temperature (~22 °C) in a purged atmosphere with ~9% relative humidity.

Optics EXPRESS

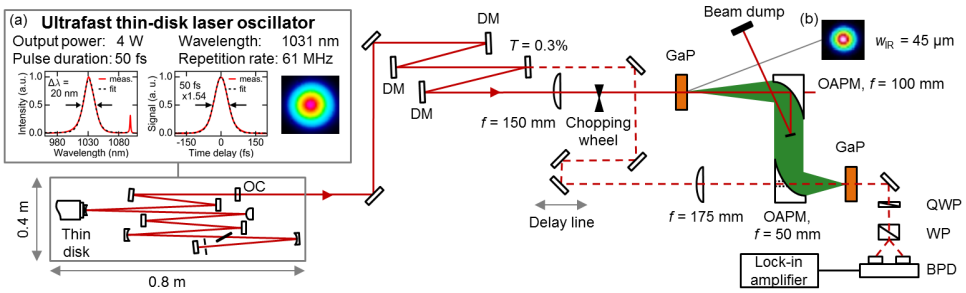

Fig. 1. Experimental setup for THz generation driven by the output of an ultrafast thin-disk laser oscillator. The inset (a) shows (from left to right) the optical spectrum, the autocorrelation trace and the output beam profile of the laser; the inset (b) shows the beam profile of the near-infrared laser at the focus. BPD: balanced photo-detector; DM: dispersive mirror; OAPM: off-axis parabolic mirror; OC: output coupler; QWP: quarter-wave plate; T: transmission; WP, Wollaston prism; w_{IR}: infrared beam radius.

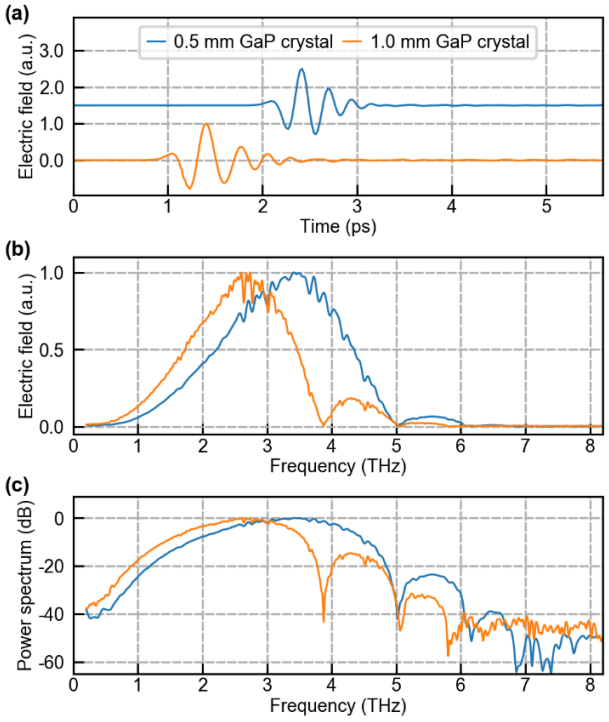

Fig. 2. (a) Time-resolved THz signals generated and detected in 0.5 mm (blue) and 1.0 mm (orange) thick GaP crystals (an offset in time and electric field has been added for better visibility) and (b) corresponding spectra of the electric field amplitude after Fourier transformation. (c) Corresponding power spectrum represented in logarithmic scale.

Quasi-single-cycle THz pulses were produced via optical rectification in 0.5 mm and 1.0 mm GaP crystals. The THz waveforms acquired in single scans with 30 ms and 10 ms integration constant, respectively, are shown in Fig. 2(a). They are detected via EOS using crystals with the same thicknesses as the rectification crystals. The corresponding THz spectra obtained by Fourier transformation of the waveforms have a central frequency at around 3.4 THz and 2.7 THz and extend up to nearly 6 THz and 7 THz, respectively [Fig. 2(b)]. The noise-like features in the spectrum are caused by residual water absorption. For both measurements, a dynamic range greater than 40 dB is achieved [Fig. 2(c)].

Optics EXPRESS

We evaluated the THz average power produced in the configuration with 1.0 mm GaP crystal using a calibrated pyroelectric photodetector (Ophir, RM9-THz) placed at the position of the detection crystal. The total path length from crystal to the detector is ~50 cm. Two filters made of black paper and fabric are used to block residual pump light. At a relative humidity level of ~25%, we measured an average power of 0.2 µW. We calibrated the measurement by characterizing the filters spectral transmission using the EOS setup. They exhibit a 2% total transmission for our spectrum. Thus the estimated THz average power is in the order of 10 µW, implying a conversion efficiency in the order of 10^{-6}, which is in a reasonable agreement with results obtained with similar laser parameters [22,23,25].

3. Spectroscopic characterization of GaP

Prompted by the discrepancies among the published data [31,32], we performed an independent measurement of the refractive index of GaP in the THz region via THz-TDS [3,4]. For this, we inserted a 1.0 mm <110>-cut GaP test-crystal into the collimated THz beam between two 0.5 mm GaP rectification and detection crystals. Comparing the spectral phase of this measurement to a reference measurement without the test-crystal allows to extract the refractive index of GaP [4]. Our data shown in Fig. 3 are consistent with [31] but disagree with more recent work [32]. Using our data in the range 1-6 THz and the data from [33] in the near infrared, the refractive index n is fitted to the Sellmeier equation given by

$$n^2 = 1 + \frac{B_1\lambda^2}{\lambda^2 - \lambda_1^2} + \frac{B_2\lambda^2}{\lambda^2 - \lambda_2^2}, \tag{1}$$

with $B_1 = 2.064$, $\lambda_1 = 27.284\,\mu\text{m}$, $B_2 = 8.089$ and $\lambda_2 = 0.2707\,\mu\text{m}$ and λ the wavelength in µm.

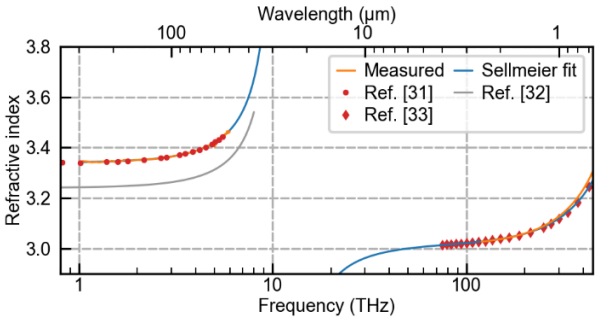

Fig. 3. Refractive index of GaP. In the THz region, it is retrieved from a THz time-domain spectroscopy measurement and compared to values taken from [31,32]. In the near-infrared range, is it measured by spectroscopic ellipsometry combined with transmission data and compared to [33].

The origin of the pronounced modulations in the THz spectra, e.g. at 5 THz, can be explained by phase matching. It accounts for the difference between the group velocity of GaP in the near-infrared and its phase velocity in the THz domain. The curves presented in Fig. 4 are calculated using the model introduced in [18] taking into consideration both generation and detection processes. In the calculation, we used a value of 3.31 for the optical group index of GaP at 1031 nm [33] and the refractive index in the THz range given by Eq. (1). Our calculated spectra are in a reasonable agreement with the measured ones in the range from 2 to 5 THz. In comparison, the refractive index given in [32] would yield a much broader phase matching for our system. The low-frequency behavior is not explained by this

simple calculation because it does not include the influence of the pump pulse shape and propagation effects. The discrepancies in the amplitude at frequencies above 5 THz are due to the linear absorption in GaP and vanishing nonlinear constant [32]. Based on phase matching considerations, we estimate an optimal crystal thickness to be 150 µm for producing a gap-less spectrum spanning up to 7 THz using an Yb-based driving laser source.

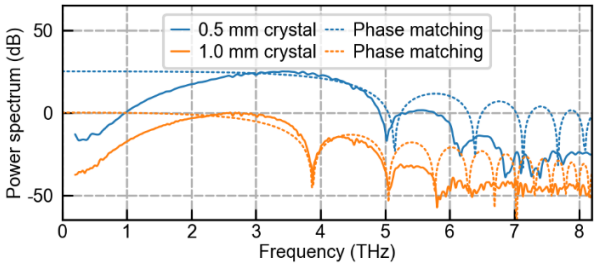

Fig. 4. THz spectra generated in 0.5 mm and 1.0 mm thick GaP crystals (solid lines). The corresponding phase matching curves (dashed lines) are calculated following the model presented in [18], using a value of 3.31 for the optical group index of GaP at 1031 nm and the refractive index in the THz domain given by (1).

4. THz spectroscopy of water vapor

To confirm the suitability of the system for broadband THz-TDS, we performed a benchmarking spectroscopic measurement of water vapor absorption [2] [Fig. 5]. For this, we compared the THz spectra acquired at two humidity levels (23% and 9% relative humidity) in a setup using 1.0 mm GaP crystals for generation and detection. Each data set is acquired in a single scan with 10 ms integration constant. The water vapor absorption coefficient is given by the logarithm of the ratio of the two amplitude spectra as a function of the frequency. The resulting water vapor absorption spectrum is compared to the one reported in [34]. Water vapor lines are reliably detected with a sub-50-GHz resolution up to 5 THz. A better reliability in the 5-6 THz range could be obtained by averaging over multiple scans or by increasing the integration time constant. A finer spectral resolution is achievable by acquiring longer temporal scans including the echo pulses from the reflections inside the crystals, which would not affect the data analysis as they divide out in the frequency domain [2].

Optics EXPRESS

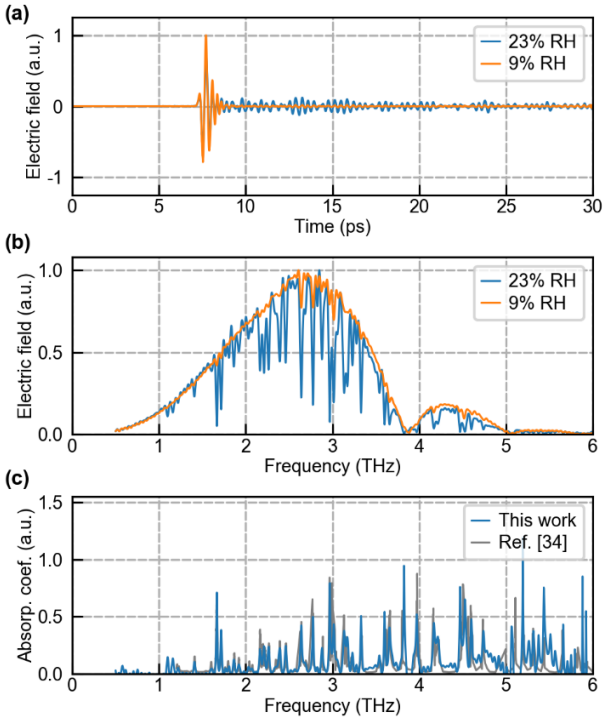

Fig. 5. (a) THz time-domain waveforms and (b) THz power spectra generated in a 1.0 mm GaP crystal at different relative humidity (RH) levels. (c) Frequency-dependent absorption coefficient of the water vapor, compared to the data taken from [34].

5. Conclusion and outlook

In conclusion, we have demonstrated broadband THz generation at MHz repetition rate using an ultrafast TDL oscillator as pump source. This simple single-stage laser source enabled the generation and detection of spectra with frequency content extending up to nearly 7 THz. We performed a spectroscopic measurement of GaP and refined its Sellmeier equation in the THz range. It is used for phase matching calculations, which are consistent with the acquired THz spectra. We conducted benchmarking linear THz-TDS experiment, measuring water vapor absorption spectrum with a sub-50-GHz resolution achieved in a frequency range between 0.5 and 5 THz.

We believe that higher THz frequencies are within reach by using thinner GaP crystals for improved phase matching or different types of emitters [35] such as ZnTe [20], nonlinear organic crystals [36], plasma [37] or metallic spintronic emitters [38]. On the other hand, higher THz average power should be achievable by using thicker crystals, albeit at the expense of a reduced bandwidth. A compromise fulfilling the demands of a particular experiment is certainly possible. Similar to the case of THz generation in $LiNbO_3$ [7], our preliminary calculations indicate that a pump pulse duration of 50 fs is not optimal for efficient THz generation with a targeted bandwidth of 7 THz. As a next step, we will investigate the influence of the pulse duration on the THz generation in GaP crystals. TDL oscillators delivering more than 10 W of average power with 90 fs pulses at 61 MHz repetition rate have been as well recently demonstrated [26]. We expect that such parameters would allow increasing the THz average power due to the availability of higher pump power and longer pulses offering an adequate spectral bandwidth for efficient conversion. Therefore, we believe that TDL oscillators are a promising technology for scaling up the average power

Optics EXPRESS

of broadband THz radiation. We expect that such compact sources of broadband THz pulses based on thin-disk laser oscillators will be beneficial for linear static THz-TDS and time-resolved THz spectroscopy.

Funding

German Ministry of Education and Research (BMBF) (FKZ 13N14192); Alexander von Humboldt Foundation and the Cluster of Excellence RESOLV (EXC 1069); National Center of Competence in Research for Molecular Ultrafast Science and Technology (NCCR-MUST) and the Swiss National Science Foundation (SNF) (200021_159931; 200020_179146).

Acknowledgements

We thank Gregory Gäumann, Yannik Wäber, Prof. Thomas Feurer (IAP, Bern) and Prof. J. P. Wolf (GAP, Geneva) for scientific discussions on terahertz generation and for the contributed equipment. We are grateful to Dr. Nicholas Karpowicz (MPQ, Garching, Germany) for fruitful personal scientific communication.

C. K. acknowledges financial support by the German Ministry of Education and Research (BMBF) (FKZ 13N14192). C. J. S. acknowledges financial support by the Alexander von Humboldt Foundation and the Cluster of Excellence RESOLV (EXC 1069). T. S. acknowledges financial support by the National Center of Competence in Research for Molecular Ultrafast Science and Technology (NCCR-MUST) and the Swiss National Science Foundation (SNF) (200021_159931; 200020_179146).

References

1. K. P. Cheung and D. H. Auston, "A novel technique for measuring far-infrared absorption and dispersion," Infrared Phys. **26**(1), 23–27 (1986).
2. M. Exter, C. Fattinger, and D. Grischkowsky, "Terahertz time-domain spectroscopy of water vapor," Opt. Lett. **14**(20), 1128–1130 (1989).
3. D. Grischkowsky, S. Keiding, M. van Exter, and C. Fattinger, "Far-infrared time-domain spectroscopy with terahertz beams of dielectrics and semiconductors," J. Opt. Soc. Am. B **7**(10), 2006–2015 (1990).
4. P. U. Jepsen, D. G. Cooke, and M. Koch, "Terahertz spectroscopy and imaging – Modern techniques and applications," Laser Photonics Rev. **5**(1), 124–166 (2011).
5. T. A. A. Oliver, "Recent advances in multidimensional ultrafast spectroscopy," R. Soc. Open Sci. **5**(1), 171425 (2018).
6. K. Reimann, "Table-top sources of ultrashort THz pulses," Rep. Prog. Phys. **70**(10), 1597–1632 (2007).
7. J. A. Fülöp, L. Pálfalvi, G. Almási, and J. Hebling, "Design of high-energy terahertz sources based on optical rectification," Opt. Express **18**(12), 12311–12327 (2010).
8. P. Russbueldt, T. Mans, J. Weitenberg, H. D. Hoffmann, and R. Poprawe, "Compact diode-pumped 1.1 kW Yb:YAG Innoslab femtosecond amplifier," Opt. Lett. **35**(24), 4169–4171 (2010).
9. J.-P. Negel, A. Loescher, A. Voss, D. Bauer, D. Sutter, A. Killi, M. A. Ahmed, and T. Graf, "Ultrafast thin-disk multipass laser amplifier delivering 1.4 kW (4.7 mJ, 1030 nm) average power converted to 820 W at 515 nm and 234 W at 343 nm," Opt. Express **23**(16), 21064–21077 (2015).
10. T. Nubbemeyer, M. Kaumanns, M. Ueffing, M. Gorjan, A. Alismail, H. Fattahi, J. Brons, O. Pronin, H. G. Barros, Z. Major, T. Metzger, D. Sutter, and F. Krausz, "1 kW, 200 mJ picosecond thin-disk laser system," Opt. Lett. **42**(7), 1381–1384 (2017).
11. M. Müller, M. Kienel, A. Klenke, T. Gottschall, E. Shestaev, M. Plötner, J. Limpert, and A. Tünnermann, "1 kW 1 mJ eight-channel ultrafast fiber laser," Opt. Lett. **41**(15), 3439–3442 (2016).
12. C. J. Saraceno, F. Emaury, O. H. Heckl, C. R. E. Baer, M. Hoffmann, C. Schriber, M. Golling, T. Südmeyer, and U. Keller, "275 W average output power from a femtosecond thin disk oscillator operated in a vacuum environment," Opt. Express **20**(21), 23535–23541 (2012).
13. J. Brons, V. Pervak, E. Fedulova, D. Bauer, D. Sutter, V. Kalashnikov, A. Apolonskiy, O. Pronin, and F. Krausz, "Energy scaling of Kerr-lens mode-locked thin-disk oscillators," Opt. Lett. **39**(22), 6442–6445 (2014).
14. C. J. Saraceno, F. Emaury, C. Schriber, A. Diebold, M. Hoffmann, M. Golling, T. Südmeyer, and U. Keller, "Toward millijoule-level high-power ultrafast thin-disk oscillators," IEEE J. Sel. Top. Quantum Electron. **21**(1), 106–123 (2015).
15. C. J. Saraceno, O. H. Heckl, C. R. E. Baer, C. Schriber, M. Golling, K. Beil, C. Kränkel, T. Südmeyer, G. Huber, and U. Keller, "Sub-100 femtosecond pulses from a SESAM modelocked thin disk laser," Appl. Phys. B **106**(3), 559–562 (2012).
16. C. J. Saraceno, "Mode-locked thin-disk lasers and their potential application for high-power terahertz generation," J. Opt. **20**(4), 044010 (2018).

17. Y. Ochi, K. Nagashima, M. Maruyama, M. Tsubouchi, F. Yoshida, N. Kohno, M. Mori, and A. Sugiyama, "Yb:YAG thin-disk chirped pulse amplification laser system for intense terahertz pulse generation," Opt. Express **23**(11), 15057–15064 (2015).
18. Q. Wu and X.-C. Zhang, "7 terahertz broadband GaP electro-optic sensor," Appl. Phys. Lett. **70**(14), 1784–1786 (1997).
19. A. Leitenstorfer, S. Hunsche, J. Shah, M. C. Nuss, and W. H. Knox, "Detectors and sources for ultrabroadband electro-optic sampling: experiment and theory," Appl. Phys. Lett. **74**(11), 1516–1518 (1999).
20. Q. Wu and X.-C. Zhang, "Free-space electro-optics sampling of mid-infrared pulses," Appl. Phys. Lett. **71**(10), 1285–1286 (1997).
21. I. D. Vugmeyster, J. F. Whitaker, and R. Merlin, "GaP based terahertz time-domain spectrometer optimized for the 5-8 THz range," Appl. Phys. Lett. **101**(18), 181101 (2012).
22. G. Chang, C. J. Divin, C.-H. Liu, S. L. Williamson, A. Galvanauskas, and T. B. Norris, "Power scalable compact THz system based on an ultrafast Yb-doped fiber amplifier," Opt. Express **14**(17), 7909–7913 (2006).
23. J. Li, L. Chai, J. Shi, F. Liu, B. Liu, B. Xu, M. Hu, Y. Li, Q. Xing, C. Wang, A. B. Fedotov, and A. M. Zheltikov, "Generation of 0.3 mW high-power broadband terahertz pulses from GaP crystal pumped by negatively chirped femtosecond laser pulses," Laser Phys. Lett. **10**(12), 125404 (2013).
24. J. Hamazaki, K. Furusawa, N. Sekine, A. Kasamatsu, and I. Hosako, "Effects of chirp of pump pulses on broadband terahertz pulse spectra generated by optical rectification," Jpn. J. Appl. Phys. **55**(11), 110305 (2016).
25. J. Xu, B. Globisch, C. Hofer, N. Lilienfein, T. Butler, N. Karpowicz, and I. Pupeza, "Three-octave terahertz pulses from optical rectification of 20-fs, 1-µm, 78-MHz pulses in GaP," J. Phys. At. Mol. Opt. Phys. **51**(15), 154002 (2018).
26. C. Paradis, N. Modsching, V. J. Wittwer, B. Deppe, C. Kränkel, and T. Südmeyer, "Generation of 35-fs pulses from a Kerr lens mode-locked Yb:Lu_2O_3 thin-disk laser," Opt. Express **25**(13), 14918–14925 (2017).
27. C. Kränkel, "Rare-earth-doped sesquioxides for diode-pumped high-power lasers in the 1-, 2-, and 3-µm spectral range," IEEE J. Sel. Top. Quantum Electron. **21**(1), 250–262 (2015).
28. Y. Li, F. Liu, Y. Li, L. Chai, Q. Xing, M. Hu, and C. Wang, "Experimental study on GaP surface damage threshold induced by a high repetition rate femtosecond laser," Appl. Opt. **50**(13), 1958–1962 (2011).
29. Q. Wu and X.-C. Zhang, "Free-space electro-optic sampling of terahertz beams," Appl. Phys. Lett. **67**(24), 3523–3525 (1995).
30. A. Nahata, D. H. Auston, T. F. Heinz, and C. Wu, "Coherent detection of freely propagating terahertz radiation by electro-optic sampling," Appl. Phys. Lett. **68**(2), 150–152 (1996).
31. D. F. Parsons and P. D. Coleman, "Far infrared optical constants of gallium phosphide," Appl. Opt. **10**(7), 1683 (1971).
32. S. Casalbuoni, H. Schlarb, B. Schmidt, P. Schmüser, B. Steffen, and A. Winter, "Numerical studies on the electro-optic detection of femtosecond electron bunches," Phys. Rev. Spec. Top. Accel. Beams **11**(7), 072802 (2008).
33. W. L. Bond, "Measurement of the refractive indices of several crystals," J. Appl. Phys. **36**(5), 1674–1677 (1965).
34. B. Clough, J. Dai, and X.-C. Zhang, "Laser air photonics: beyond the terahertz gap," Mater. Today **15**(1), 50–58 (2012).
35. B. Ferguson and X.-C. Zhang, "Materials for terahertz science and technology," Nat. Mater. **1**(1), 26–33 (2002).
36. X.-C. Zhang, X. F. Ma, Y. Jin, T.-M. Lu, E. P. Boden, P. D. Phelps, K. R. Stewart, and C. P. Yakymyshyn, "Terahertz optical rectification from a nonlinear organic crystal," Appl. Phys. Lett. **61**(26), 3080–3082 (1992).
37. K. Y. Kim, J. H. Glownia, A. J. Taylor, and G. Rodriguez, "Terahertz emission from ultrafast ionizing air in symmetry-broken laser fields," Opt. Express **15**(8), 4577–4584 (2007).
38. T. Seifert, S. Jaiswal, U. Martens, J. Hannegan, L. Braun, P. Maldonado, F. Freimuth, A. Kronenberg, J. Henrizi, I. Radu, E. Beaurepaire, Y. Mokrousov, P. M. Oppeneer, M. Jourdan, G. Jakob, D. Turchinovich, L. M. Hayden, M. Wolf, M. Münzenberg, M. Kläui, and T. Kampfrath, "Efficient metallic spintronic emitters of ultrabroadband terahertz radiation," Nat. Photonics **10**(7), 483–488 (2016).

Optical rectification of ultrafast Yb-lasers: Pushing power and bandwidth of THz generation in GaP

JAKUB DRS,[1,*] NORBERT MODSCHING,[1] CLÉMENT PARADIS,[1] CHRISTIAN KRÄNKEL,[2] VALENTIN J. WITTWER,[1] OLGA RAZSKAZOVSKAYA,[1] AND THOMAS SÜDMEYER[1]

[1]*Laboratoire Temps-Fréquence (LTF), Institut de Physique, Université de Neuchâtel, Avenue de Bellevaux 51, Neuchâtel, Switzerland*
[2]*Center for Laser Materials, Leibniz-Institut für Kristallzüchtung, Max-Born-Str. 2, Berlin, Germany*
**jakub.drs@unine.ch*

Abstract: We demonstrate broadband high-power THz generation at MHz repetition rates by optical rectification in GaP driven by an ultrafast Yb-based thin-disk laser oscillator. We investigate the influence of pulse duration in the range of 50 fs to 220 fs and thickness of the GaP crystal on the THz generation. Optimization of these parameters with respect to the broadest spectral bandwidth yields a gap-less THz spectrum extending to nearly 7 THz. We further tailor the driving laser and the THz generation parameters for the highest average power, demonstrating 0.3 mW THz radiation with a spectrum extending to 5 THz. This was achieved using a 0.5 mm thick GaP crystal pumped with a 95 fs, 20 W thin disk laser, operating at 48 MHz repetition rate. We also provide a comprehensive method to estimate the THz spectrum, which can be used for design and optimization of similar THz systems.

1. Introduction

Increasing both the average power and the repetition rate of broadband THz sources is of high interest for various spectroscopic and imaging THz applications [1]. So far, tabletop high-power broadband THz sources have been mostly driven by high energy laser amplifier systems, typically based on Ti:sapphire gain material, operating at kHz repetition rates and modest average powers of several watts.

In the last years Yb-based directly diode-pumped solid-state lasers have become a promising alternative to Ti:sapphire systems. The higher Stokes efficiency of the Yb-doped gain medium together with the direct diode pumping scheme allows for substantial increase in average power, albeit at the expense of longer pulse durations due to the narrower gain bandwidth of Yb-doped media. Several studies investigated the potential of Yb-based amplifier systems for high-power THz generation. A chirped pulse thin-disk laser amplifier has been used to generate 4 mW of THz average power in $LiNbO_3$ with a spectrum extending to 1 THz [2]. Li *et al.* demonstrated generation of 0.3 mW THz radiation with a spectrum extending to 2 THz by optical rectification in GaP driven by a 21 W, 52 fs fiber amplifier [3]. More recently, broadband THz systems with spectra extending to 5 and 6 THz have been demonstrated, however, yet in a few-µW average power range [4,5].

Ultrafast Yb-based thin-disk laser (TDL) oscillators operating at MHz repetition rates reach high output powers directly out of the oscillator circumventing the necessity for amplification stages. They usually emit transform-limited soliton pulses without pre- or post-pulses in a TEM_{00} beam. Nearly 300 W have been obtained from TDL oscillators with several hundred fs pulse durations [6,7]. In the last years, there was also a large progress in the development of ultrafast thin-disk lasers operating directly in the sub-100-fs regime [8–13]. The shortest pulse durations of ultrafast thin-disk lasers have been reduced to 30 fs [14], and power levels up to

20 W have been achieved in 95-fs pulses [15], making TDL oscillators very attractive sources to drive broadband high-power THz generation [16].

Recently, we demonstrated the generation of broadband THz radiation with a gap-less spectrum extending to 5 THz at a few µW of average power [17]. This was achieved by optical rectification in GaP of 50-fs pulses, delivered by a 4-W TDL oscillator. Shortly after, Meyer *et al.* demonstrated the potential for increasing the available THz power by using a high-power TDL oscillator as a driving source [18]. They showed that 100 W of average laser power with 580 fs pulse duration could be optically rectified in GaP, yielding 80 µW of average THz power with a spectrum extending up to 1.6 THz.

In this study, we show that optical rectification in GaP allows for high average THz powers approaching the mW range also with broadband spectra. We investigate the influence of the pulse duration of the driving laser and the thickness of the GaP crystal on the THz generation. Optimization of these parameters with respect to spectral bandwidth allowed us to generate THz radiation with a spectrum extending to nearly 7 THz. This is to our knowledge the broadest gap-less THz spectrum obtained from an Yb-based laser driven system. Optimization with respect to average power yielded 0.3 mW of THz radiation with a spectrum extending to nearly 5 THz. We further provide a comprehensive guideline to estimate the generated THz spectrum based on pulse duration and thickness of the crystal, which we believe can be a very useful tool for the optimization of similar THz systems.

2. Experimental setup

The driving laser of our setup described in [13] is a Kerr lens mode-locked TDL oscillator (Fig. 1) based on the gain material Yb:Lu_2O_3 [19] emitting at a center wavelength of 1.03 µm. It generates transform limited soliton pulses at 60 MHz repetition rate with pulse durations between 50 and 220 fs at typical average powers of several watts and diffraction limited beam quality (M^2 < 1.05). Pulse duration and average power of the laser oscillator can be modified by changing the intra-cavity dispersion (replacing dispersive mirrors), the output-coupling rate and by variation of the hard aperture size (elements shown in blue in Fig. 1). This approach is limited to discrete operation parameters and does not allow for a large continuous tuning range; however, it ensures maintaining transform-limited soliton pulses and TEM_{00} beam profile at all the accessible pulse durations. This allowed us to perform high-fidelity measurements of the influence of pulse duration on the THz generation. In the second part of the study, focused on optimization of the THz average power, we utilized a power-scaled version of the driving TDL oscillator, delivering a higher average power of 20 W at 95 fs pulse duration.

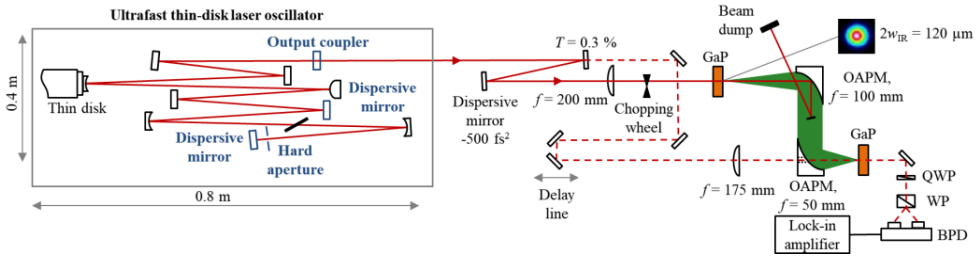

Fig. 1. Experimental setup for THz generation via optical rectification and detection by electro-optic sampling driven by an ultrafast TDL oscillator. Pulse duration and average power of the driving laser can be modified by replacing the cavity elements highlighted in blue. OAPM: off-axis parabolic mirror; QWP: quarter-wave plate; WP: Wollaston prism; BPD: balanced photo-detector; T: output coupler; w_{IR}: beam radius at $1/e^2$.

The THz radiation is generated via optical rectification in uncoated <110>-cut GaP crystals of different thickness. The pump pulses are pre-chirped by -500 fs^2 to compensate for the

focusing lens and crystal dispersion. The beam is chopped at a frequency of 2.5 kHz for lock-in detection and focused into the crystal at a $1/e^2$ beam diameter of 120 µm. The unconverted infrared (IR) light is separated from the THz radiation by a 5-mm diameter mirror placed on the optical axis. Due to the much stronger divergence of the THz radiation, this does not create significant losses for the THz beam.

The generated THz radiation is detected by electro-optic sampling (EOS) in a second <110>-cut uncoated GaP crystal. The EOS signal is sent to the lock-in amplifier with a typical time constant of 30 ms. The delay line is moved by fixed steps and remains on the spot during each measured point. This avoids vibrations and eliminates dependence on stage speed and lock-in time constant. The system is operated at room temperature in a dry air purged environment with residual relative humidity of ~7%.

3. Influence of pulse duration and crystal thickness on the THz spectrum

The THz spectrum generated by optical rectification in GaP is mainly determined by the pulse duration of the driving laser and the thickness of the nonlinear crystal. While the corresponding parameters are well investigated for Ti:sapphire lasers emitting at 800 nm, their influence in the emission wavelength range of Yb-based lasers around 1 µm remains relatively less explored, which motivated our investigations.

In a first experiment, we investigated the influence of the GaP crystal thickness on the THz spectrum. We used 50-fs pulses and measured the THz spectra for three different crystal thicknesses (see Fig. 2 a). The experiment demonstrates how the thickness of the GaP crystals limits the THz spectrum due to the mismatch between the group velocity of the IR pulse and the phase velocity of the THz radiation [20]. The theoretical phase matching curves are plotted as dashed lines for reference. The solid blue and orange curves depict spectra for crystals thicker than optimum for the generation of broadest spectra, which show frequency cut-offs at 4 and 5 THz, respectively. The green curve demonstrates the results with a thinner crystal, where the phase mismatch frequency cut-off at 7.3 THz is not anymore the main limiting factor and the THz spectrum is mostly limited by the pulse duration of the driving laser. The phase matching conditions between the IR and THz pulse in GaP were calculated according to [20] based on a Sellmeier fit of the THz refractive indices presented in [17] and a group refractive index for the IR pulse $n_g = 3.31$ calculated from [21] (see Tab. 1 in the appendix).

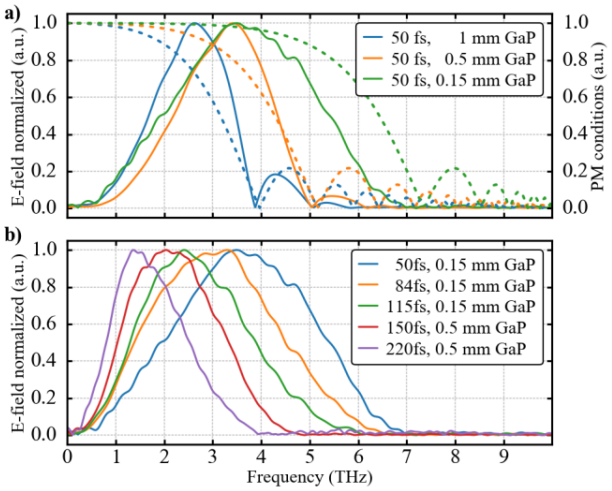

Fig. 2 a) THz spectra generated by optical rectification of 50 fs pulses in GaP crystals of different thicknesses. The use of thick crystals (blue and orange) poses a frequency cut-off on the measured THz spectrum due to the phase mismatch between the IR and THz pulses. The theoretical phase matching curves are plotted by dashed lines for reference. The green curve shows a spectrum for a crystal thin enough to prevent phase mismatch being the most limiting factor. b) Experimental measurement of the achievable THz spectra for different pulse durations of the driving laser. The thickness of the crystal is adapted to the respective pulse duration in order to maximize the signal, while avoiding the phase mismatch frequency cut-off.

In a second experiment, we studied the influence of the pulse duration of the driving laser. The experiment was designed to assess the maximum spectral bandwidth at each pulse duration. To this end, we adapted the crystal thickness to maximize the THz signal, while avoiding the phase mismatch frequency cut-off in the THz spectrum. Five different configurations of the driving laser were chosen for the experiment with pulse durations between 50 and 220 fs at average powers of 3 to 7 W. Despite the different average power levels obtained at different pulse durations, we did not observe any significant dependence of the THz spectral shape on the driving laser average power in our experiments. We therefore used the full available power of each configuration to drive the THz generation.

The THz spectra measured for different pulse durations are shown in Fig. 2 b). The central frequency shifts from 1.5 THz for 220-fs pulses to 3.5 THz for the 50-fs configuration. The broadest THz spectrum acquired in the 50-fs configuration extends to nearly 7 THz.

We further verify the THz spectral bandwidth of our system by performing a THz time domain spectroscopy measurement of water vapor shown in the appendix of this study in Fig 5. The measurement was taken using 84 fs pulse duration (orange curve in Fig. 2b) and shows a good agreement with the theoretical absorption of water vapor obtained from the HITRAN database [22] in a frequency range between 1 and 6 THz with < 20 GHz spectral resolution.

4. Estimation of the THz spectrum

Understanding of the underlying mechanisms of the THz generation and detection is a key requirement for optimization of THz systems. Although solving a nonlinear coupled wave equation is generally required to fully describe the THz generation process [23,24], according to our measurements, the THz spectrum can be reasonably approximated by decoupled multiplicative factors in the frequency domain. This approach provides a comprehensive tool to isolate the influence of different parameters and determine the key limitations. The considered frequency factors and their parameters are shown in Eq. (1) and depicted graphically

in Fig. 3. For the convenience of the reader, we also include all the formulas in Table 1 in the appendix.

$$E_{\mathrm{THz}}(\omega) \approx E_{0\ \mathrm{THz}}(\omega, \tau_{\mathrm{laser}}) \cdot \mathrm{PM}_{\mathrm{Gen}}(\omega, n_{\mathrm{g}}, d_{\mathrm{crystal}}) \cdot \mathrm{EOS}(\omega, \tau_{\mathrm{laser}}) \cdot \mathrm{PM}_{\mathrm{Det}}(\omega, n_g, d_{\mathrm{crystal}}) \cdot r_{41}(\omega) \cdot t_{\mathrm{GaP}}(\omega, d_{\mathrm{crystal}}) \quad (1)$$

The maximum bandwidth of the THz field $E_{0\ \mathrm{THz}}$ generated by optical rectification in $\chi^{(2)}$ nonlinearity (shown in blue in Fig. 3) can be approximated by the 2nd derivative of the IR pulse intensity envelope with respect to time [25]. Both the generation and the detection of the THz radiation are affected by the phase matching (PM) condition between the phase velocity of the THz radiation and the group velocity of the IR pulse in the nonlinear crystal. The factor $\mathrm{PM}_{\mathrm{Gen}} \cdot \mathrm{PM}_{\mathrm{Det}}$ (red curve in Fig. 3) is strongly dependent on the thickness of the GaP crystal d_{crystal} and the center wavelength of the driving laser through the group refractive index n_{g}. The response of the EOS detection can be described as a cross correlation between the THz field and the intensity envelope of the IR probing pulse as derived in [26], i.e., multiplication with the IR pulse intensity spectrum (depicted in orange in Fig. 3) in the frequency domain. The THz radiation is further affected by an electro-optic coefficient r_{41} (purple curve in Fig. 3) and the THz transmission t_{GaP} of the GaP crystal (gray curve in Fig. 3), determined by Fresnel reflection and material absorption. Both curves are based on Lorentzian fits to third party experimental data obtained from [27]. The fits might have significant uncertainties; however, they do not have a major influence on most of our data compared to the phase matching condition.

We present three example spectral estimates for pulse durations of 220 fs, 95 fs, and 50 fs and different crystal thicknesses. In the case of longest pulse duration (Fig. 3a), the THz spectrum is mostly limited by the EOS detection. The phase matching condition for the 0.5 mm thick GaP crystal does not strongly influence the THz spectrum at such long pulse durations. For sub-100-fs pulses, the thickness of the crystal starts to play an important role. Due to the indirect phonon resonance of GaP at 11 THz [28], higher THz frequencies are getting rapidly phase mismatched with the driving IR pulse. Thus, the use of thin crystals is required in order to support the highest spectral bandwidth. Fig. 3b) shows that the phase mismatch in the 0.5 mm thick GaP crystal already slightly limits the THz spectrum for a 95-fs driving laser (see the dip at 5 THz). The shortest pulses of 50 fs duration (Fig. 3c) finally require a more than three times thinner crystal to support the THz spectrum extending to 7 THz.

The described method slightly overestimates the spectral bandwidth, as it does not take into account processes like dispersion and self-focusing of the IR pulses in GaP or the coupled nonlinear propagation of IR and THz pulses. It predicts that THz frequencies beyond 7 THz are within reach for pulse durations shorter than 50 fs and crystal thickness bellow 0.15 mm. The credibility of the prediction for these higher THz frequencies, approaching the phonon resonance of GaP, is however further reduced by the uncertainties of the used material properties. Nevertheless, according to our measurements, the model provides valid estimates for pulse durations in excess of 50 fs.

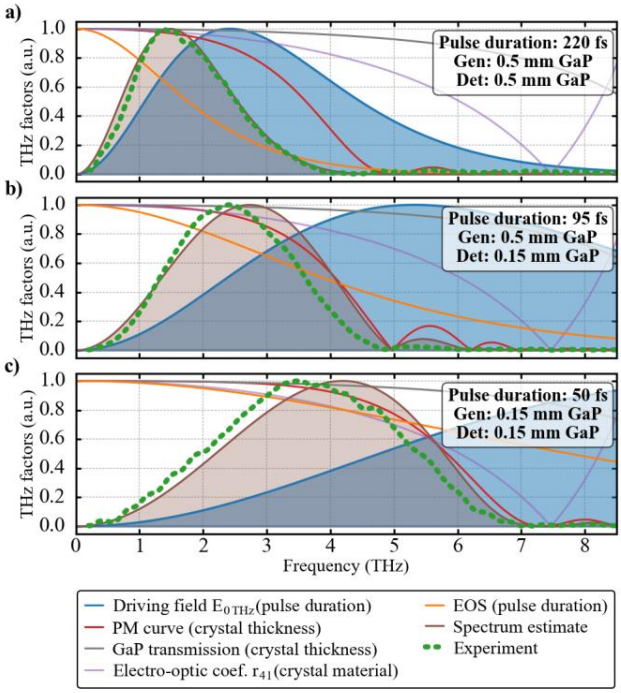

Fig. 3. Estimate of the THz spectra considering multiplicative factors in frequency domain. The blue curve depicts the maximum bandwidth of the driving THz field $E_{0\,\mathrm{THz}}$. The red curve shows the phase matching condition for 1 µm IR pulse and THz radiation considering both the detection and the generation GaP crystal. The orange curve determines the EOS corresponding to the probing pulse intensity spectrum. Violet and gray curves depict GaP transmission and electro-optic coefficient r_{41}. The overall spectral estimate E_{THz} calculated according to Eq. 1 is shown by the brown filled curve, the corresponding experimental data are shown in dashed green.

5. Toward high THz powers

In order to investigate the achievable power levels of our THz system, we utilized a power-scaled version of our TDL oscillator optimized for high output power in the sub-100-fs regime as a compromise between achievable average power and shortest pulse duration. This laser configuration, described in detail in [15], delivers 95-fs transform limited soliton pulses at 20 W average power and 48 MHz repetition rate, which corresponds to 3.9 MW peak power and 0.4 µJ pulse energy. The laser beam is focused into the generation crystal by a 200 mm focusing lens. The THz average power is measured by an Ophir pyroelectric THz power detector. Corresponding THz spectra are measured by EOS in a 0.15 mm thick GaP crystal. In order to prevent all unconverted IR light from reaching the pyroelectric detector and influencing the power measurement we use a small mirror centered on the optical axis deflecting the main beam into a beam block combined with two layers of black plastic foil to block the residual IR light scattered from the crystal. The THz transmission of one layer of the plastic foil was determined to be 46% and the presented average THz power was corrected accordingly.

We first investigated the influence of the driving field peak intensity in the crystal by performing a 1 cm z-scan of the focusing lens. The spot size diameter in the crystal was varied between 200 and 370 µm. We limited ourselves to peak intensities of 20 GW/cm^2 to avoid damage of the crystals. The result of the experiment for 0.5 and 0.15 mm thick crystals is shown

in Fig. 4a). Although the $\chi^{(2)}$ origin of the optical rectification suggests quadratic dependence of the THz power on the peak intensity, our result already shows an onset of saturation. The highest driving peak intensity of 20 GW/cm^2 thus seems to be close to the maximum efficiency at this pulse duration. It yields an average THz power of 65 µW for the 0.15 mm thick crystal and 0.3 mW for 0.5 mm thickness, corresponding to an optical-to-optical efficiency of $3.2 \cdot 10^{-6}$ and $1.5 \cdot 10^{-5}$, respectively, for the 20-W driving laser.

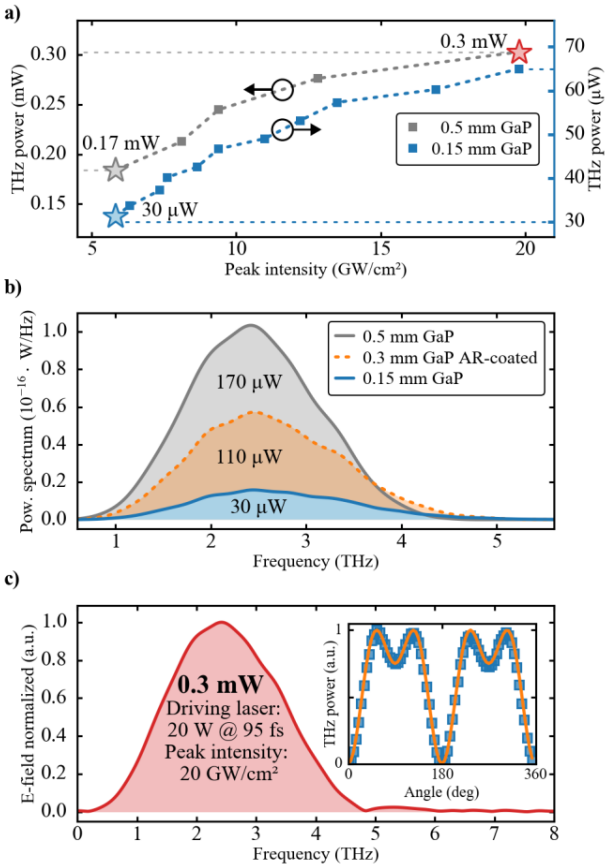

Fig. 4 a) Z-scan experiment showing the dependence of the THz power on the peak intensity in the crystal. The curves for 0.5 mm and 0.15 mm thick crystals are plotted on two different power scales (left and right axis) sharing same zero. The stars in the graph correspond to the same colored spectra shown below. b) THz spectral power density for different crystal thicknesses measured with a 1/e^2 focus diameter of 370 µm, corresponding to peak intensities of 5.8 GW/cm^2 for the 0.5 mm and 0.15 mm crystals and 7.2 GW/cm^2 for the AR-coated 0.3 mm crystal (dashed orange line). c) The electric field spectrum at maximum THz average power generated in a 0.5 mm GaP crystal at 200 µm spot size diameter (20 GW/cm^2 peak intensity). The blue markers in the inset graph show the measured dependence of the THz power on the crystal orientation compared with a theoretical curve in orange, proving the $\chi^{(2)}$ origin of the THz generation.

In the second part of the experiment, we investigated the influence of the GaP crystal thickness on the THz power. We used three crystal thicknesses of 0.5, 0.3 and 0.15 mm, with a modest focusing spot size diameter of 370 µm measured at 1/e^2. The corresponding spectral power densities are depicted in Fig. 4b). Accounting for 20% Fresnel reflection for the uncoated crystals, the used spot size corresponds to peak intensities of 5.8 GW/cm^2 and amounts to 7.2 GW/cm^2 for the 0.3 mm crystal, which is AR coated and thus plotted by dashed line.

Fig. 4c) finally shows the electric field amplitude spectrum of the highest generated THz average power. The 0.5 mm GaP crystal already slightly limits the spectral bandwidth. The spectra shown in Fig. 4b) and c) correspond to the data points marked with same color stars in Fig. 4a).

We further validated the $\chi^{(2)}$ nonlinear origin of the THz radiation by measuring the THz power as a function of the crystal orientation, comparing it with the theoretical values [25] for the <110>-cut zincblende structure of the GaP crystal. The experiment, shown in the inset of Fig. 4c), agrees very well with the theoretical curve.

6. Conclusion

We have demonstrated that broadband high-power THz radiation approaching mW power levels can be efficiently generated in a simple collinear phase matching scheme in GaP driven by a sub-µJ-pulse-energy MHz-repetition-rate Yb-based TDL oscillator. We generated 0.3 mW of THz power with a spectrum extending to nearly 5 THz in a 0.5 mm GaP crystal using a 20 W, 95 fs driving laser operating at 48 MHz repetition rate.

Benefiting from the excellent beam quality and transform-limited soliton pulses of our driving laser, we provide high-fidelity measurements of the influence of the pulse duration, the peak intensity, and the crystal thickness on both the THz average power and the THz spectral bandwidth for the less-investigated 1 µm emission range of Yb-lasers. Optimization of these parameters allowed us to extend the THz spectrum to nearly 7 THz, which is to our knowledge the broadest gap-less THz spectrum generated by an Yb-based laser.

We further show that the measured THz spectrum can be reasonably approximated by considering decoupled multiplicative factors in the frequency domain, providing a simple and comprehensive method for the design and optimization of similar THz systems.

In agreement with [18], we thus conclude that optical rectification in GaP is highly suitable for broadband THz generation driven by high-power Yb-based lasers. Further power scalability has been recently confirmed by Meyer *et al.* utilizing a high power TDL oscillator combined with an external pulse compression delivering 88-fs pulses at 112 W of average power as a driving source. This yielded 1.35 mW THz radiation with a spectrum extending to 4 THz [29]. Since further improvements in the area of ultrafast TDL are expected, we believe that broadband THz sources delivering tens of mW of average power at MHz repetition rates are soon within reach.

Funding

Swiss National Science Foundation (SNSF) (179146, 170772, 144970); German Ministry of Education and Research (BMBF) (13N14192).

7. Appendix

In order to verify the usable spectral range of our system we performed a simple THz-TDS measurement of water vapor as depicted in Fig. 5. The measurement was taken using 84 fs pulse duration and shows a good agreement with the reference HITRAN database [22] water absorption spectrum in the frequency range between 1 and 6 THz with < 20 GHz resolution.

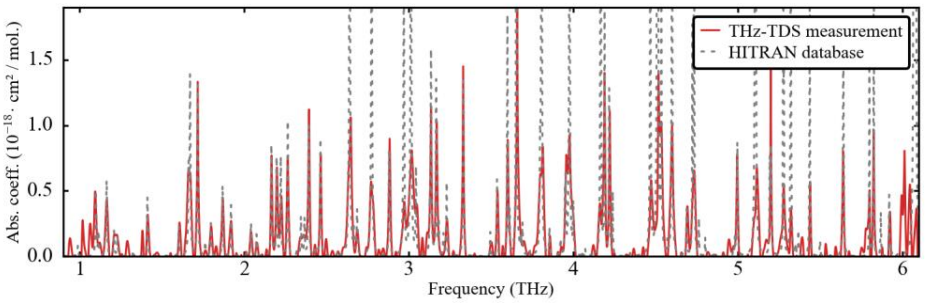

Fig. 5. THz-TDS measurement of water vapor absorption obtained by comparing two 40 ps THz scans at 40% and 10% relative humidity, respectively. The measurement is compared with the absorption spectrum from the HITRAN database [22].

Table 1. Equation for estimation of the THz spectrum.[a]

Process	Equation	Ref.
IR sech^2 pulse intensity envelope, where τ_{laser} ·1.76 corresponds to the FWHM pulse duration	$I_{IR}(t) = \mathrm{sech}^2\left(\frac{t}{\tau_{laser}}\right)$	
Driving THz field, defined by second derivative of the driving pulse intensity envelope I_{IR} with respect to time	$E_{0\,THz}(\omega) = \mathrm{F}\left(\frac{d^2 I_{IR}(t)}{dt^2}\right)(\omega)$	[25]
Sellmeier equation for refractive index of GaP	$n_{THz}^2 = 1 + \frac{B_1 \lambda^2}{\lambda^2 - \lambda_1^2} + \frac{B_2 \lambda^2}{\lambda^2 - \lambda_2^2}$, $B_1 = 2.064$, $\lambda_1 = 27.284\,\mu m$, $B_2 = 8.089$, $\lambda_2 = 0.2707\,\mu m$	[17]

Phase matching condition for group velocity of the IR pulse and THz radiation phase velocity, where d_{crystal} determines thickness of the GaP crystal	$\mathrm{PM}(\omega)=\frac{e^{i\omega\delta(\omega)}-1}{i\omega\delta(\omega)}$, $\delta(\omega)=\frac{n_{\text{g}}(\lambda_0)-n_{\text{THz}}(\omega)}{c_{\text{light}}}d_{\text{crystal}}$, $n_{\text{g}}(1.03\ \mu\text{m})=3.31$	[20]
EOS response, determined by intensity envelope spectrum of the probing IR pulse	$\mathrm{EOS}(\omega)=\mathrm{F}\ \left(I_{\text{IR}}(t)\right)(\omega)$	[26]
GaP absorption coefficient	$k(\omega)=\mathrm{Im}\left(\varepsilon_{\text{el}}+\frac{\mathrm{S}_0\,\omega_0^2}{\omega_0^2-\omega^2-i\Lambda_0\omega}\right)$, $\varepsilon_{\text{el}}=8.7,\ S_0=1.8,$ $\Lambda_0=0.126\cdot10^{12}\ \text{rad/s},$ $\omega_0=69\cdot10^{12}\ \text{rad/s}$	[27]
GaP transmission, based on Fresnel reflection and material absorption, where d_{crystal} determines thickness of the GaP crystal	$t_{\text{GaP}}(\omega)=\frac{2}{n_{\text{THz}}(\omega)+1}\cdot e^{-k\frac{\omega\cdot d_{\text{crystal}}}{c_{\text{light}}}}$	
Electro-optic coefficient r_{41} of GaP	$r_{41}(\omega)=d_{\text{E}}\left(1+\frac{C_0\,\omega_0^2}{\omega_0^2-\omega^2-i\Lambda_0\omega}\right)$, $d_{\text{E}}=10^{-12}\ \text{m/V},\ C_0=-0.53,$ $\Lambda_0=0.126\cdot10^{12}\ \text{rad/s},$ $\omega_0=69\cdot10^{12}\ \text{rad/s}$	[27]
Overall THz field estimate	$E_{\text{THz}}=E_{0\ \text{THz}}\cdot\mathrm{PM}_{\text{Det}}\cdot\mathrm{PM}_{\text{Gen}}\cdot\mathrm{EOS}\cdot t_{\text{GaP}}\cdot r_{41}$	
Dependence of THz average power on angle θ of <110>-cut GaP crystal with respect to laser polarization	$P(\theta)\propto\sin^2(2\theta)+\sin^4(\theta)$	[25]

[a] $I_{\text{IR}}(t)$: soliton pulse intensity envelope; t: time (s); $\tau_{\text{laser}}\cdot1.76$: FWHM pulse duration (s); $E_{0\ \text{THz}}$: driving THz field; ω: angular frequency of the THz radiation (rad/s); n_{THz}: refractive index for THz frequencies; PM: Phase matching condition; λ_0: laser central wavelength; n_{g}: group refractive index; EOS: electro-optic sampling; k: absorption coefficient; t_{GaP}: GaP transmission; d_{crystal}: thickness of the GaP crystal; c_{light}: speed of light (m/s); r_{41}: electro-optic coefficient of GaP (m/V); E_{THz}: estimate of THz spectrum; $P(\theta)$: THz power (W)

References

1. P. U. Jepsen, D. G. Cooke, and M. Koch, "Terahertz spectroscopy and imaging – Modern techniques and applications," Laser & Photon. Rev. **5**(1), 124–166 (2011).
2. Y. Ochi, K. Nagashima, M. Maruyama, M. Tsubouchi, F. Yoshida, N. Kohno, M. Mori, and A. Sugiyama, "Yb:YAG thin-disk chirped pulse amplification laser system for intense terahertz pulse generation," Opt. Express **23**(11), 15057–15064 (2015).
3. J. Li, L. Chai, J. Shi, F. Liu, B. Liu, B. Xu, M. Hu, Y. Li, Q. Xing, C. Wang, A. B. Fedotov, and A. M. Zheltikov, "Generation of 0.3 mW high-power broadband terahertz pulses from GaP crystal pumped by negatively chirped femtosecond laser pulses," Laser Phys. Lett. **10**(12), 125404 (2013).
4. J. Xu, B. Globisch, C. Hofer, N. Lilienfein, T. Butler, N. Karpowicz, and I. Pupeza, "Three-octave terahertz pulses from optical rectification of 20-fs, 1-μm, 78-MHz pulses in GaP," J. Phys. B: At. Mol. Opt. Phys. **51**(15), 154002 (2018).
5. W. Cui, A. W. Schiff-Kearn, E. Zhang, N. Couture, F. Tani, D. Novoa, P. St. J. Russell, and J.-M. Ménard, "Broadband and tunable time-resolved THz system using argon-filled hollow-core photonic crystal fiber," APL Photonics **3**(11), 111301 (2018).
6. C. J. Saraceno, F. Emaury, O. H. Heckl, C. R. E. Baer, M. Hoffmann, C. Schriber, M. Golling, T. Südmeyer, and U. Keller, "275 W average output power from a femtosecond thin disk oscillator operated in a vacuum environment," Opt. Express **20**(21), 23535–23541 (2012).
7. J. Brons, V. Pervak, E. Fedulova, D. Bauer, D. Sutter, V. Kalashnikov, A. Apolonskiy, O. Pronin, and F. Krausz, "Energy scaling of Kerr-lens mode-locked thin-disk oscillators," Opt. Lett. **39**(22), 6442–6445 (2014).
8. T. Südmeyer, C. Kränkel, C. R. E. Baer, O. H. Heckl, C. J. Saraceno, M. Golling, R. Peters, K. Petermann, G. Huber, and U. Keller, "High-power ultrafast thin disk laser oscillators and their potential for sub-100-femtosecond pulse generation," Appl. Phys. B **97**(2), 281–295 (2009).
9. C. J. Saraceno, O. H. Heckl, C. R. E. Baer, C. Schriber, M. Golling, K. Beil, C. Kränkel, T. Südmeyer, G. Huber, and U. Keller, "Sub-100 femtosecond pulses from a SESAM modelocked thin disk laser," Appl. Phys. B **106**(3), 559–562 (2012).
10. A. Diebold, F. Emaury, C. Schriber, M. Golling, C. J. Saraceno, T. Südmeyer, and U. Keller, "SESAM mode-locked Yb:$CaGdAlO_4$ thin disk laser with 62 fs pulse generation," Opt. Lett. **38**(19), 3842–3845 (2013).
11. C. Schriber, L. Merceron, A. Diebold, F. Emaury, M. Golling, K. Beil, C. Kränkel, C. J. Saraceno, T. Südmeyer, and U. Keller, "Pushing SESAM modelocked thin-disk lasers to shortest pulse durations," in Advanced Solid State Lasers (Optical Society of America, 2014), paper AF1A.4.
12. J. Zhang, J. Brons, M. Seidel, V. Pervak, V. Kalashnikov, Z. Wei, A. Apolonski, F. Krausz, and O. Pronin, "49-fs Yb:YAG thin-disk oscillator with distributed Kerr-lens mode-locking," in European Quantum Electronics Conference (Optical Society of America, 2015), paper PD_A_1.
13. C. Paradis, N. Modsching, V. J. Wittwer, B. Deppe, C. Kränkel, and T. Südmeyer, "Generation of 35-fs pulses from a Kerr lens mode-locked Yb:Lu_2O_3 thin-disk laser," Opt. Express **25**(13), 14918–14925 (2017).
14. N. Modsching, C. Paradis, F. Labaye, M. Gaponenko, I. J. Graumann, A. Diebold, F. Emaury, V. J. Wittwer, and T. Südmeyer, "Kerr lens mode-locked Yb:CALGO thin-disk laser," Opt. Lett. **43**(4), 879–882 (2018).
15. N. Modsching, J. Drs, J. Fischer, C. Paradis, F. Labaye, M. Gaponenko, C. Kränkel, V. J. Wittwer, and T. Südmeyer, "Sub-100-fs Kerr lens mode-locked Yb:Lu_2O_3 thin-disk laser oscillator operating at 21 W average power," Opt. Express **27**(11), 16111–16120 (2019).
16. C. J. Saraceno, "Mode-locked thin-disk lasers and their potential application for high-power terahertz generation," J. Opt. **20**(4), 044010 (2018).
17. C. Paradis, J. Drs, N. Modsching, O. Razskazovskaya, F. Meyer, C. Kränkel, C. J. Saraceno, V. J. Wittwer, and T. Südmeyer, "Broadband terahertz pulse generation driven by an ultrafast thin-disk laser oscillator," Opt. Express **26**(20), 26377–26384 (2018).
18. F. Meyer, N. Hekmat, S. Mansourzadeh, F. Fobbe, F. Aslani, M. Hoffmann, and C. J. Saraceno, "Optical rectification of a 100 W average power mode-locked thin-disk oscillator," Opt. Lett. **43**(24), 5909–5912 (2018).
19. C. Kränkel, "Rare-earth-doped sesquioxides for diode-pumped high-power lasers in the 1-, 2-, and 3-μm spectral range," IEEE J. Sel. Top. Quantum Electron. **21**(1), 250–262 (2015).
20. Q. Wu and X.-C. Zhang, "7 terahertz broadband GaP electro-optic sensor," Appl. Phys. Lett. **70**(14), 1784–1786 (1997).
21. W. L. Bond, "Measurement of the refractive indices of several crystals," J. Appl. Phys. **36**(5), 1674–1677 (1965).
22. contact: HITRAN online, https://hitran.org/.
23. T. Hattori and K. Takeuchi, "Simulation study on cascaded terahertz pulse generation in electro-optic crystals," Opt. Express **15**(13), 8076–8093 (2007).
24. K. Aoki, J. Savolainen, and M. Havenith, "Broadband terahertz pulse generation by optical rectification in GaP crystals," Appl. Phys. Lett. **110**(20), 201103 (2017).
25. Y.-S. Lee, *Principles of Terahertz Science and Technology* (Springer US, 2009).

26. G. Gallot and D. Grischkowsky, "Electro-optic detection of terahertz radiation," J. Opt. Soc. Am. B **16**(8), 1204–1212 (1999).
27. S. Casalbuoni, H. Schlarb, B. Schmidt, P. Schmüser, B. Steffen, and A. Winter, "Numerical studies on the electro-optic detection of femtosecond electron bunches," Phys. Rev. ST Accel. Beams **11**(7), 072802 (2008).
28. E. D. Palik, *Handbook of Optical Constants of Solids* (Academic Press, 1997).
29. F. Meyer, N. Hekmat, T. Vogel, A. Omar, S. Mansourzadeh, F. Fobbe, M. Hoffmann, Y. Wang, and C. J. Saraceno, "1.35 mW, MHz-Repetition-Rate Broadband THz Source Driven by a 112 W, 88 fs Thin-Disk Laser," in Conference on Lasers and Electro-Optics (Optical Society of America, 2019), paper JTh5A.3.

Research Article | Vol. 29, No. 15 / 19 July 2021 / Optics Express 23729
Optics EXPRESS

Intra-oscillator broadband THz generation in a compact ultrafast diode-pumped solid-state laser

MARIN HAMROUNI,* JAKUB DRS, NORBERT MODSCHING, VALENTIN J. WITTWER, FRANÇOIS LABAYE, AND THOMAS SÜDMEYER

Laboratoire Temps-Fréquence (LTF), Institut de Physique, Université de Neuchâtel, Avenue de Bellevaux 51, 2000 Neuchâtel, Switzerland
*marin.hamrouni@unine.ch

Abstract: We demonstrate broadband and powerful terahertz (THz) generation at megahertz repetition rate based on intra-oscillator optical rectification (OR) in gallium phosphide (GaP). By placing the nonlinear crystal directly inside the cavity of a Kerr-lens mode-locked ultrafast diode-pumped solid-state laser (DPSSL) oscillator, we demonstrate a compact and single-stage THz source. Using only 7 W of diode-pump power, we drive OR in a GaP crystal with 22 W of average power at ~80 MHz repetition rate. In a first configuration, using a 0.3-mm-thick GaP and 105 fs driving pulses, we generate up to 150 μW of THz radiation with a spectrum extending to 5.5 THz. In a second configuration allowing for sub-50-fs pulse duration, we generate up to 7 THz inside a 0.1-mm-thick GaP crystal. This performance is well suited for THz time-domain spectroscopy and THz imaging. Intra-oscillator THz generation in sub-100-fs DPSSLs is a promising way to scale down footprint, complexity and cost of powerful broadband THz sources.

1. Introduction

During the last decades, broadband terahertz (THz) generation driven by ultrafast lasers has opened up access to numerous applications such as THz time-domain spectroscopy or spectral imaging [1]. However, the conversion efficiency between the driving laser and the THz radiation is typically relatively low, ranging between a few parts per million up to a few percent. Although several microwatts of THz average power are sufficient for some applications such as terahertz time-domain spectroscopy, many others such as THz imaging or spectroscopy of highly absorptive samples would strongly benefit from higher THz average powers [2]. In recent years, we have witnessed a considerable progress in the development of high-power THz systems. New THz sources based on plasmonic-enhanced photoconductive antennas [3,4] and organic nonlinear crystals [5,6] achieve milliwatt-class broadband THz generation from moderate pump power levels of only a few watts. Another highly promising direction for increased THz power is the use of well-established techniques such as optical rectification (OR) in nonlinear crystals or two-color laser filamentation at much higher pump power levels from novel ultrafast lasers. Up to 1.35 mW of THz average power with a spectrum reaching up to 6 THz have been generated by driving OR in gallium phosphide (GaP) with a 100-W nonlinearly compressed thin-disk laser (TDL) oscillator [7]. Later on, driving OR in lithium niobite instead of GaP, 66 mW of THz average power with a spectrum extending up to 2 THz were generated using the same driving laser [8]. Finally, 50 mW of THz average power with a spectrum expected to extend up to 30 THz was demonstrated using two-color laser filamentation in a neon gas target driven by a 160-W chirped-pulse fiber-amplifier system at 100 kHz repetition rate [9]. However, the complexity, the size and the cost of these systems due to, e.g., the required diode pump power or the vacuum

#426750 https://doi.org/10.1364/OE.426750
Journal © 2021 Received 1 Apr 2021; accepted 4 May 2021; published 12 Jul 2021

Optics EXPRESS

chamber might still be a limiting factor for many applications requiring small and compact sources.

Driving a nonlinear frequency conversion process inside a laser cavity has proven to be a successful approach for reducing the complexity of the system and increasing the overall efficiency [10–12]. Similarly, placing the THz generation crystal in a laser cavity allows for recycling of the unconverted pulse energy in each cavity roundtrip. This strongly increases the available driving power in comparison to the outcoupled beam. However, previous demonstrations of intra-cavity THz generation were so far strongly restricted in the demonstrated power levels. In [13], intra-oscillator THz generation reaching up to 7 µW of THz average power was achieved by a transient photocurrent at the surface of a semiconductor saturable absorber mirror, which also initiated and stabilized the pulses in a femtosecond Ti:sapphire oscillator. In 2008, this intra-oscillator technique was applied in a soliton fiber laser [14]. Here a THz yield of 4 µW and a conversion efficiency of 3.1×10^{-5} were achieved. In the same year, passive enhancement cavities were used for the generation of THz radiation using OR [15] and THz generation inside a dual frequency optical parametric oscillator via difference frequency generation in DAST was achieved [16]. The first optical rectification inside a femtosecond oscillator was demonstrated in 2010 using a Ti:sapphire laser oscillator [17]. However, the THz average power was not measured and the THz spectrum was restricted to 2.5 THz due to the 1-mm-thick zinc telluride crystal used for OR.

In the last decade, ultrafast technology strongly progressed [18–20]. Today, ultrafast solid-state laser oscillators can operate at several hundred watts of intra-oscillator average power with sub-100-fs pulses [21–25] which is required for powerful and broadband THz generation [7,26–28].

In our experiment, we drive OR in a GaP crystal which is placed inside the cavity of a Kerr-lens mode-locked (KLM) Yb:CALGO bulk laser oscillator. Yb:CALGO is an outstanding gain material for ultrafast lasers thanks to its broadband gain emission spectrum combined with a low quantum defect and relatively high thermal conductivity [29–31], making it particularly attractive for compact and efficient ultrafast DPSSLs [32]. For example, 30-fs pulses at optical-to-optical efficiencies of ~30% were recently achieved [33]. Moreover, it can be pumped by low cost 980 nm multimode pump diodes. In our intra-oscillator THz system, OR was driven in a GaP crystal at 22 W of intra-cavity laser power, 105 fs pulse duration, and 75 MHz repetition rate. We achieve up to 150 µW of THz average power with a spectrum extending to 5.5 THz using only 7 W of diode pump power. Compared to a single-pass system with similar performance [27], the intra-cavity approach requires 20 times less pump power. We also demonstrate that the THz spectrum can be extended up to ~7 THz at the expense of THz average power using a thinner GaP crystal combined with shorter pulse duration. These results show that intra-oscillator THz generation via OR is a promising way to simplify and reduce the size of the current state-of-the-art THz sources. GaP can support more than hundred watts of driving power [34], and we expect that milliwatt THz power levels are within reach of this technology.

2. Experimental setup

The experimental setup is shown in Fig. 1. The laser oscillator is based on a 3-mm-long, antireflection-coated (AR) Yb(3 at.%):CALGO crystal. The crystal is mounted in a water-cooled copper holder and optically pumped at 980 nm by a commercially available 10-W multimode fiber coupled laser diode module. The positive group delay dispersion (GDD) introduced by the gain medium, the GaP crystal, and the self-phase modulation is compensated by several dispersive mirrors (DM). A 2.7-mm diameter hard aperture enables stable KLM operation. An output coupler (OC) with a transmission of 1.5% is placed as a folding mirror, thus providing two out-coupled beams. One beam is used to characterize the driving laser while the other beam is used for electro-optic sampling (EOS). The GaP crystal is placed close to the end mirror of

Optics EXPRESS

the laser cavity without any active cooling. Both faces of the GaP crystal have an AR coating which was designed and grown in our own ion beam sputtering coating facility. The THz radiation is generated in two directions inside the GaP crystal, however, only one direction is characterized. The strongly diverging THz beam is directed by two off-axis parabolic mirrors (OAPM) onto a second 0.15-mm-thick GaP crystal for EOS. The THz beam is mechanically chopped at around 75 Hz for subsequent lock-in detection. The THz average power is measured by placing a pyroelectric power meter at the position of the GaP crystal used for the detection. Three layers of black plastic foil were inserted between the two OAPMs in order to prevent any of the parasitic scattered infrared light from reaching the detector. Their individual THz transmission of 46% has been determined in a previous study [27] and the here stated measured THz average powers were corrected by this transmission factor. The system was purged by dry air to decrease the relative humidity to below 20% in order to reduce the water vapour absorption of the THz radiation.

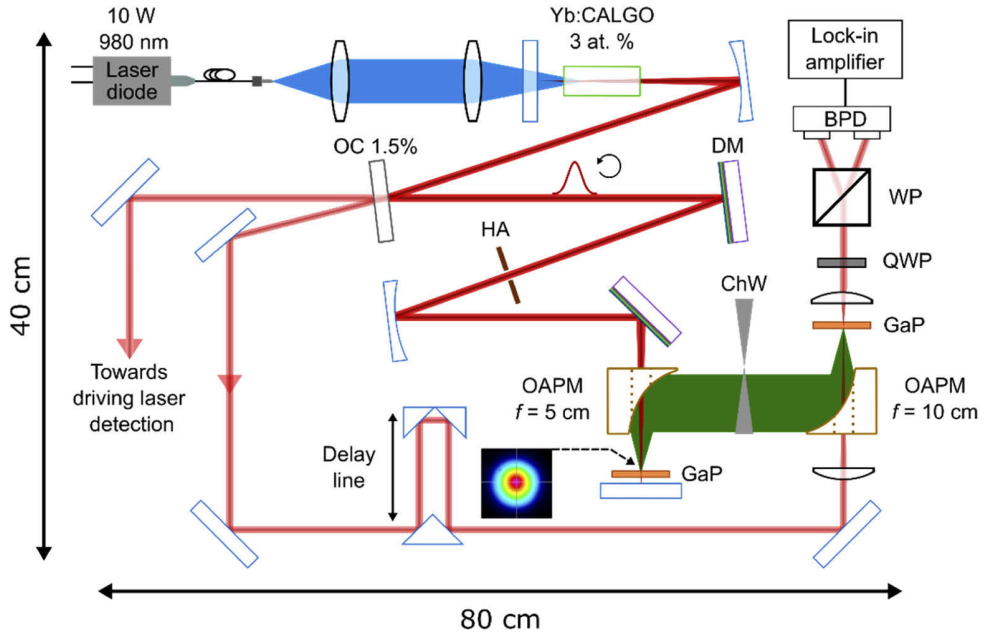

Fig. 1. Experimental setup for intra-oscillator THz generation and detection by electro-optic sampling. OC, 1.5% transmission output coupler; DM, dichroic mirror; HA, hard aperture; OAPM, off-axis parabolic mirror; ChW, chopper wheel; QWP, quarter waveplate; WP, Wollaston prism; BPD, balanced photodetector. The footprint of the overall system is 80 cm × 40 cm.

3. Experimental results

We characterized the system in two different configurations optimized for either high THz average power or for a broader THz spectrum. Table 1 summarizes the characteristics of the driving laser and the resulting THz performance. The first configuration optimized for high THz average power uses a 0.3-mm-thick GaP crystal. OR in GaP was driven at 22 W of intra-cavity average power with 105 fs pulse duration corresponding to 12.2 nm of full width at half maximum (FWHM) spectral bandwidth [Figs. 2(a) and 2(b)] and 75 MHz repetition rate.

The pulse duration was adapted to the phase matched window of the 0.3-mm GaP crystal according to [27]. The beam diameter inside the crystal was ~400 µm, corresponding to a

Optics EXPRESS

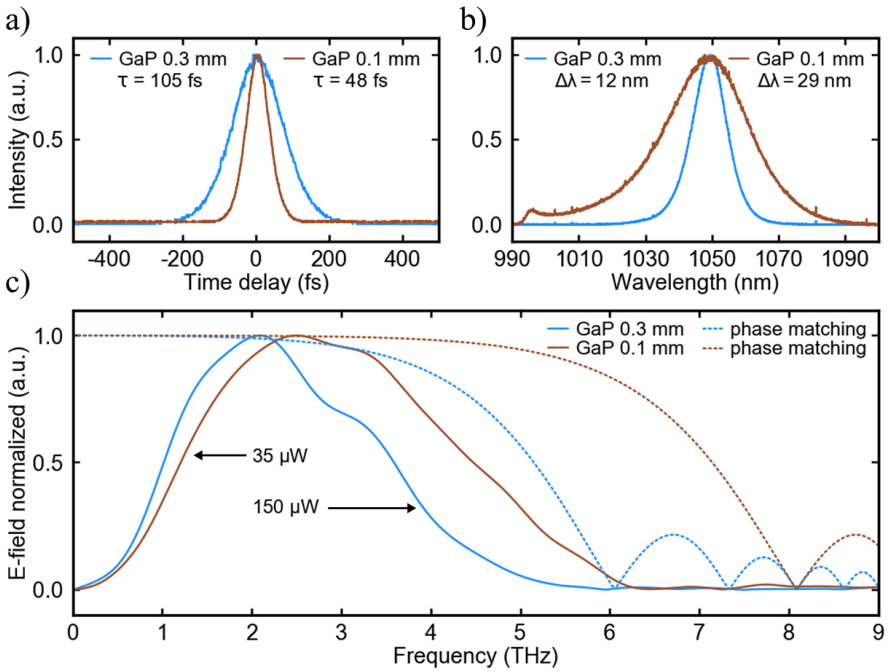

Fig. 2. a) Autocorrelation trace and b) optical spectrum of the driving pulse for the configuration 1 (using a 0.3-mm-thick GaP) and the configuration 2 (using a 0.1-mm-thick GaP). c) Normalized THz E-field in the frequency domain detected by electro-optic sampling (plain line) and the corresponding theoretical phase matching curves (dashed lines) for both configurations. τ, FWHM pulse duration; $\Delta\lambda$, FWHM spectral bandwidth.

Table 1. Driving laser parameters and resulting THz performance corresponding to the configuration 1 using a 0.3-mm-thick GaP crystal and the configuration 2 using a 0.1-mm-thick crystal.[a]

	Driving laser							THz results	
GaP thickness	P_{pump} (W)	$P_{av,intra}$ (W)	f_{rep} (MHz)	τ (fs)	$\Delta\lambda$ (nm)	2ω ($1/e^2$) (μm)	I_p (GW/cm^2)	$P_{av,THz}$ (μW)	$\nu_{THz,max}$ (THz)
0.3 mm	6.5	22	75	105	12.2	400	4	150	5.5
0.1 mm	7	20	80	48	29.4	350	9	35	7

[a] P_{pump}, pump power of the laser; $P_{av,intra}$, intra-cavity average power; f_{rep}, repetition rate; τ, FWHM pulse duration; $\Delta\lambda$, FWHM spectral bandwidth; 2 ($1/e^2$), beam diameter in the GaP; I_p, peak intensity in the GaP, $P_{av,THz}$, THz average power; $\nu_{THz,max}$, maximal THz spectrum frequency.

peak intensity of ~4 GW/cm^2, significantly below the damage threshold of 60 GW/cm^2 [35]. Figure 2(c) shows the generated THz spectrum (blue line) retrieved from the EOS measurement in the frequency domain. The THz spectrum is centred at 2 THz and extends up to 5.5 THz, slightly below the limit imposed by the phase matching condition. We measured up to 150 μW of THz average power leading to an optical-to-optical efficiency of 7×10^{-6} and 2×10^{-5} with respect to the driving laser and the multimode pump diode average power, respectively.

The second configuration aims to further exploit the potential of the ultrafast driving source for broadband THz generation. It utilizes a 0.1-mm GaP crystal allowing for a phase-matched window extending up to ~8 THz. However, the broader phase-matched window of the thinner

Optics EXPRESS

GaP crystal comes at the expense of a reduced THz average power due to the shorter interaction length. The pulse duration was adjusted to 48 fs corresponding to 12.2 nm of FWHM spectral bandwidth by reducing the negative GDD introduced by the DMs. The laser beam diameter inside the GaP crystal was decreased to ~350 µm by slightly adjusting the cavity length. The decrease of the pulse duration and beam diameter led to a higher peak intensity inside the GaP crystal estimated to be ~9 GW/cm^2 in this configuration. Driving OR at 20 W of intra-cavity average power and 80 MHz repetition rate resulted in the generation of 35 µW of THz average power with a spectrum centred at 3 THz and extending up to ~7 THz. The drop of the average THz power is consistent with the change in the crystal thickness and the driving laser peak intensity. The measured spectrum does not reach the 8-THz phase-matching limit mostly due to the thicker GaP crystal of 0.15 mm used for EOS, restricting the measurement range to approximately 7 THz.

In the current setup we were limited to intra-cavity average powers of ~20 W by the onset of a continuous-wave lasing breakthrough at higher pumping powers. We attribute this effect to the thermal lens and multiphoton absorption inside the GaP crystal disrupting the KLM operation. We expect that optimization of the cavity layout to accommodate the thermal lens combined with higher repetition rate will allow for significant increase of the intra-cavity driving power. Further advances are expected by implementing efficient cooling of the GaP crystal.

4. Conclusion

In this proof-of-principle experiment, we have demonstrated efficient and broadband THz generation based on OR in GaP in a simple collinear geometry directly inside the cavity of an ultrafast laser oscillator. In a first configuration, the system generated up to 150 µW of THz average power with an optical spectrum extending up to 5.5 THz and 35 µW with a spectrum extending up to 7 THz in a second configuration. This simple concept of intra-oscillator THz generation allows for high average driving powers in combination with short pulse duration which are otherwise available only from more complex laser systems requiring diode pump powers exceeding the 100 W range. For instance, in comparison to a single-pass THz-source based on OR in GaP driven by a high-power TDL oscillator utilizing the same GaP thickness, our intra-oscillator approach requires 20 times lower pump power at a fraction of the component cost [27]. We also expect a further improvement of the technology is easily within reach. Since up to 1.35 mW of THz average power has already been generated by single-pass OR in GaP [7], we believe that the intra-oscillator approach will soon reach a comparable performance.

Funding. Schweizerischer Nationalfonds zur Förderung der Wissenschaftlichen Forschung (200021_188456, SPARK CRSK-2_190593).

Disclosures. The authors declare that there are no conflicts of interest related to this article.

Data availability. Data underlying the results presented in this paper are available in Ref. [36].

References

1. P. U. Jepsen, D. G. Cooke, and M. Koch, "Terahertz spectroscopy and imaging – Modern techniques and applications," Laser & Photon. Rev. **5**(1), 124–166 (2011).
2. M. Tonouchi, "Cutting-edge terahertz technology," Nat. Photonics **1**(2), 97–105 (2007).
3. N. T. Yardimci, S.-H. Yang, C. W. Berry, and M. Jarrahi, "High-power terahertz generation using large-area plasmonic photoconductive emitters," IEEE Trans. Terahertz Sci. Technol. **5**(2), 223–229 (2015).
4. N. T. Yardimci, S. Cakmakyapan, S. Hemmati, and M. Jarrahi, "A High-Power Broadband Terahertz Source Enabled by Three-Dimensional Light Confinement in a Plasmonic Nanocavity," Sci. Rep. **7**(1), 1–8 (2017).
5. T. O. Buchmann, E. J. Railton Kelleher, M. Jazbinsek, B. Zhou, J.-H. Seok, O.-P. Kwon, F. Rotermund, and P. U. Jepsen, "High-power few-cycle THz generation at MHz repetition rates in an organic crystal," APL Photonics **5**(10), 106103 (2020).
6. C. Vicario, M. Jazbinsek, A. V. Ovchinnikov, O. V. Chefonov, S. I. Ashitkov, M. B. Agranat, and C. P. Hauri, "High efficiency THz generation in DSTMS, DAST and OH1 pumped by Cr:forsterite laser," Opt. Express **23**(4), 4573–4580 (2015).

Optics EXPRESS

7. F. Meyer, N. Hekmat, T. Vogel, A. Omar, S. Mansourzadeh, F. Fobbe, M. Hoffmann, Y. Wang, and C. J. Saraceno, "Milliwatt-class broadband THz source driven by a 112 W, sub-100 fs thin-disk laser," Opt. Express **27**(21), 30340–30349 (2019).
8. F. Meyer, T. Vogel, S. Ahmed, and C. J. Saraceno, "Single-cycle, MHz repetition rate THz source with 66 mW of average power," Opt. Lett. **45**(9), 2494–2497 (2020).
9. J. Buldt, M. Mueller, H. Stark, C. Jauregui, and J. Limpert, "Fiber laser-driven gas plasma-based generation of THz radiation with 50-mW average power," Appl. Phys. B **126**(2), 1–5 (2020).
10. R. G. Smith, K. Nassau, and M. F. Galvin, "Efficient continuous optical second harmonic generation," Appl. Phys. Lett. **7**(256), 129 (1965).
11. Q. H. Xue, Q. Zheng, Y. K. Bu, F. Q. Jia, and L. S. Qian, "High-power efficient diode-pumped Nd:YVO_4/LiB_3O_5 457 nm blue laser with 46 W of output power," Opt. Lett. **31**(8), 1070 (2006).
12. L. McDonagh and R. Wallenstein, "Low-noise 62 W CW intracavity-doubled TEM_{00} Nd:YVO_4 green laser pumped at 888 nm," Opt. Lett. **32**(7), 802–804 (2007).
13. J. Darmo, T. Müller, G. Strasser, K. Unterrainer, T. Le, A. Stingl, and G. Tempea, "Voltage-controlled intracavity terahertz generator for self-starting Ti:sapphire lasers," Opt. Lett. **27**(21), 1941 (2002).
14. G. Matthäus, B. Ortaç, J. Limpert, S. Nolte, R. Hohmuth, M. Voitsch, W. Richter, B. Pradarutti, and A. Tünnermann, "Intracavity terahertz generation inside a high-energy ultrafast soliton fiber laser," Appl. Phys. Lett. **93**(26), 261105 (2008).
15. M. Theuer, D. Molter, K. Maki, C. Otani, J. A. L'huillier, and R. Beigang, "Terahertz generation in an actively controlled femtosecond enhancement cavity," Appl. Phys. Lett. **93**(4), 041119 (2008).
16. T. Shibuya, T. Akiba, K. Suizu, H. Uchida, C. Otani, and K. Kawase, "Terahertz-Wave Generation Using a 4-Dimethylamino-*N*-methyl-4-stilbazolium tosylate Crystal Under Intra-Cavity Conditions," Appl. Phys. Express **1**, 042002 (2008).
17. S. Xu, J. Liu, G. Zheng, and J. Li, "Broadband terahertz generation through intracavity nonlinear optical rectification," Opt. Express **18**(22), 22625–22630 (2010).
18. U. Keller, "Ultrafast solid-state laser oscillators: a success story for the last 20 years with no end in sight," Appl. Phys. B **100**(1), 15–28 (2010).
19. H. Fattahi, H. G. Barros, M. Gorjan, T. Nubbemeyer, B. Alsaif, C. Y. Teisset, M. Schultze, S. Prinz, M. Haefner, M. Ueffing, A. Alismail, L. Vámos, A. Schwarz, O. Pronin, J. Brons, X. T. Geng, G. Arisholm, M. Ciappina, V. S. Yakovlev, D.-E. Kim, A. M. Azzeer, N. Karpowicz, D. Sutter, Z. Major, T. Metzger, and F. Krausz, "Third-generation femtosecond technology," Optica **1**(1), 45 (2014).
20. D. T. Reid, C. M. Heyl, R. R. Thomson, R. Trebino, G. Steinmeyer, H. H. Fielding, R. Holzwarth, Z. Zhang, P. Del'Haye, T. Südmeyer, G. Mourou, T. Tajima, D. Faccio, F. J. M. Harren, and G. Cerullo, "Roadmap on ultrafast optics," J. Opt. **18**(9), 093006 (2016).
21. A. Greborio, A. Guandalini, and J. Aus der Au, "Sub-100 fs pulses with 12.5-W from Yb:CALGO based oscillators," in *Proc. SPIE*, (2012), paper 823511.
22. A. Diebold, F. Emaury, C. Schriber, M. Golling, C. J. Saraceno, T. Südmeyer, and U. Keller, "SESAM mode-locked Yb:$CaGdAlO_4$ thin disk laser with 62 fs pulse generation," Opt. Lett. **38**(19), 3842–3845 (2013).
23. A. Klenner, M. Golling, and U. Keller, "High peak power gigahertz Yb:CALGO laser," Opt. Express **22**(10), 11884–11891 (2014).
24. S. Hakobyan, V. J. Wittwer, K. Gürel, A. S. Mayer, S. Schilt, and T. Südmeyer, "Carrier-envelope offset stabilization of a GHz repetition rate femtosecond laser using opto-optical modulation of a SESAM," Opt. Lett. **42**(22), 4651–4654 (2017).
25. J. Fischer, J. Drs, F. Labaye, N. Modsching, V. Wittwer, and T. Südmeyer, "Intra-oscillator high harmonic generation in a thin-disk laser operating in the 100-fs regime," Opt. Express **29**(4), 5833–5839 (2021).
26. C. Paradis, J. Drs, N. Modsching, O. Razskazovskaya, F. Meyer, C. Kränkel, C. J. Saraceno, V. J. Wittwer, and T. Südmeyer, "Broadband terahertz pulse generation driven by an ultrafast thin-disk laser oscillator," Opt. Express **26**(20), 26377–26384 (2018).
27. J. Drs, N. Modsching, C. Paradis, C. Kränkel, V. J. Wittwer, O. Razskazovskaya, and T. Südmeyer, "Optical rectification of ultrafast Yb lasers: pushing power and bandwidth of terahertz generation in GaP," JOSA B **36**(11), 3039–3045 (2019).
28. G. Barbiero, H. Wang, J. Brons, B.-H. Chen, V. Pervak, and H. Fattahi, "Broadband terahertz solid-state emitter driven by Yb:YAG thin-disk oscillator," J. Phys. B: At. Mol. Opt. Phys. **53**(12), 125601 (2020).
29. J. Petit, P. Goldner, and B. Viana, "Laser emission with low quantum defect in Yb:$CaGdAlO_4$," Opt. Lett. **30**(11), 1345–1347 (2005).
30. Y. Zaouter, J. Didierjean, F. Balembois, G. L. Leclin, F. Druon, P. Georges, J. Petit, P. Goldner, and B. Viana, "47-fs diode-pumped Yb^{3+}:$CaGdAlO_4$ laser," Opt. Lett. **31**(1), 119–121 (2006).
31. F. Druon, F. Balembois, and P. Georges, "New Materials for Short-Pulse Amplifiers," IEEE Photon. J. **3**(2), 268–273 (2011).
32. P. Sévillano, P. Georges, F. Druon, D. Descamps, and E. Cormier, "32-fs Kerr-lens mode-locked Yb:$CaGdAlO_4$ oscillator optically pumped by a bright fiber laser," Opt. Lett. **39**(20), 6001–6004 (2014).

Optics EXPRESS

33. F. Labaye, V. J. Wittwer, N. Modsching, O. Razskazovskaya, E. Cormier, and T. Südmeyer, "Yb:CALGO bulk oscillator generating ultrashort pulses at high efficiency by cross-polarized optical pumping," in *9th EPS-QEOD Europhoton conference*, (2020), paper We-A1.4.
34. N. Hekmat, T. Vogel, Y. Wang, S. Mansourzadeh, F. Aslani, A. Omar, M. Hoffmann, F. Meyer, and C. J. Saraceno, "Cryogenically cooled GaP for optical rectification at high excitation average powers," Opt. Mater. Express **10**(11), 2768–2782 (2020).
35. Y. Li, F. Liu, Y. Li, L. Chai, Q. Xing, M. Hu, and C. Wang, "Experimental study on GaP surface damage threshold induced by a high repetition rate femtosecond laser," Appl. Opt. **50**(13), 1958–1962 (2011).
36. M. Hamrouni, J. Drs, N. Modsching, V. J. Wittwer, F. Labaye, and T. Sudmeyer, *EUDAT B2SHARE repository: b2share*," (2021), http://doi.org/10.23728/b2share.089c82b5f3594c558af796e13285beaa

4 Conclusion

Within the frame of this thesis, three main topics were investigated and the results were published in international journals. The common denominator of the presented work has been the development of ultrafast KLM TDL oscillators operating in the sub-100-fs regime. Over the four years of this thesis, we significantly improved the performance of these lasers. In 2019, we demonstrated a 20-W 100-fs TDL oscillator which was already twice more powerful than previous demonstrations of similar lasers. In 2020, we pushed this frontier even further, increasing the average power to 100 W, while shortening the pulse duration to 50 fs. In the same year, we also demonstrated the shortest pulse duration of any TDL oscillator of 27 fs.

The developed TDL oscillators have been further utilized for nonlinear frequency conversion toward THz and XUV wavelengths. In 2018, we demonstrated for the first time the suitability of TDL oscillators for driving broadband THz generation. In this study, we used a 50-fs, 5-W self-developed TDL oscillator as a driving source and reached 10 µW of average THz power with a broad 7-THz-spanning spectrum. Later we increased the THz average power to 0.3 mW by utilizing a newly developed 20-W version of the driving laser. Finally, we have showed that the THz generation setup can be largely simplified by placing the generation nonlinear crystal directly inside the laser cavity. This allowed replacing the high-power TDL by a small bulk oscillator while strongly improving the overall THz generation efficiency of the setup.

The major motivation for developing ultrafast TDL oscillators in our group has been their application for intra-oscillator HHG. The TDL technology has been designed to withstand highest peak and average powers inside the gain material. This makes these lasers ideal candidates for driving extreme nonlinear processes such as HHG directly inside the laser cavity. The concept of HHG inside a high power TDL has been first demonstrated in our group shortly before the start of this thesis. Building upon this result, we developed a second generation of the intra-oscillator HHG system. Major modifications were implemented throughout this process. The original SESAM mode-locking scheme was replaced by KLM enabling a significant increase of the laser performance. The gain material of the laser was switched from Yb:LuO to Yb:YAG, which has an advantage of being commercially available. The system has further un-

dergone countless mechanical, electrical and thermal management modifications strongly improving the operation routine and the stability of the laser. The result of these modifications has been an increase of the generated XUV flux over four orders of magnitude, starting from 0.5 nW up to 10 µW, while also increasing the photon energy from 13 eV to 30 eV. These demonstrations might lead to the development of a new class of compact coherent XUV sources based on the well-established and commercially available TDL technology. Such affordable sources would highly benefit many applications both in science and industry.

Acknowledgments

In the first place, I would like to thank my whole family, my parents, my grandparents, my brothers. They have been supporting me throughout my studies, and up to nowadays and helped orienting me towards where I am standing right now.

The second greatest thank goes to Thomas, who took me onboard to his group and provided the greatest research environment for pursuing my doctoral studies. He has given us a lot of freedom in organizing the research projects, always supporting our ideas, but also providing many advices and contacts, as well as numerous bottles of champagne to celebrate our results.

Then Valentin, who's been the technical advisor of the whole group, always ready to help with whatever issue we were able to come up with. Starting from aligning autocorrelators, over RF measurements, preparing python code for our experiments, fulfilling our needs of hundreds of optical coatings, while still finding some time for organizing a ski weekend in his apartment in Mürren.

A lot of gratitude belongs to my colleagues at LTF. To Maxim, who helped me to get to the group in the first place and later introduced me to the intra-oscillator HHG. Clément and Olga for kicking off the THz project and being of great support during my first years at LTF. Norbert for all the laser night-shifts spent together for the last minute results and the scientific discussions shared over a beer. François for sharing his knowledge of HHG. Marin for his adventurous climbing and mountaineering ideas and trips. Julian for pulling together the HHG project as well as some skiing adventures. Patricia for being so helpful with the administrative stuff, but also organizing many group events. And all the other colleagues who have not been mentioned yet for creating a great atmosphere and group spirit at the LTF.

Finally, I would like to thank all my friends here in Switzerland for all the hikes, barbeques, parties, and other events which we shared together. Pieter, Julie, Malwina, Rafa, Kasia, Alexandros, Christos, Yvan, Johan, Mélanie, Maxim, Thomas and many others, you have been great friends and I so much appreciate the time we have spent together.

My greatest thanks to You all.

Curriculum Vitae

Contact Information

Jakub Drs
Rue du Rocher 24
2000 Neuchatel
Switzerland

Cell phone: +41 798 670 668
E-mail: jakub.drs@unine.ch

Education

University of Neuchâtel **2017 - 2022**

PhD in physics, Time and Frequency laboratory

- Thesis Topic: "Thin-disk lasers and their applications for nonlinear frequency conversion toward THz and XUV"
- Thesis director: Prof. Thomas Südmeyer

Czech Technical University in Prague **2009 - 2015**

Master degree program - Cybernetics and robotics

- Thesis Topic: "Micromanipulation platform for droplets"

Bachelor degree program - Cybernetics and robotics

- Thesis Topic: "Four-sector microelectrode array for dielectrophoresis"

Research experience

University of Neuchâtel **2017 - 2022**
Doctoral studies at Time and Frequency laboratory (LTF)
Thin-disk lasers and their applications for nonlinear frequency conversion toward THz and XUV

École polytechnique fédérale de Lausanne & FEMTOprint SA **2016 - 2017**
CTI project - design of the R&D laser polishing setup

University of Technology in Eindhoven, Netherlands **(3 months) 2014**
Lab internship at Microsystems research group

Honors and Awards

Prize of Josef Hlavka for the Best Students and Graduates **2012**
EOS award for the best student presentation at EOSAM conference **2021**

Professional Skills

- Design of lasers and optical systems
- Laser microstructuring and micromachining
- Electronic design, embedded programming

Languages

- English: Fluent
- French: Beginner
- Czech: Mothertongue

Personal interests

- DIY projects
- Music: playing guitar violin and learning piano
- Traveling